Discovery, systematics, and taxonomy of new marine Apicomplexa and a myzozoan relative

アピコンプレックス類および
近縁のミゾゾア類における未記載種の発見
およびそれらの系統分類学的研究

Naoki Davis Iritani

Submitted for the degree of Doctor of Philosophy

Graduate School of Science, Hokkaido University

Department of Natural History Sciences

2020 September

Abstract

Taxonomy in its essence posits that the entire biosphere is connected by common descent. The binomial system of nomenclature suggested by Carl Linnaeus relies on both similarities and differences among species. Shared traits among species as a result of common ancestry unite organisms into taxonomic units. On the other hand, the different adaptations that make each lineage unique are carefully scrutinized to distinguish related taxa. This seemingly simple and traditional practice has, of course, various challenges that slow the impetus to the classification of life. For example, experts often disagree on what makes two lineages sufficiently different, literature old and new is scattered across obscure journals in various languages, and natural mechanisms such as convergent evolution can confound classification. Taxonomy, despite these complex obstacles, continues to form the foundation of biology by creating an ever-expanding lexicon of nomenclature. Without the proper vocabulary to refer to all life on Earth, interdisciplinary communication and navigating through the disciplinary matrix of biology would be near impossible.

The research included in this dissertation aims to contribute to taxonomy by delving into an enigmatic group of parasitic eukaryotes known as the Apicomplexa and its close relatives. These parasites are speciose and have devastating medical impacts on human life and the natural ecosystem. However, there is a noticeably disproportionate depth of knowledge between what is known about a select group of apicomplexan species and what is known about apicomplexan biology as a whole. This dissertation presents descriptions of a new genus, five new species of apicomplexan parasites, and the characterization of an undescribed apicomplexan relative isolated from various animal hosts. These descriptions employ the use of both traditional morphology as well as molecular systematics in an effort to better reconcile morphological data with molecular phylogenetics. At the very core of this work is my attempt at making a humble contribution to the creation of a

taxonomy that reflects phylogeny and to help rectify the lack of taxon sampling through species discovery and the acquisition of novel data.

The first chapter is a general introduction to apicomplexan biology, taxonomy, and systematics. It aims to provide an overview of the history of apicomplexan biology while highlighting the major lineages within the group and their main characteristics. The chapter most heavily articulates the Gregarinasina – the main focal taxon of the research included herein. Finally, this review of literature demonstrates that the major obstacles to apicomplexan biology include poor taxon sampling, a lack of research on non-medically significant species, and the dissonance between taxonomy and phylogenetics.

The second chapter describes the discovery of a new species of marine gregarine, *Cuspisella ishikariensis* gen. nov., sp. nov., from a scale worm host found in Hokkaido, Japan. The observation of unusual morphological traits in this new species provided an opportunity to re-evaluate the degree of morphological innovation in marine gregarines. The molecular identity of a previously described scale worm parasite, *Loxomorpha harmothoe*, was also recovered and given a phylogenetic position as *Loxomorpha* cf. *harmothoe*. These scale worm parasites form a distinct lineage within the greater marine gregarine phylogeny and a new genus was created to accommodate this discovery.

The third chapter presents four new species of marine gregarines discovered from ascidian hosts from New Zealand: *Lecudina kaiteriteriensis* sp. nov., *L. dolabra* sp. nov., *L. savignyii* sp. nov., and *L. pollywoga* sp. nov. These novel taxa were characterized morphologically using microscopy and phylogenetically using small subunit rDNA (SSU rDNA) sequences. The analyses revealed a colourful history of marine gregarines switching hosts between annelid and ascidian hosts. The classification of these new species led to a deep delve into traditional literature whereupon previously undetected taxonomic issues became apparent. To reconcile taxonomy with this improved understanding of evolutionary history, *Lankesteria*, a large, traditional genus of ascidian parasites containing 45 species is combined with *Lecudina*.

The fourth chapter discusses *Platyproteum* sp., a species of parasite found from

a sipunculid host in Hokkaido, Japan. This parasite was originally classified as an apicomplexan until a recent phylogenomic analysis showed that it is instead a species situated deep in the myzozoan phylogeny and diverging from the base of the Apicomplexa, chromerids, and colpodellids. In corroboration of this idea, *P.* sp. was shown to be a biflagellate, similar to other non-apicomplexan myzozoans, and the associated flagellar apparatus was characterized using electron microscopy. A phylogenetic analysis of SSU rDNA sequences was also consistent with the identity of *P.* sp. as a deep branching myzozoan parasite.

Through the discoveries and data included in this dissertation, a small contribution has hopefully been made to address the following: (1) the lack of taxon sampling in apicomplexan biology; (2) improving the understanding of early branching apicomplexans and their relatives; and (3) the addition and emendation of names to help taxonomy better reflect contemporary phylogenetics.

> ...as it seems to me, that man with all his noble qualities, with sympathy which feels for the most debased, with benevolence which extends not only to other men but to the humblest living creature, with his godlike intellect which has penetrated into the movements and constitution of the solar system - with all these exalted powers - Man still bears in his bodily frame the indelible stamp of his lowly origin.
>
> ---
>
> *The Descent of Man*
>
> *Charles Darwin*

Contents

List of Figures

List of Tables

Acknowledgements

I am grateful for all the professional and personal support I have received over the past three years from my mentors, colleagues, friends, and family. I did not, nor could not, have come to this stage of my academic career alone. I will be forever appreciative to the people who stayed by me through various challenges and hardships.

I thank the faculty members and colleagues from the Natural History Sciences department at Hokkaido University for nurturing my growth as a scientist. In particular, I would like to thank my supervisor Dr. Takeo Horiguchi who kindly supported my project and mentored me through this academic experience. He was always an exemplary figure both as an accomplished biologist and as a person. I appreciate having met my advisor Dr. Kevin C. Wakeman without whom I could not have started nor finished my doctoral degree. I am sincerely grateful to Dr. Kazuhiro Kogame who was always willing to offer help in the laboratory and for his constructive feedback on this dissertation. Furthermore, I am deeply thankful to Dr. Hiroshi Kajihara for his help in improving the quality of this dissertation through his many editorial suggestions and for being a philosophically and scientifically inspiring role model. I wish to acknowledge Mr. Fumimasa Sugimoto for all his support in the field and his work managing the Oshoro Marine Station. I am also grateful to the faculty staff and students who were part of my teaching experiences at the university. I discovered a love and passion for teaching that I will no doubt carry with me through what journeys await me next. Special regard goes to the Ministry of Education, Culture, Sports, Science and Technology of Japan who funded the entirety of my doctoral

program.

I owe my deepest gratitude to my friends and family who have always remained supportive and believed in me. There are too many people I am indebted to and I could not possibly list them all here. However, I would like to mention by name my parents, Itsuko and Toshiya Iritani, whose limitless encouragement, advice, and inspiration continues to drive me forward. To my closest colleagues and friends: thank you for all the personal and professional growth you have spurred in me through countless hours of discussions, developing hobbies, and providing unique perspectives. By no means do the following names cover all who were fundamental to my happiness over the past few years, but I would like to leave my sincerest thanks to: Dr. Mahmutjan Dawut, Dr. Alex Pettitt, Dr. Katrina-Kay Alaimo, Dr. Timo van der Zwan, Dr. Tom Czertowicz, Mr. Masakazu Hoshino, Mr. Alexander McKinley, Mr. Genta Azumaya, and Ms. Tomoe Matsuhashi.

Thank you all for standing by me through the best and worst of times.

Naoki Davis Iritani
Sapporo, Japan
18th June 2020

1

Introduction

1.1 Objective

Biology from its inception has, by necessity, been concerned with the study of organisms and how they relate to one another. Even before the universally accepted system of modern taxonomy was pioneered by Carl Linnaeus, people who were well attuned to the natural world noticed similarities among the life forms that surrounded them. For instance, Aristotle is credited for having categorized animals into “blooded” and “bloodless” forms which resemble the modern classifications of vertebrates and invertebrates. Perhaps the desire to categorize the immense biodiversity of the planet into organized, understandable units is human nature or simply inevitable for unravelling the mysteries of the biological world.

Taxonomy, in this regard, is an indispensable practice in biology that works to classify life in a hierarchical framework. Although specific names and ranks have changed continually in unison with an ever-expanding knowledge of taxa, the paradigm of unifying organisms by common characteristics has been consistent. Taxonomy forms the foundation for other avenues of biological research by providing the lexicon for which biological phenomena can be discussed. In other words, taxonomy provides biology with the vocabulary to study the biosphere by organizing life into workable units such as phyla, genera, and species.

The publication of Darwin's "On the Origin of Species" in 1859 shed new light on taxonomy. Until then, the classification of plants and animals was based on similarities and dissimilarities between organisms without the theory of evolution to explain the association between ancestry and shared traits. The history of characteristics shared by taxa as a result of common descent can be elegantly retraced and depicted as a phylogenetic tree. Systematics is the branch of biology that works to understand phylogeny and accurately describe the evolutionary history and diversification of life. Modern taxonomy, to this end, is necessarily tied to systematics in that classification should reflect evolutionary history.

The body of work described in the current dissertation aims to humbly contribute to the biological frontier by adding newly discovered species to the tree of life within a taxonomic framework that reflects their evolutionary history to the best of my ability. The main objectives for this research were to: (1) discover new species from the parasitic phylum Apicomplexa and its close relatives; (2) identify and describe the traits of these new parasitic species; and (3) add resolution to the basal myzozoan phylogeny in the hopes of aiding future research in the field.

1.2 The Apicomplexa

The Apicomplexa is a major phylum of parasitic, unicellular eukaryotes. There are over 6000 named apicomplexans classified in $\sim$350 genera (Adl et al., 2019) and the most

infamous species have devastating impacts on human life. For example, *Plasmodium* is responsible for 228 million cases of malaria per year resulting in 405,000 deaths (WHO, 2019), *Toxoplasma* infects 30% of the global human population (Schlüter et al., 2014) with toxoplasmosis often leading to death or congenital defects in newborns (Flegr et al., 2014), and *Cryptosporidium* manifests as cryptosporidiosis resulting in death and malnutrition for children in developing countries (Checkley et al., 2015). Outside of such well known taxa, however, the Apicomplexa remains largely enigmatic and most species are still undiscovered (Morrison, 2009).

Taxonomically, apicomplexans constitute one of three major lineages within the Alveolata Cavalier-Smith 1991; the other two lineages being the Ciliophora and Dinoflagellata. All three alveolate lineages are unified by the presence of flattened, cortical vesicles beneath the plasma membrane called alveoli (Cavalier-Smith, 2004). These alveolar sacs serve different functions for different taxa. For example, the ciliates store calcium in their alveoli (Plattner and Klauke, 2001) whereas the dinoflagellates fill them with protective thecal plates in an exemplary display of structural modification (Lee and Kugrens, 1992). In contrast, the alveoli in many apicomplexans play a role in the gliding motility used for host invasion (Dubremetz et al., 1998). Despite such shared morphological similarities, the alveolates embrace strikingly different modes of life. Most ciliates are heterotrophic, whereas dinoflagellates can be autotrophic, heterotrophic, or parasitic. The Apicomplexa is unique in that it is comprised entirely of parasitic species.

Apicomplexans are associated with several diagnostic traits. The current criteria include having at least one life cycle stage with flattened subpellicular vesicles, subpellicular microtubules, and an apical complex constituted by a polar ring and secretory organelles including the rhoptries and micronemes (Adl et al., 2019). Sexual reproduction occurs by syngamy and is followed by meiosis to produce haploid progeny. The haploid stages can undergo asexual reproduction by binary fission, endodyogeny, endopolyogeny, or merogony. Motility is achieved by gliding, flexion, longitudinal ridges, and/or cilia. An important structure seen in most apicomplexans, but not all, is a relict red algal plastid

known as the apicoplast. A challenge in identifying the unifying character traits for the Apicomplexa is that the group is speciose and encompasses a diversity of morphological forms across several life stages.

The phylogenetic relationships among apicomplexans are not well resolved and many taxa are still undescribed. Apicomplexans are found distributed across a wide range of habitats and all animals taxa are thought to host at least one apicomplexan species (Morrison, 2009). Perhaps as a result of such immense diversity, taxon sampling has thus far been largely opportunistic and efforts to fill critical gaps in the apicomplexan phylogeny have been limited (Barta, 2001; Morrison, 2009). Most intensive studies of apicomplexans have focused on causative members of medical and veterinary diseases. Consequently, many of the morphological and genetic character traits associated with apicomplexans represent those found by studies where the main focus was treatment or drug development. Such biases in taxon sampling have lead to erroneous phylogenetic conclusions in the past. For example, *Cryptosporidium* was considered to be a sister lineage to the Apicomplexa when evidence arose to indicate that it does not belong with other coccidians (Morrison, 2009). Later phylogenetic analyses included the gregarines, however, and current consensus places *Cryptosporidium* within the gregarines (Adl et al., 2019; Cavalier-Smith, 2014; Ryan et al., 2016). Other major groups included in the Apicomplexa are similarly incomplete in terms of taxon sampling and represent taxonomic utility. Whether these classifications reflect evolutionary history, therefore, is questionable. Apicomplexan species are still continually discovered and the taxonomy continues to change in accordance to this expanding knowledge (Adl et al., 2019, 2012, 2007, 2005).

Molecular phylogenetics has contributed to the increased resolution of apicomplexan relationships. Taxonomically reliable morphological characters are limited among apicomplexans and inferences into the homology of traits, such as cellular surface morphology, is difficult (Morrison, 2009). Molecular data for apicomplexan taxa has been limited, however, in that most phylogenies are based on ribosomal small subunit sequences (SSU rDNA). Therefore, the presently accepted relationships among apicom-

plexan taxa is based on the evolutionary history of the SSU rRNA gene and are not necessarily reflective of species relationships. More robust apicomplexan phylogenies could be built with datasets that include multiple, phylogenetically relevant genes or a combination of morphological and molecular data.

The Apicomplexa remains one of the most poorly understood groups despite its parasitological importance (Morrison, 2009). Further progress toward a resolved apicomplexan phylogeny requires an improved understanding of evolutionary history and taxonomy that accurately reflects this history. Bias in taxon sampling and the lack of character traits are two of the primary obstacles that need to be addressed in order to achieve phylogenetic and taxonomic clarity. To this end, species discovery and fundamental studies on apicomplexan taxa outside of medical studies remain critical.

1.3 Apical complex

The Apicomplexa derives its name from the apical complex: a characteristic collection of structural and secretory components common to the infectious stages of apicomplexan parasites (Katris et al., 2014). The apical complex was first discovered by transmission electron microscopy of *Toxoplasma* (Agar et al., 1954) and consists of a polar ring, rhoptries, micronemes, and dense granules. There is diversity in apical complex morphology within the Apicomplexa and some taxa (e.g., *Toxoplasma*, *Eimeria*, and *Sarcocystis*) possess an additional structure known as the conoid (Morrissette and Sibley, 2002). The presence of the apical complex makes apicomplexan cells highly polarized as many of the organelles essential for parasitism are physically focused around this point. Apicomplexans use the various components of the apical complex to accomplish the various steps involved in host-cell invasion.

The apical complex is structurally supported by a polar ring that acts as a microtubule organizing center (Morrissette and Sibley, 2002). Microtubules extend in an array from the polar ring towards the posterior beneath the inner membrane complex (Katris et al., 2014; Morrissette and Sibley, 2002). The inner membrane complex refers to the

combination of alveoli which are supported on the cytoplasmic side by a network of filamentous proteins (Anderson-White et al., 2011). In taxa that possess a conoid, the conoid protrudes and retracts from within the polar ring (Morrissette and Sibley, 2002). The conoid is built out of tubulin (Swedlow et al., 2002) that spirals counter clockwise and is thought to play a role in physically invading the host cell. The structural scaffolding of the apical complex serves as a focal point for the secretory components — micronemes, rhoptries, and dense granules — that are employed in sequence (Baum et al., 2008).

Micronemes are the smallest of the secretory components that are concentrated at the apical end of the apicomplexan parasite (Gubbels and Duraisingh, 2012). Inside the micronemes are proteins that are released onto the surface of the host cell in preparation for host-cell invasion. One of these proteins secreted from micronemes is the thrombospondin-related adhesive protein (TRAP), first found in malaria, which serves as a crucial ligand that binds to host receptor cells (Tomley and Soldati, 2001). An intracellular motor complex involving myosin motors, anchored to the inner membrane complex, and actin filaments uses these extracellular TRAPs to create a gliding motion for the parasite (Baum et al., 2008). As a result, the microneme grants motility for the apicomplexan parasite on the host cell surface.

Rhoptries are pear-shaped secretory organelles that are attached at one end to the polar ring (Gubbels and Duraisingh, 2012; Morrissette and Sibley, 2002). The rhoptries play a crucial role in the formation of the parasitophorous vacuolar membrane (PVM). Following secretion from the micronemes, the apicomplexan parasite will move into the host cell and reside inside a newly formed PVM (Cesbron-Delauw et al., 2008). The PVM acts as a physical barrier between the parasite and the cytoplasm of the host cell. Having this barrier offers both protection from host defenses and an interface for host–parasite interaction. Rhoptries, therefore, are responsible for creating an intracellular safehouse for the parasite to carry out its functions inside the host cell.

Dense granules are distributed throughout the apicomplexan cell and are continually secreted following host cell invasion (Gubbels and Duraisingh, 2012). The exact

functions and mechanisms by which dense granules play a role in host cell invasion are not clearly known (Mercier et al., 2005). However, there has been suggestion that dense granules are required for making modifications to the host cell as well as having an indispensable role in building the PVM. Further studies on protein and lipid trafficking of apicomplexans are required to better understand how dense granules function in parasite pathogenesis (Mercier et al., 2005).

The apical complex used for parasitism is an innovation for the Apicomplexa, but very similar structures are found in closely related alveolate lineages (Gubbels and Duraisingh, 2012; Leander and Keeling, 2003). For example, colpodellids are alveolates that possess an open conoid and associated rhoptries used for predation (Leander and Keeling, 2003). Moreover, some dinoflagellates feed upon prey cells using an apical structure known as the peduncle which has been suggested to be homologous to the apical complex (Norén et al., 1999; Schnepf and Deichgräber, 1984). As it currently stands, there is still much to be learned about the how the apical complex aids in apicomplexan parasitism. Understanding the evolutionary history of various alveolate feeding strategies would shed light on the transition of apicomplexans from free-living organisms to parasites. Unravelling the mechanisms that underly host-cell invasion, and parasite proliferation is critical to elevating the understanding of apicomplexan pathogenesis (Hu et al., 2006).

1.4 Apicoplast

The evolution of plastids is one of the biggest topics in biology due to the fundamental role that photosynthesis plays in shaping the world (Bhattacharya and Medlin, 1995). The term plastid refers to both the photosynthetically active organelles found in plants and algae as well as the non-photosynthetic, modified versions such as those found in underground plant tissues (Foth and McFadden, 2003). These organelles take on a variety of forms and colours that range from green chloroplasts, bright red rhodoplasts, and golden chromoplasts. A long-standing enigma surrounding the origin of plastids is the observation that while plastids are closely related, their hosts are not (Keeling, 2013). This

seemingly paradoxical fact is a consequence of endosymbiosis and subsequent evolutionary events.

Endosymbiotic theory (Margulis, 1970), supported by an overwhelming body of evidence, suggests that plastids arose by integration of a free-living cyanobacterium inside a heterotrophic eukaryotic host (Bodył et al., 2009a; Cavalier-Smith et al., 2003; Gould et al., 2008). This event, known as primary endosymbiosis, gave rise to the characteristic two-membrane plastids found in glaucophytes, red algae, green algae, and terrestrial plants (Archibald, 2012; Cavalier-Smith, 2000; Palmer, 2003). Molecular phylogenetics of these groups show that the plastid is monophyletic and of a common origin. A second engulfment and permanent integration of green or red algal endosymbionts by other non-photosynthetic eukaryotic lineages is known as secondary endosymbiosis. Plastids formed by secondary endosymbiosis have a total of three or four membranes (Palmer, 2003). Euglenophytes, chlorarachniophytes, chromists, and alveolates possess plastids from secondary endosymbiosis (Archibald, 2012). The exact number of times secondary endosymbiosis has occurred throughout eukaryotic history remains contentious (Bodył, 2005; Keeling, 2013; Palmer, 2003). Some lineages have gone a step further to acquire plastids through tertiary endosymbiosis. For example, the dinoflagellates *Karinia* and *Karlodinium* possess haptophyte endosymbionts (Tengs et al., 2000) and *Kyrptoperidinium* has a diatom endosymbiont (Inagaki et al., 2000). Following engulfment, the endosymbionts became permanent organelles in their hosts over time through a transfer of essential genes from the plastid to the nuclear genome of the host (Bodył et al., 2009a).

The Apicomplexa possess a relict, red algal plastid from secondary endosymbiosis known as the apicoplast (Arisue and Hashimoto, 2015; Foth and McFadden, 2003). The first indications of its presence were early images of circular DNA molecules (McFadden and Yeh, 2016) in *Plasmodium* (Kilejian, 1975) and *Toxoplasma* (Borst et al., 1984). However, because apicomplexans are parasitic and were classified as protozoa at the time, this circular extrachromosomal DNA was thought to represent the mitochondrial genome. This was refuted when a separate molecule encoding for mitochondrial genes was found

(McFadden and Yeh, 2016). Further evidence for the true origins of the apicoplast came from molecular analyses which showed that the circular DNA shared closer ancestry to the plastids of plants than to mitochondria (Gardner et al., 1991). The discovery of an algal organelle in the Apicomplexa had immense implications for parasitology and malarial drug development (Foth and McFadden, 2003).

The apicomplexan endosymbiont is heavily reduced and modified having lost all its nuclear, cytoskeletal, and all photosynthetic functions (Gleeson, 2000) and the thylakoid membranes (McFadden, 2011). The retained features are the genome, stroma, and four bounding membranes. These membranes represent the phagocytotic membrane from the apicomplexan ancestor, the plasma membrane of the red algal endosymbiont, and the two bounding membranes of the original primary plastid. The exact origins of this red algal endosymbiont have been a topic of debate and much controversy.

The chromalveolate hypothesis (Cavalier-Smith, 1999; Cavalier-Smith et al., 2003) suggests that the acquisition of a red algal endosymbiont happened only once to form a monophyletic origin for the chromists (Heterokontophyta, Haptophyta, and Cryptophyta) and Alveolata (Apicomplexa, Perkinsidae, Dinophyta, Ciliata). Therefore, the common ancestor of chromists and alveolates integrated a red alga and formed the Chromalveolates. Many authors, however, have offered counter evidence and refutations to the chromalveolate origin of the chromists and alveolates (e.g., Bodył 2005; Bodył et al. 2009b; Burki et al. 2008; Harper et al. 2005; Keeling 2009).

What function the apicoplast serves for apicomplexans is not well known (McFadden and Yeh, 2016). The general consensus is that the apicoplast is indispensable for the parasites by playing a critical role in metabolism. The apicoplast encompasses a collection of metabolic pathways associated with plastids and the production of molecules essential for the parasite's survival (McFadden, 2011). For instance, the organelle contains genetic information for the synthesis of fatty acids, haem, and isoprenoid precursors (McFadden, 2011; McFadden and Yeh, 2016; Ralph et al., 2004). However, nothing is known to be exported out of the apicoplast (McFadden, 2011). The apicoplast genome

has been carefully scrutinized, but no clear purpose for its existence has ever been found (McFadden and Yeh, 2016; Wilson et al., 1996). Adding to the mystery, apicoplasts have not been found in *Cryptosporidium* (Zhu et al., 2000). Further comprehensive genetic, proteomic, and biochemical studies of apicoplasts from a wider range of apicomplexans as well as closely related relatives is required to more clearly elucidate its function (Sato, 2011).

The apicoplast is essential to the survival of apicomplexan parasites, therefore, is a prime target for anti-apicomplexan drugs. For example, following genetic or pharmacological perturbation of the apicoplast, the parasite undergoes a delayed death whereby it continues to grow, but dies upon infecting a new host-cell (Fichera and Roos, 1997; Ralph et al., 2004). As mentioned previously, most genes found in the apicoplast are associated with the synthetic pathways for fatty acids, haem, and isoprenoid precursors (Ralph et al., 2004). Haem is required for mitochondrial respiration, isoprenoids are needed for mitochondrial ubiquinones, and the fatty acids are likely used to form phospholipids. Furthermore, some of these compounds are likely essential for the host-parasite interface particularly the production of the parasitophorous vacuole (Ralph et al., 2004). As these apicomplexan pathways, with bacterial origins, are significantly different from analogous human pathways, apicoplast targeted drugs could be the answer for the development of antiparasitic drugs with acceptable side effects (Foth and McFadden, 2003; Ralph et al., 2004).

1.5 Aconoidasida Mehlhorn et al. 1980

The Aconoidaidasida Mehlhorn et al. 1980 is one of two currently accepted classes within the Apicomplexa (Adl et al., 2019). This class was formerly known as the Hematozoa Vivier 1982 and includes apicomplexans with the following traits: an apical complex lacking a conoid in asexual motile stages, some diploid motile zygotes with a conoid, macrogametes and microgametes that form independently, and heteroxenous life cycles (Adl et al., 2019). Within the Aconoidasida are the Haemospororida Danilewsky 1885,

Piroplasmorida Wenyon 1926, and Nephromycida Cavalier-Smith 1993, emend. Adl et al. 2019.

1.5.1 Haemospororida Danilewsky 1885

The Haemospororida are generally intraerythrocytic parasites as part of their life cycles and are classified into 12 genera: *Dionisia*, *Haemocystidium*, *Haemoproteus*, *Hepatocystis*, *Leucocytozoon*, *Mesnilium*, *Nycteria*, *Parahaemoproteus*, *Plasmodium*, *Polychromophilus*, *Rayella*, and *Saurocytozoon* (Adl et al., 2019). These taxa are unified by motile zygotes (ookinetes) with a conoid, ciliated microgametes produced by schizogony, and oocysts that contain sporozoites. A large portion of the Haemospororida literature focuses on *Plasmodium* and *Leucocytozoon* due to their widespread medical and veterinary implications.

Plasmodium, the causative agent of malaria, is responsible for 228 million cases of malaria per year resulting in 405,000 deaths (WHO, 2019). This disease is hugely detrimental to global health and the rise in travel and immigration among countries has resulted in more cases of imported malaria than in the past (Trampuz et al., 2003). Furthermore, thousands of travellers from developed countries are thought to contract malaria every year (Kain and Keystone, 1998). Four *Plasmodium* species are known to cause malaria in humans (*P. falciparum*, *P. malariae*, *P. ovale*, and *P. vivax*) and a single person can be co-infected by multiple species (Trampuz et al., 2003). These parasites are mainly transmitted by the *Anopheles* mosquito, but transmission through exposure to infected blood or congenital transmission is also possible.

A bite from a mosquito carrying *Plasmodium* causes sporozoites to enter the host's bloodstream (Trampuz et al., 2003). The sporozoites move from the bloodstream into liver cells where schizogony takes place to produce merozoites. Some species can enter a dormant state (hypnozoite) and remain in the liver before further reproduction. The merozoites eventually leave the liver and develop into trophozoites that infect erythrocytes. These trophozoites become schizonts and produce enough merozoites by schizogony to

lyse the host erythrocyte. The freed merozoites move on to infect new erythrocytes, thus, starting a new cycle of schizogony by autoinfection. Some merozoites will eventually form gametocytes to complete the life cycle back to the mosquito host.

The symptoms associated with malaria are the result of repetitive schizogony and the consequent excessive death of erythrocytes (Trampuz et al., 2003). Interestingly, the incubation period (i.e., the time between sporozoites entering the bloodstream and the development of symptoms) can range from several days to months to even years depending on the species of *Plasmodium*; the longest recorded incubation period is 30 years (White and Cook, 1996). Severe forms of malaria leading to death are almost exclusively caused by *P. falciparum* (Trampuz et al., 2003). The most widely employed treatment for malaria is intravenously administered quinine, but the side effects include hearing loss, blindness, and cardiac arrhythmia in severe cases alongside a multitude of less serious effects (Trampuz et al., 2003).

Another member of the Haemospororida that has received special attention is the genus *Leucocytozoon*. This group consists of species that exclusively parasitize birds across a diverse range of habitats (Freund et al., 2016; Valkiunas, 2005). As with other Aconoidasida, *Leucocytozoon* requires multiple hosts to complete its life cycle, thus involves a vector for transmission (Adl et al., 2019; Freund et al., 2016). The vectors for leucocytozoids are various species of blood-sucking black flies of the family Simuliidae (Freund et al., 2016). The specificity of associations between the host, vector, and *Leucocytozoon* is not well understood. Infection by *Leucocytozoon* can cause symptoms similar to malaria that can be fatal to both domestic and wild avian populations (Freund et al., 2016; Imura et al., 2014; Morii, 1992). Thus, the implications for conservation and economy are quite significant.

Hosts of particular concern are chickens and corvids (Freund et al., 2016; Morii, 1992). *Leucocytozoon caulleryi* is known to cause reduced egg production and thinner egg shells as a direct result of large schizonts spatially occupying the oviduct and compression of associated organs (Nakamura et al., 1997). Corvids, on the other hand, potentially act

as a reservoir for such bloodborne parasites (Kim and Tsuda, 2010; Leclerc et al., 2014). Many corvids have adapted to the continued expansion of cities and have become an important part of the urban ecosystem. The prevalence and diversity of *Leucocytozoon* in corvids is especially high and there is suspicion that bird migrations spread the parasites to new areas (Yoshimura et al., 2014).

The taxonomic history of Haemospororida, as is the pattern for all apicomplexan taxa, is long and complex. The confusion stems in large part from poor taxon and character sampling compounded by past phylogenetic studies that omitted major lineages that were not of medical concern (Galen et al., 2018). As a result, many early hypotheses on character evolution and host transitions were based on incomplete data. Contributing to these challenges is the rarity of these parasite taxa which make comprehensive studies difficult (Galen et al., 2018). To illustrate the long-lasting effects of early, utilitarian taxonomy, it is noteworthy to state that *Plasmodium* was recently shown to be polyphyletic (Galen et al., 2018). This discovery came from molecular phylogenetic analyses that employed a broad range of haemospororidian taxa in contrast to similar studies which are restricted to only a subset of anthropologically important parasites. All analyses recovered phylogenetic relationships that showed that *Plasmodium* is not a monophyletic genus. Galen et al. (2018) offered a solution by suggesting that subgeneric names reflecting evolutionary history be created instead of replacing the genus name *Plasmodium*. This was in light of the resistance that came with an ICZN sanction to change *Plasmodium* to *Laverania* which to many was too dramatic a nomenclatural change for such a model organism. Despite these recent advances, there are still many gaps in the haemospororidian phylogeny including members of *Leucocytozoon*; it is critical that what is already known from morphological studies is compared to recent molecular discoveries and reviewed from this new perspective (Galen et al., 2018).

1.5.2 Piroplasmorida Wenyon 1926

The Piroplasmorida Wenyon 1926 are tick-borne parasites that are mostly known for causing disease in domestic and wild animals (Mans et al., 2015; Uilenberg, 2006; Watts et al., 2016). They are defined as being piriform, round, rod-shaped, or amoeboid with no conoid or cilia in any stage, having a polar ring, and without oocysts (Adl et al., 2019). There are eight accepted genera within the Piroplasmorida: *Anthemosoma*, *Babesia*, *Cytauxzoon*, *Echinozoon*, *Haemohormidium*, *Sauroplasma*, *Serpentoplasma*, and *Theileria* (Adl et al., 2019). *Babesia* and *Theileria* are the best known of the piroplasmids due to their negative veterinary and economic impact.

Babesia was discovered in the late 1800's by Babes when he observed microbes in the red blood cells of cattle (Babes, 1888). Around the same time, a parasite transmitted to cattle by ticks was described from the United States and was called *Pyrosoma bigeminum* (Smith and Kilborne, 1893). The genus name *Pyrosoma* was already in use, however, and the name *Babesia* took its place (Starcovici, 1893). *Babesia* parasites are often pear-shaped following reproduction and have also been named *Piroplasma* or piroplasms to reflect this morphology (Uilenberg, 2006). All members of the genus *Babesia* use ticks as vectors and are transmitted with the saliva of the tick following a bite (Uilenberg, 2006). The sporozoites are injected into the host, and the parasites directly enter host red blood cells upon transmission as is characteristic of *Babesia* species. These sporozoites then develop and multiply into daughter cells that continue to infect new erythrocytes. *Babesia* only reproduces inside host red blood cells, therefore, are not considered *Babesia* taxonomically if schizogony is observed to occur in the vertebrate host (Uilenberg, 2006).

The vector tick is exposed to *Babesia* through ingestion of red blood cells containing "piroplasms," or more specifically, gametocytes (Uilenberg, 2006). Development into male and female gametes takes place inside the gut of the tick and fuse to form motile zygotes (Mehlhorn and Schein, 1985). The zygotes can multiply and transmit vertically by invading organs such as the ovaries. Subsequent to this transovarial transmission, the parasites undergo sporogony in the salivary glands of the vertically infected ticks. The sporo-

zoites mature upon invading the red blood cells of the next vertebrate host. It is within these vertebrate hosts in which *Babesia* species can have debilitating impacts. Common symptoms of acute babesiosis among various hosts include fever, anemia, hemoglobinuria, jaundice, malaise, lethargy, and anorexia (Schnittger et al., 2012).

Babesia infections of domestic animals are of particular concern from an economic perspective. For example, red water fever, also known as bovine babesiosis, is considered to have the most severe economic implications out of all arthropod transmitted diseases of cattle (Schnittger et al., 2012). Significant financial loss stems from mortality, decreased production of meat and milk, as well as the costs associated with control and restriction of infected cattle. Bovine babesiosis was the first disease ever eradicated from the United States owing to a four-decade campaign to exterminate the cattle tick (Schnittger et al., 2012). Millions of dollars were invested into this effort and epidemiological surveillance is ongoing despite the declared eradication of the disease. The estimated savings for the industry, however, are at least three billion dollars per year (Schnittger et al., 2012). Babesiosis is receiving renewed attention as reports of human infections, fatal in some cases, have increased in the past few decades. Furthermore, it is evident that more *Babesia* species than initially thought are able to infect humans (Schnittger et al., 2012). Cattle, rodents, deer, and other animals may play a role in the transmission of *Babesia* to humans by acting as reservoirs of the parasites and their vectors. Other vertebrate taxa that play host to *Babesia* include lions, lynxes, panthers, elephants, giraffes, antelopes, water buffalo, wolves, raccoons, hyaenas, mongooses, rhinoceroses, horses, pigs, various small ruminants, and birds such as seagulls and kiwis (Kjemtrup and Conrad, 2006; Schnittger et al., 2012; Uilenberg, 2006).

The understanding of *Babesia* phylogenetics and diversity is limited due to the heavy bias in the number of studies concerned with controlling the disease for anthropocentric interests. However, *Babesia* has been reported from an immensely diverse range of vertebrate hosts and there are likely many more animal hosts waiting to be discovered (Schnittger et al., 2012). New *Babesia* infections from unexpected host taxa are in fact

continually being discovered (Mans et al., 2015; Schnittger et al., 2012). The taxonomic details of *Babesia* and the number of valid species is uncertain for the time being. Much of this confusion is a consequence on the poor understanding of vector specificity, immunity, and pathogenicity for many *Babesia*–host relationships (Uilenberg, 2006). Furthermore, there are inconsistencies among authors about what criteria must be met to constitute distinct *Babesia* species and taxonomic changes have been slow to permeate the literature. A parasite of horses now called *Theileria equi*, for example, has been in three other genera in the past including *Babesia* (Uilenberg, 2006). Parasitological evidence eventually indicated its correct taxonomic position as a member of *Theileria*, but the name *Babesia equi* is still seen in many publications from later dates.

Theileria sporozoites, in contrast to *Babesia*, infect the leukocytes in the vertebrate host instead of erythrocytes (Mans et al., 2015; Uilenberg, 2006). The sporozoites are released when an infected tick feeds from a vertebrate host. The sporozoites multiply by merogony and the merozoites are released to infect erythrocytes and become gametocysts. A tick feeding from this vertebrate host ingests the gametocysts, zygotes are formed in the gut, and then they divide to create motile kinetes that migrate through the epithelial lining of the digestive tract and ultimately into the salivary glands. Sporogony takes place inside the salivary glands to create multiple sporozoites that are ready to infect a new vertebrate host when the tick begins feeding.

Theileria is transmitted to a variety of domestic and wild animals including cattle, goats, sheep, and buffalo where they can cause economic loss as a result of mortality and decreased production of goods (Bishop et al., 2004). The detection of *Theileria* species in various carrier animals was traditionally described based on observations using light microscopy (Mans et al., 2015). The limitations of diagnosis by light miscopy, paired with a dearth of morphological differences among *Theileria* species, has resulted in many taxa going unnoticed. The use of molecular methods for detection, however, has been shown to be orders of magnitude more sensitive than solely using conventional microscopy (Criado-Fornelio, 2007). As such, there has been an increase in the number of newly discovered

Theileria species and genotypes in the past decade (Mans et al., 2015). These discoveries have also brought with them the realization that *Theileria* infections are more diverse and complex than previously believed including the possibility that domestic animals play host to a multitude of mixed infections.

1.6 Conoidasida Levine 1988

The Conoidasida Levine 1988 is one of two currently accepted classes, the other being Aconoidasida, within the Apicomplexa (Adl et al., 2019). The taxonomic criteria for the Conoidasida are as follows: complete apical complex with a closed conoid in the asexual stages, cilia only found on microgametes, motility generally via gliding, and both homoxenous and heteroxenous life cycles. The two major lineages that fall under these criteria are the Coccidia Lecukart 1879 and the Gregarinasina Dufour 1828. The Conoidasida, however, is comprised of many subtaxa that are classified based on utility and not phylogeny; therefore, this group is not monophyletic and the taxonomic divisions remain open for improvement (Adl et al., 2019).

1.6.1 Coccidia Leuckart 1879

The Coccidia Leuckart 1879 are arguably most infamous for causing toxoplasmosis and coccidiosis. Members of the Coccidia have gametes that mature intracellularly, microgamonts that produce numerous microgametes, no syzygy, generally non-motile zygotes, and sporocysts that form within oocysts (Adl et al., 2019). The two subdivisions of the Coccidia are Adeleorina Léger 1911 and Eimeriorina Léger 1911.

1.6.2 Adeleorina Léger 1911

The biological and phylogenetic understanding of Adeleorina and its constituent taxa is poor (Barta, 1989; Barta et al., 2012). Adeleorinid coccidians infect a broad range of host taxa and many of their descriptions are limited to the gamonts found in the blood cells of

their vertebrate hosts (Siddall, 1995; Smith et al., 2000). Thus, these descriptions omit half of the life cycle in cases where the parasites are heteroxenous. Most of the taxonomic classifications of Adeleorina species are based on morphological characteristics, alterations they make to the host-cell, and host specificity. Furthermore, there is little consensus on what character traits are homoplastic and how much weight to give such traits when discriminating among species (Barta et al., 2012). The addition of molecular phylogenetic data, especially the use of SSU rDNA sequences, has recently brought some resolution to the relationships among subtaxa.

The adeleorinid life cycle is complex with multiple cycles of reproduction involving merogony followed by gametogony, syngamy, and sporogony (Barta et al., 2012). *Hepatozoon* is a genus within the Adeleorina that can infect dogs (Allen et al., 2011; Potter and Macintire, 2010). A typical life cycle first involves the ingestion of *Hepatozoon* oocysts found in the hemocoel of an infected tick (Potter and Macintire, 2010). Sporozoites break free within the small intestine of the dog and are taken up by macrophages. The parasites exploit these macrophages to migrate into skeletal or cardiac muscles and lodge between the muscle fibers. The infected host macrophage secretes multiple, concentric layers of mucopolysaccharide material to produce the characteristic onion skin lesion (Cummings et al., 2005; Panciera et al., 1998); so called due the resemblance to an onion cut in half. Merozoites are released by lysis of the host-cell resulting from multiple rounds of merogony. The rupture of the host-cells triggers a severe inflammatory response. The merozoites can either develop into gamonts inside leukocytes or restart merogonic cycles. A tick feeding from the infected vertebrate host subsequently ingests the *Hepatozoon* gamonts. The gamonts leave the leukocytes once inside the gut of the tick and undergo gametogenesis. Fertilization yields zygotes that divide and form oocysts containing hundreds of sporozoites. The sporozoites will infect the next vertebrate host after the tick is ingested. Fever, muscle pain, and chronic muscle wasting are potential consequences of the innumerable merozoites a single one of these sporozoites can produce (Potter and Macintire, 2010).

There are at least 20 genera classified within Adeleorina (Adl et al., 2019). In addition to *Hepatozoon*, *Adelina* and *Haemogregarina* are also considered major genera (Barta et al., 2012). Members of *Adelina* are generally monoxenous parasites of insects (Kopečná et al., 2006) whereas *Haemogregarina* are heteroxenous parasites of arthropods and vertebrates (Davies et al., 2004). *Haemogregarina bigemina* is a particularly widespread species and has been reported from 96 species of fishes across 70 genera and 34 families (Davies et al., 2004). Whether these parasites truly constitute a single species, however, is highly questionable and Davies et al. (2004) call for the need of a molecular survey of intraspecific genetic differences. The lack of phylogenetic clarity and overall poor understanding of adeleorid biology is especially problematic in regard to the causative agents of veterinary diseases. For example, over 4000 species of *Hepatozoon* have been described of which two are known to cause disease in dogs (Potter and Macintire, 2010). Infection by *Hepatozoon* is incurable (Allen et al., 2011) and can have severe repercussions if not diagnosed and treated swiftly (Potter and Macintire, 2010). Further studies that clarify the host and vector specificity, geographical distribution, and the molecular phylogenetic relationships among Adeleorina genera are needed to further improve the understanding of their biology.

1.6.3 Eimeriorina Léger 1911

The Eimeriorina Léger 1911 consists of 34 genera (Adl et al., 2019), of which, the most well-known are undoubtedly *Toxoplasma* which causes toxoplasmosis and *Eimeria* which causes coccidiosis. Members of the Eimeriorina undergo syzygy and have microgamonts that produce large quantities of ciliated microgametes (Adl et al., 2019). The life cycle can be either homoxenous (Chartier and Paraud, 2012) or heteroxenous (Dubey, 2009). *Toxoplasma*, for instance, is a parasite of cats that uses non-felines including humans as the intermediate host (Dubey, 2009). The life cycle of *Toxoplasma* took over 60 years to complete following its discovery (Dubey, 2009) despite its medical importance, which is indicative of how much remains to be understood about Eimeriorina lineages.

Toxoplasma gondii is found on all continents (Dubey, 2020) and can infect virtually all warm-blooded animals (Robert-Gangneux and Dardé, 2012). Moreover, it is extremely prevalent and one third of the world's human population is estimated to carry a chronic *T. gondii* infection (Schlüter et al., 2014). Transmission to humans occurs though ingestion of undercooked meat containing tissue cysts or through exposure to cat faeces containing oocysts (Dubey, 2020). The parasite uses domestic cats and other felines as the definitive host and sexual reproduction occurs inside the intestinal epithelial cells (Petersen and Dubey, 2001). The infectious forms of *T. gondii* are called the tachyzoite which is a rapidly dividing stage found in tissues, the bradyzoite which is found inside tissue cysts, and the sporozoite which is found inside the oocyst in cat faeces. It is generally believed that the merozoites develop into microgametes and macrogametes found most frequently in the ileum of an infected cat (Petersen and Dubey, 2001). The microgamete is biflagellate and fertilizes a macrogamete inside a host enterocyte. The fertilization initiates the production of a wall which forms around the resulting zygote to create an oocyst. These oocysts are released into the intestinal lumen of the cat when the enterocytes rupture. Sporozoites are contained inside the oocysts which are eventually shed inside the host's faeces. Asexual reproduction by schizogony can occur in the cat host or an intermediate host if the parasites penetrate through the epithelial lining of the intestine and encyst in the tissue. For non-feline hosts, these tachyzoites can spread throughout the body by exploiting macrophages and lymphocytes until the host cells start to lyse as a result of parasite overload. The tissue cysts can lead to autoinfection or infect another warm-blooded host if the tissue is ingested such as in the case of undercooked meat eaten by a human. Infections by *T. gondii* is often asymptomatic for immunocompetent intermediate hosts, but can be fatal for immunocompromised individuals including patients combating AIDS or cancer (Dubey, 2020; Wang et al., 2017).

Coccidiosis is a disease caused by members of the genus *Eimeria*. Its notoriety stems in part from the devastating impact it had on the poultry industry which was only recently mitigated by advances in control, therapy, and vaccination (Chapman, 2014).

Research into *Eimeria* was slow relative to the advances that were made in neighbouring apicomplexan taxa such as *Toxoplasma* and *Plasmodium*. Initial studies were focused on describing the life cycle, morphology, host specificity, pathogenicity, and how to delineate species (Chapman, 2014). The field subsequently benefited from ultrastructural, biochemical, and pathological investigations eventually leading to the discovery of drugs and vaccines. Coccidiosis is also known to occur in small ruminants and can negatively affect production in domestic species (Chartier and Paraud, 2012). The parasites are thought to be strictly host specific and do not transmit between different ruminant species. Infection can cause diarrhea, acute weight loss, and sudden mortality among other symptoms (Chartier and Paraud, 2012; Keeton and Navarre, 2018). Prevention and treatment of coccidiosis mainly relies on maintaining hygienic environments and the use of anticoccidial drugs.

1.7 Gregarinasina Dufour 1828

Gregarines are an understudied group of phylogenetically early diverging apicomplexans within the Conoidasida found in both terrestrial and marine environments (Leander, 2008). They parasitize nearly every large group of invertebrates including annelids (Desportes and Schrével, 2013; Field and Michiels, 2005; Iritani et al., 2017, 2018; Leander, 2007; Rueckert et al., 2010; Simdyanov et al., 2017; Wakeman et al., 2014b), ascidians (Levine, 1981; Mita et al., 2012; Rueckert et al., 2015), and arthropods (Clopton et al., 1992; Criado-Fornelio et al., 2017; Simdyanov et al., 2015). The gregarines are characteristically different from other apicomplexan taxa in having particularly large extracellular feeding stages, known as trophozoites, as part of their monoxenous (single host) life cycles (Leander, 2008). Additionally, gregarine infections occur most commonly in the intestinal lumen of their hosts in contrast to the intracellular parasitism of some other apicomplexan taxa (e.g., *Toxoplasma* and *Plasmodium*; Baum et al. 2008). In special cases, however, gregarines have been observed to infect coelomic spaces (e.g., urosporidians; Leander et al. 2006) or reproductive organs (e.g., *Monocystis agilis*; Field and Michiels

2005). From a phylogenetics standpoint, gregarines are of particular interest due to the plesiomorphic characters that they retain and their implications for understanding early apicomplexan diversification (Leander, 2008).

Many of the character traits described above, such as large trophozoites, monoxeny, and intestinal parasitism are in stark contrast to the more derived members of the Apicomplexa. For example, *Plasmodium falciparum* has similarly sized stages (Bannister et al., 2000) throughtout a dioxenous life cycle that requires an arthropod host, human liver cells, and intracellular parasitism of human erythrocytes (Aikawa, 1971). Sexual reproduction between a haploid female gamete and a haploid male gamete by syzygy is also characteristic of gregarine life cycles (Desportes and Schrével, 2013). Another difference between gregarines and other apicomplexan taxa is observed in the mechanisms involved in feeding from their hosts. Some gregarine taxa are known to attach to host cells extracellularly and steal cytoplasmic content via myzocytosis which is a feeding mechanism observed in some other, non-apicomplexan alveolates (Gubbels and Duraisingh, 2012; Janouškovec et al., 2013; Keeling, 2010; Schrével et al., 2016). Feeding off of host cells by myzocytosis requires use of the apical complex, which in taxa such as *Toxoplasma*, is used mainly for host invasion whereby secretory organelles work in succession so the parasite can gain entry into the cytoplasm of the host cell (Katris et al., 2014). The differences in morphology and parasitic mechanisms between gregarines and other apicomplexan taxa has led to the general understanding that gregarines represent a “primitive” lineage with characteristics that resemble those of the common ancestor of the Apicomplexa (Leander, 2008).

Molecular phylogenetic studies corroborate the idea that gregarines are early branching apicomplexans. However, it has also been shown that certain lineages within the gregarines can be highly divergent, for example, in terms of cytoskeletal morphology (Leander, 2008). Thus, it seems most accurate to consider gregarines plesiomorphic and early branching, but quite complex and divergent in their own right. The earliest branching gregarines, which in turn are the earliest branching apicomplexans, are found from ma-

rine habitats (Leander, 2008). Marine gregarines are regularly detected in environmental sequencing studies (Rueckert et al., 2011b) and have also been found from the deep sea (Wakeman et al., 2017). The high prevalence and wide distribution of marine gregarines are reflective of their descent from a free-living, marine ancestor.

The wide geographical distribution of gregarine species across both terrestrial and marine environments is indicative of the immense diversity of gregarine species, but most remain undiscovered (Leander, 2008; Levine, 1976, 1971). The taxonomic gaps left by a lack of taxon sampling have led to poor phylogenetic resolution and there is still much ongoing discussion about the relationships among gregarine taxa (e.g., chapter 3 of this dissertation; Mathur et al. 2019; Morrison 2009; Simdyanov et al. 2017). To further compound these phylogenetic challenges, the formal taxonomic descriptions that do exist are often scattered across journals, some obscured by time, in various languages (e.g., Bogolepova 1953; Grassé 1953; Mingazzini 1891; Ormières 1965; Simdyanov 1996). Moreover, early descriptions of gregarine taxa were limited to non-ultrastructural morphological observation and distinguishing among species relied heavily on comparing line drawings (e.g., Levine 1981, 1977, 1971). Gregarine morphology, at the best of times, can be taxonomically uninformative due to the challenge of identifying the range of variation of a given morphological trait without first knowing the degree of intraspecific morphological plasticity. Some studies have offered insight into the use of morphology in gregarine taxonomy and systematics (Clopton, 2004; Rueckert et al., 2011b), but authors still disagree whether certain morphological characters are the result of inheritance by evolutionary descent (Simdyanov et al., 2017) or convergence (Wakeman et al., 2014a,b). It is now becoming evident that gregarines are a necessary piece to understanding the Apicomplexa as a whole (Boisard and Florent, 2020; Morrison, 2009; Ryan et al., 2016). A greater sample of taxa is needed to address the dearth of described gregarine species and to identify synapomorphic traits that unify each major gregarine lineage.

Despite the challenges, current apicomplexan taxonomists have settled on four major groups of gregarines (Adl et al., 2019): Archigregarinorida Grassé 1953, Eugregari-

norida Léger 1900, Neogregarinorida Grassé 1953, and Cryptogregarinorida Cavalier-Smith 2014, emend. Adl et al. 2019. These lineages encompass a variety of hosts, morphologies, and parasitic strategies. Furthermore, whether these groups have reliable diagnostic characteristics that allow one species to be conclusively distinguished from another remains to be seen. Gregarine taxonomy is updated in regular intervals, but the deepest relationships still remain unresolved (Adl et al., 2019, 2012, 2007). The continued discovery of gregarine species and the construction of a taxonomic framework that accurately reflects phylogeny is undoubtedly one of the pre-requisites for further elucidation of the apicomplexan enigma.

1.7.1 Archigregarinorida Grassé 1953

The gregarines were traditionally classified into two groups based on whether schizogony was part of their life cycle (Levine, 1971). Taxa with schizogony were called the Schizogregarinidia and taxa without schizogony were called the Eugregarinida. It is important to note that schizogony is a general term that refers to asexual reproduction by multiple fission. Asexual reproduction of gametes (gametogony), sporozoites (sporogony), and trophozoites (merogony) are all types of schizogony. Some authors, however, use schizogony interchangeably with merogony. Grassé (1953) recognized that within the Schizogregarinidia was a mixture of taxa with considerable differences. He offered a solution by establishing two further taxonomic divisions and created the orders Archigregarina and Neogregarina. The Archigregarina consisted of species with merogony that infect annelids, hemichordates, and primitive chordates. In contrast, the Neogregarina consisted of species with merogony that infect insects. Moreover, it was said that the Neogregarina arose from septate eugregarines and that their merogony is a secondary acquisition (Grassé, 1953). *Selenidium* was selected as the type genus for Archigregarina and *Ophyrocystis* as the type genus for Neogregarina.

Much of what is currently known about archigregarines is based on *Selenidium* Giard 1884 from the family Selenidiidae Brasil 1907 (Desportes and Schrével, 2013).

The type species *Selenidium pendula* is a crescent-shaped gregarine discovered from the intestine of *Scolelepis squamata* (formerly *Nerine ciratulus*) and was named for its pendular movement (Giard, 1884). The early histological work from the 1900's (e.g., Brasil 1907; Caullery and Mesnil 1901, 1900; Ray 1930) and the subsequent ultrastructural and molecular work from the 1960's to the present (e.g., Leander 2007; Rueckert and Leander 2009; Vivier and Schrével 1966, 1964; Wakeman and Leander 2012) has made considerable contributions to the overall understanding of archigregarines. Initial observations of *Selenidium*, isolated from the intestine of a polychaete worm, noted that the trophozoites were flat and motile (Léger, 1892). Thus, the name *Platycystis* was proposed. *Selenidium* was proposed several years later to encompass archigregarines with pendular or nematode-like motility (Caullery and Mesnil, 1899) which was markedly distinct from the usual gliding motility observed in eugregarines (Desportes and Schrével, 2013). It is now accepted that *Selenidium* species can also move by rolling, twisting, and euglenoid metaboly-like movements (Desportes and Schrével, 2013). Certain aspects of defining *Selenidium*, however, have been taxonomically problematic.

Grassé, and authors before him, had recognized that merogony is not a universally observed trait among *Selenidium* speices (Levine, 1971); extensive histological study of *Selenidium* found in *Scololepis fuliginosa*, for example, failed to recover evidence for merogony despite high abundance of trophozoites (Mackinnon and Ray, 1933). Although the lack of evidence is not evidence for the absence of merogony, it is likely that merogony has been abandoned by members of the genus (Levine, 1971). The diagnosis for the archigregarines, therefore, was emended to omit all mention of merogony (Schrével, 1971). As a result, the new criteria for archigregarines was limited to trophozoites that are morphologically similar to sporozoites, have a well-defined pellicular fibrillar system, and parasitize the intestinal tract of polychaetes. Levine (1971) heavily disputed this change by arguing that these criteria are insufficient for distinguishing between orders. He additionally argued that without more comprehensive knowledge, it is difficult to conclude that all archigregarine species have trophozoites that are similar to the sporozoite

stage. Similarly, it is equally difficult to say that eugregarine trophozoites are always considerably different from their sporozoite stages. Levine (1971) was also in disagreement with using the presence of a subpellicular fibrillar system as a diagnostic trait for archigregarines because this does not distinguish them from the eugregarines. The solution for these taxonomic challenges offered by Levine (1971) was to split *Selenidium* into a new genus with merogony and a new genus without merogony. Moreover, he argued that the definition for archigregarines should include schizogony. The presently accepted diagnostics for archigregarines are as follows: aseptate trophozoites, sexual reproduction by syzygy, encystment of gamonts, and oocysts that contain between four to eight, or more, sporozoites (Adl et al., 2019). Evidently, schizogony is no longer considered a trait for the archigregarines as a whole.

In addition to *Selenidium*, there are several other archigregarine genera including *Filipodium*, *Merogregarina*, *Meroselenidium*, *Platyproteum*, *Selenocystis*, *Veloxidium* (Adl et al., 2019). The hosts for these parasites are mostly Sedentaria polychaetes, but also include sipunculids and hemichordates. It has further been observed that no archigregarines have thus far been found from Errantia polychaetes in direct contrast to the eugregarines which are prevalent in them (Desportes and Schrével, 2013). The most primitive genus is thought to be *Selenidium* with polychaetes perhaps representing the first hosts to be parasitized by the earliest gregarine (Levine, 1971) . Further speculation suggests that *Selenidium* gave rise to the eugregarines and that the eugregarines in turn gave rise to the neogregarines. With the accumulation of molecular data, unravelling the co-evolutionary history between polychaetes and archigregarines is an avenue of research well worth pursuing (Desportes and Schrével, 2013).

1.7.2 Eugregarinorida Léger 1900

The Eugregarinorida Léger 1900 is the largest gregarine group and consequently represents the majority of known marine gregarine taxa (Adl et al., 2019; Levine, 1976). Taxonomically, they are defined as gregarines in which the trophozoite has an epimerite or

mucron depending on the presence or absence of an internal septum, syzygy followed by the encystment of gamonts, and oocysts that contain eight sporozoites (Adl et al., 2019). This aforementioned septum is used to further classify the eugregarines into one of two suborders: Aseptatorina Charkravarty, 1960 and Septatorina Lankester, 1885.

The aseptate eugregarines (also monocystid or acephaline) are so called due to their lack of an internal division that would otherwise separate their trophozoite stage into three distinct compartments (Desportes and Schrével, 2013). Instead, aseptate trophozoites possess a mucron or epimerite at the anterior end of the cell. The mucron is thought to allow the gregarine trophozoite to feed from host cells by myzocytosis in contrast to the epimerite which involves appendages that help the parasite insert deep into the host cell (Desportes and Schrével, 2013). The septate gregarines are suggested to be particularly abundant in marine annelid hosts and there are an estimated 100 genera containing one to two thousand species if not more (Desportes and Schrével, 2013).

The septate eugregarines (also polycystid or cephaline) refer to those with trophozoites that are divided by a septum, observable under light microscopy, into three distinct compartments: the epimerite, the protomerite, and the deutomerite. The nucleus is always found in the deutomerite (Desportes and Schrével, 2013). In some cases, there are species considered to be intermediates between aseptate and septate forms that are known as dicystid gregarines. These species display a clear distinction between an ectoplasmic area and a deutomerite. In general, however, the septum is a morphological character identified for utility and offer little actual taxonomic merit in terms of reflecting phylogeny (Desportes and Schrével, 2013). For example, it has been shown that in the superfamily Cephaloidophoridae, which contains the Ganymedidae, Uradiophoridae, Porosporidae and Cephaloidophoridae as subclades, both septate and aseptate species are found. Therefore, the Aseptatorina and Septatorina represent morphological suborders that do not reflect phylogeny. The bulk of septate eugregarines have been found from arthropod hosts and the group is thought to contain more than 150 genera.

Eugregarines are found as parasites to a plethora of invertebrate host taxa. The an-

nelids, for instance, are heavily parasitized by marine gregarines in general. Interestingly, the Sedentaria polychaetes and sipunculids play host to archigregarines whereas the Errantia infections are restricted to eugregarines (Desportes and Schrével, 2013). *Lecudina* Mingazinni 1891 is a genus of eugregarines consisting of about 40 species that parasitize a variety of polychaete hosts (Levine, 1976). In crustaceans, six families of gregarines have been identified: Cephaloidophoridae, Cephalolobidae, Ganymedidae, Porosporidae, Uradiophoridae, and Thiriotiidae. The eugregarines from these families are reported from a variety of environments including both freshwater and marine habitats. *Lankesteria* Mingazinni 1891 is a major genus of gregarines that infect ascidian hosts. The genus *Lankesteria* was originally a collection of gregarines isolated from various hosts including marine urochordates and terrestrial insects. Grassé (1953) removed the insect gregarines from *Lankesteria* and established *Ascocystis* while Ormières (1965) retained *Lankesteria* as a genus name for only the urochordate parasites. The validity of *Lankesteria* and its evolutionary relationship to *Lecudina* is discussed in detail in Chapter 3 of the current dissertation. The diversity of eugregarines is likely much greater than what is currently described especially when considering the high diversity of the animal groups they parasitize (Desportes and Schrével, 2013).

Monophyly has been suggested for the eugregarines along with a set of common characteristics that were offered to unify the clade (Simdyanov et al., 2017). These character traits include the epimerite, epicytic crests, and gliding motility. In direct contrast, studies by other authors suggest that the wide range of morphological forms among eugregarines are a consequence of convergent evolution from ancestral, archigregarine lineages that have given rise to independent lineages of gregarines with superficial similarities (Wakeman and Leander, 2012; Wakeman et al., 2014b,a). These disagreements in the higher-level classification of gregarines is largely due to the difficulty in identifying morphological characters that can be used to reliably infer evolutionary history. In other words, traits such as gliding motility, epimerites, and the submembrane architecture of surface folds are not clearly resolved on any molecular dataset and these traits

can be extraordinarily plastic even among seemingly closely related taxa (Rueckert et al., 2013; Simdyanov et al., 2017; Wakeman and Leander, 2012; Wakeman et al., 2014a,b). The phylogenetic distribution of such character traits sheds doubts on the validity of eugregarines as a taxonomic group. Better taxon sampling and subsequent construction of datasets that detail the range of morphological forms and molecular diversity found among eugregarine taxa is necessary to resolve eugregarine relationships. The discovery of new subclades and integration of molecular data with morphological data has, indeed, already contributed to progress towards a better understanding of eugregarine phylogenetics (Rueckert et al., 2013, 2010).

1.7.3 Neogregarinorida Grassé 1953

The neogreagrines are one of two groups, the other being the archigregarines, that emerged as a subdivision of the traditional Schizogregarinida Léger 1900 (Levine, 1971). All gregarines were formerly classified on the basis of having merogony (Schizogregarinida) or not having merogony (Eugregarinida) as part of their life cycle. Grassé (1953) recognized a taxonomic problem with this simplistic classification, however, because the Schizogregarinida embraced gregarines of vastly differing characteristics. As a solution, he separated the Schizogregarinida into the Archigregarina and Neogregarina. The neogregarines are all parasites of terrestrial invertebrates.

The currently accepted taxonomic criteria for the Neogregarinorida Grassé 1953 are the following: trophozoites with an epimerite or mucron, multiple rounds of schizogony/merogony, pairing of gamonts, and oocysts that contain eight sporozoites (Adl et al., 2019). Sixteen genera are recognized, and their constituent species infect a range of terrestrial hosts. There are five aseptate families and one septate family found in insects (Desportes and Schrével, 2013). These neogregarine families are known as the Caulleryellidae, Gigaductidae, Lipotrophidae, Ophryocystidae, Schizocystidae, and Syncystidae. Arachnids and myriapods are also infected by neogregarines of the family Lipotrophidae. Gregarine infections in insects have been observed to adversely affect host development,

survival, and fecundity (Altizer and Oberhauser, 1999; Cowley, 1989; Jouvenaz and Anthony, 1979; Münster-Swendsen, 1991; Zuk, 1987a,b).

The schizogony observed in neogregarines is secondarily acquired whereas the schizogony observed in archigregarines is thought to be a primitive form retained from their ancestor (Desportes and Schrével, 2013; Grassé, 1953). Furthermore, the occurrence of schizogony in the septate family Gigaductidae provides evidence for neogregarines having diverged from within the eugregarines (Desportes and Schrével, 2013). Sexual reproduction is modified in some neogregarine species, *Coelogregarine ephestiae* for example, and involves gamonts pairing without the production of gametes. Interestingly, the gamonts fuse to form a zygote which then becomes a spore; this is in contrast to other gregarine species which undergo gametogony to produce countless gametes that then fuse to form multiple zygotes. The reduction of sexual stages in neogregarines is thought to be due to the small gamont size resulting from the limitation of space in the narrow tissues of insects (e.g., haemocoel, fat body, Malpighian tubules; Desportes and Schrével 2013). Sporogony, on the other hand, is similar to that of the eugregarines whereby eight sporozoites are produced in each oocyst. These oocysts are orally ingested by the next host, the sporozoites break free inside the intestinal lumen, and migrate into the haemocoel through the intestinal wall (Desportes and Schrével, 2013). There are no known cases of autoinfection by neogregarines (Clopton et al., 1992).

The higher level taxonomic relationships among the gregarines remain unstable and the neogregarines are no exception (Devetak et al., 2019). Following a molecular study of eugregarines and their SSU rDNA sequences, the neogregarines were incorporated into the eugregarines (Simdyanov et al., 2017). However, the most recent taxonomic synthesis of eukaryotic groups retains the Neogregarinorida as a distinct group (Adl et al., 2019). The disagreement is in large part due to the poor understanding of the actual diversity of neogregarines which naturally translates to a poor understanding of phylogenetics. For example, the diversity and distribution of gregarines in Europe remain largely unknown and the first report of a myriapod gregarine from Slovenia was only made in the previous

year (Devetak et al., 2019). Additionally, some studies have observed that neogregarine parasitism in important agricultural pests has implications for bio-control (Kumano et al., 2010). The sweet potato weevil is considered a major pest and has been introduced to some islands in Japan. Kumano et al. (2010) report that the presence of neogregarines reduces both longevity and fecundity of these pests. Therefore, the potential merit of continuing the search for neogregarines is not only for taxonomy, but perhaps for practical applications as well. The insects, as speciose as they are, likely play host to many more neogregarine parasites waiting to be discovered.

1.7.4 Cryptogregarinorida Cavalier-Smith 2014, emend. Adl et al. 2019

Cryptosporidium was first discovered from laboratory mice in 1907 (Tyzzer, 1907). The parasite was not known at the time to have any significant economic or medical implications (Levine, 1984). Several decades following its initial description, *Cryptosporidium* rapidly gained infamy as it was found to infect young cattle and humans with debilitating effects. Further focused medical attention and widespread recognition came after initial reports were published of *Cryptosporidium*-related deaths in immunocompromised patients such as those with AIDS (Current et al., 1983). *Cryptosporidium* is now recognized as the culprit responsible for most of the parasitic, gastrointestinal infections worldwide (Doganci et al., 2002).

In mammals, *Cryptosporidium* has only been found from the gastrointestinal tract, although it has been observed in the respiratory tract of birds (Levine, 1984). The infection occurs between the host cell cytoplasm and plasma membrane which is a distinguishing characteristic among other enteric parasites (Ramirez et al., 2004). These infections cause self-limited diarrhea in immunocompetent people and can be severely detrimental for those who are malnourished or immunocompromised (Cacciò, 2005; Checkley et al., 2015). The largest outbreak of *Cryptosporidium* occurred in 1993 in Milwaukee, USA where 403,000 people were infected (MacKenzie, 1994) leading to $96.2 million in eco-

nomic damage from a combination of medical expenses and reduced productivity (Corso et al., 2003). Although the number of reported *Cryptosporidium* cases from developing countries has increased over the years (Craun et al., 2005), diagnosis is not routine and mostly limited to immunodeficient people. Therefore, the real number of global cases is likely underreported (Ramirez et al., 2004).

Cryptosporidium is waterborne and commonly spreads via contaminated water (Sunnotel et al., 2006) where the oocysts can remain viable for months (Fayer et al., 1998). A single one of these oocysts can be enough to begin infection (Pereira et al., 2002). Transmission can also occur through direct contact via the fecal-oral route, food handled by infected people, accidental zoonotic transmission, and even aerosol transmission (Ramirez et al., 2004). Most domestic animals and a wide range of wild animals can play host to *Cryptosporidium* with repercussions similar to humans; the young are more susceptible and infections cause diarrhea that leads to dehydration and weight loss (Ramirez et al., 2004). *Cryptosporidium* cannot be destroyed by the conventional use of chlorine, but is vulnerable to treatment by ozone, UV, and ultrafiltration (Betancourt and Rose, 2004; Sunnotel et al., 2006).

The *Cryptosporidium* life cycle takes place within the gastrointestinal tract of the host. Following ingestion, the oocysts release sporozoites which infect the epithelium of the intestinal wall inside host and develop into trophozoites (Centers for Disease Control and Prevention, 2015). There are two generations of meronts, the first of which contain eight merozoites each, and the second of which contain four merozoites each (Centers for Disease Control and Prevention, 2015; Levine, 1984). The first generation merozoites are capable of merogony in some species (Ryan et al., 2016). The second generation merozoites develop into micro- and macrogamonts that fuse to form a zygote. The zygote then develops into either a thin-walled oocyst that excysts endogenously causing autoinfection or into a thick-walled oocyst that exits the host (Ramirez et al., 2004). Oocysts contain four sporozoites, are spherical, and range between 2 – 5 μm in diameter (Levine, 1984). The time between host infection and oocyst shedding can be between one to three weeks,

and the shedding itself can last days, months, or even years (O'Donoghue, 1995).

Cryptosporidium has undergone numerous taxonomic changes since it was first seen by Tyzzer. Immediately following its discovery, *Cryptosporidium* was given its own family Cryptosporidiidae Léger 1911 among other coccidians within the Apicomplexa (Levine, 1984; O'Donoghue, 1995). *Cryptosporidium* was initially thought to be highly host-specific and new species were assigned as they were discovered from different hosts (Levine, 1984). However, it became apparent that these parasites, especially *C. parvum*, are generalists and that mammalian species can infect multiple different hosts (Levine, 1984; Ramirez et al., 2004). After evidence suggesting that *Cryptosporidium* does not belong with other coccidians began to accumulate, it was taken out of the Apicomplexa entirely, and given its own place as the sister taxon to the Apicomplexa (Morrison, 2009). Current taxonomic consensus has *Cryptosporidium* back amongst other apicomplexans as a member of the Gregarinasina and represents the only genus within the Cryptogregarinorida Cavalier-Smith 2014 emend. Adl et al. 2019 (Adl et al., 2019).

The characterization and detection of *Cryptosporidium* still relies heavily on morphological observation under the microscope outside of specific research settings (Sunnotel et al., 2006). Furthermore, analysis of clinical and environmental samples depends on numerous factors including the availability of equipment, which can be limited in developing countries. Genetic detection of *Cryptosporidium* mainly targets the SSU rDNA due to the availability of comparable data, high copy number, and its ability to distinguish among *Cryptosporidium* species (Sunnotel et al., 2006). The most effective treatments for *Cryptosporidium* infection are unavailable in some developing countries and an improved understanding of parasite metabolism, gene expression, and host–parasite interaction is required to lower the number of cryptosporidiosis cases (Smith et al., 2005; Sunnotel et al., 2006).

2

Marine Gregarines *Cuspisella ishikariensis* gen. nov., sp. nov. and *Loxomorpha* cf. *harmothoe* from Western Pacific Scaleworms (Polynoidae)

2.1 Abstract

Marine gregarines are unicellular parasites of invertebrates commonly found infecting the intestine and coelomic spaces of their hosts. Diverging from the base of the api-

complexan tree, marine gregarines offer an opportunity to explore the earliest stages of apicomplexan evolution. Classification of marine gregarines is often based on the morphological traits of the conspicuous feeding stages (trophozoites) in combination with host identity and molecular phylogenetic data. Morphological characters of other life stages such as the spore are also used to inform taxonomy when such stages can be found. The reconstruction of gregarine evolutionary history is challenging, due to high levels of intraspecific variation of morphological characters combined with relatively few traits that are taxonomically unambiguous. The current study combined morphological data with a phylogenetic analysis of small subunit rDNA sequences to describe and establish a new genus and species (*Cuspisella ishikariensis* gen. nov., sp. nov.) of marine gregarine isolated from the intestine of a polynoid host (*Lepidonotus helotypus* Grube 1877) collected from Hokkaido, Japan. This new species possesses a set of unusual morphological traits including a spiked attachment apparatus and sits on a long branch on the molecular phylogeny. Furthermore, this study establishes a molecular phylogenetic position for *Loxomorpha* cf. *harmothoe*, a previously described marine gregarine, and reveals a new group of gregarines that infect polynoid hosts.

2.2 Introduction

Gregarines are a group of understudied parasites that inhabit the digestive tracts and coelomic spaces of various invertebrate hosts. Marine gregarines are especially of interest due to their early divergence in the apicomplexan tree. These lineages have retained plesiomorphic traits from the origin of the Apicomplexa and many extant species display key characteristics including monoxeny, conspicuous feeding stages, and myzocytosis (Leander, 2008). Furthermore, marine gregarines are highly prevalent throughout the ocean, but most species remain undiscovered or are ambiguously represented in molecular datasets as environmental sequences (Leander, 2008; Rueckert et al., 2011a; Sitnikova and Shirokaya, 2013). Thus, one of the primary tasks in this field is to explore the poorly understood diversity of gregarines and reconcile their taxonomy with molecular phylogenetic

data. These efforts, however, are often stifled by high levels of morphological variability, convergence onto similar morphologies, and molecular datasets that are unresolved due to quickly evolving regions along the ribosomal operon (Leander, 2008; Rueckert et al., 2010, 2011b; Wakeman and Leander, 2012, 2013b).

Gregarines are mainly characterized through a combination of morphological, life history, and small subunit rDNA (SSU rDNA) data. For instance, the gregarine life cycle involves a conspicuous feeding stage known as the trophozoite which has numerous taxonomic characters including the arrangement of cortical microtubules, attachment apparatuses, overall shape, and in some cases the capacity for asexual reproduction known as merogony (e.g., Leander et al. 2006; Rueckert et al. 2013; Schrével et al. 2016; Simdyanov et al. 2017; Wakeman and Leander 2012, 2013a). Marine gregarine systematics is concerned mainly with this trophozoite stage as other life cycle stages are difficult to find in the ocean in contrast to terrestrial gregarine systematics where oocysts and infectious stages are more commonly found. The host species and host compartment are also used for species delimitation. Gregarine infections have been mainly documented from the intestinal lumen of invertebrate hosts (e.g., Desportes and Schrével 2013; Levine 1977; Rueckert et al. 2015; Schilder and Marden 2006; Wakeman and Leander 2013b; Zuk 1987a), but some gregarines infect coelomic spaces (e.g., urosporidians; Leander et al. 2006) and reproductive tracts (e.g., *Monocystis agilis*; Field and Michiels 2005) as well. The character traits mentioned above have been used to broadly classify the gregarines into three major groups: the archigregarines, eugregarines, and neogregarines (Adl et al., 2012; Grassé, 1953; Leander, 2008). The validity of each of these broad groupings is currently in question, with the continual discovery of new taxa and in the light of ever expanding SSU rDNA phylogenies.

Eugregarines (Eugregarinorida Léger 1900) encompass most marine gregarine taxa, but the relationships and basic classifications within the group remain poorly defined and somewhat contentious. Simdyanov et al. (2017) recently established a set of characters to define all eugregarines as a monophyletic group which includes the epimerite,

epicytic crests, and gliding motility. On the other hand, other work has suggested that the varying forms among eugregarines are a consequence of convergent evolution from ancestral (archigregarine) lineages that have given rise independently to gregarines that are superficially similar (Wakeman and Leander, 2012; Wakeman et al., 2014a,b). Discrepancies in higher level classification of gregarines are largely due to the difficulty in finding morphological characters that can be used to reliably infer evolutionary history. Evolutionary traits such as gliding motility, epimerites, and the submembrane architecture of surface folds are not clearly resolved on any molecular dataset and these traits tend to vary extensively even among seemingly closely related individuals (Rueckert et al., 2013; Simdyanov et al., 2017; Wakeman and Leander, 2012; Wakeman et al., 2014a,b). The distribution of these types of traits causes uncertainty in the integrity of the eugregarines as a valid grouping and will require more comprehensive datasets detailing novel morphological forms and molecular diversity to fully resolve eugregarine systematics. The discovery of new subclades and comprehensive characterization of new species through integration of SSU rDNA data with morphological data, however, have contributed to progress towards a better understanding of eugregarine evolution (Rueckert et al., 2010, 2013).

In the present study, I describe a new species of aseptate marine eugregarine with a spiky attachment apparatus and apparent gigantism discovered from a scaleworm host in Japan. This new species possesses several uncommon morphological traits and is recovered on a divergent branch in a phylogenetic analysis of SSU rDNA sequences. A new genus was established to accommodate the new species based on host identity, comparative trophozoite morphology, and SSU rDNA phylogenetic analysis. Furthermore, I present and analyse the SSU rDNA from *Loxomorpha* cf. *harmothoe*, a previously described marine gregarine (Hoshide, 1988; Simdyanov, 1996) also from a scaleworm host. This study is the first to sequence *Loxomorpha* cf. *harmothoe* and provide a molecular phylogenetic context for the scaleworm gregarines. The discovery of the new species and its unique morphology additionally helps to highlight some of the challenges associ-

ated with incorporating morphology to inform gregarine systematics and the usefulness of molecular data in this endeavour.

2.3 Methods

2.3.1 Collection of host material and isolation of gregarine trophozoites

The annelid hosts *Lepidonotus helotypus* Grube 1877 and *Harmothoe imbricata* Linnaeus 1767 were collected on 14 April 2017 from the rocky intertidal of Ishikari Bay, Hokkaido, Japan (43°13′35.0″N 141°0′58.3″E). The geography consists of a relatively sheltered bay with large, loose rocks scattered throughout the intertidal zone among patches of brown macroalgae. The hosts were collected by hand from the underside of rocks and were dissected on the same day.

Gregarine trophozoites were found in the intestine of the host worms using an Olympus CK40 (Olympus Corp. Tokyo, Japan) inverted microscope. Each individual worm was placed in a Petri dish filled with filtered seawater and split longitudinally with fine forceps. The intestine was then extracted and torn open to spill the gut contents and gregarine trophozoites were located among food particles and digestive debris. Hand-drawn glass pipettes were used for individual cell isolations. Each trophozoite was washed three times with filtered seawater in a well slide before each was placed in its own 0.2 ml PCR tubes for subsequent SSU rDNA analysis. The remaining trophozoites were set aside for light microscopy (LM), scanning electron microscopy (SEM), and transmission electron microscopy (TEM).

2.3.2 Light microscopy

Trophozoite morphology was initially observed in differential interference contrast (DIC) with a Zeiss Axioskop 2 Plus microscope (Carl-Zeiss, Göttingen, Germany) paired to a Leica MC120 HD colour camera (Leica, Wetzlar, Germany). Light micrographs were

edited with Adobe Photoshop 11.

2.3.3 Scanning electron microscopy

Cuspisella ishikariensis gen. nov., sp. nov. trophozoites were isolated from *Lepidonotus helotypus*. Trophozoites from the hosts were pooled and fixed for SEM using 24-well tissue culture plates and plastic capsules to hold and move the trophozoites between fixation steps. The bases of 1.000 µl pipette tips were cut from the tapered ends, creating a hollow cylinder, and a 50 µl mesh was added to cover one of the open ends. The customized capsules were submerged in the wells of the tissue culture plates filled with 2.5% glutaraldehyde. Trophozoites were transferred to these capsules using hand-drawn glass pipettes. The trophozoites were left to be fixed in the glutaraldehyde for 30 min on ice. Each capsule holding the trophozoites was then moved to an adjacent well and was rinsed with filtered, chilled seawater and left to soak for 5 min. The capsules were moved to the next well filled with 1% OsO_4 and left to be soaked for 30 min on ice. Each capsule was rinsed and soaked again with filtered, chilled seawater. The trophozoites were then dehydrated in serial dilutions of ethanol by submerging the capsules for three minutes at 50%, 70%, 80%, 90%, and 100% dilutions. Following the ethanol baths, the capsules were placed in a Hitachi HCP-2 815B critical point dryer (Nissei Sangyo America, Ltd., Pleasanton, CA, USA). The mesh was then carefully peeled from the pipette tips and attached to SEM stubs using double-sided tape. Each stub was sputter coated with gold for 180 s at 15 µA. Scanning electron micrographs were taken on a Hitachi S3000N scanning electron microscope and edited with Adobe Photoshop 11.

2.3.4 Transmission electron microscopy

Trophozoites were fixed for TEM using plastic capsules like those described for the SEM fixations. The bases of 1,000 µl pipette tips were cut and one end was covered with a small piece of plastic projector transparency. The plastic capsules were then filled with filtered, chilled 2.5% glutaraldehyde. Several trophozoites were transferred from the host

dissections to each capsule with hand-drawn glass pipettes. The trophozoites were left to fix in 2.5% glutaraldehyde for 30 min on ice. The glutaraldehyde was removed with three filtered seawater washes from the capsules with 5-min soaks between each wash. Following the washes, the cells were left to soak in 4% OsO_4 for 1.5 h on ice, in the dark. The OsO_4 was removed with three seawater washes with 5-min soaks in between each wash. The trophozoites were dehydrated in serial dilutions of ethanol for 5 min at 80%, 90%, and 100%. The ethanol was replaced with a 1:1 mixture of 100% ethanol and 100% acetone for five minutes. Cells were then left to soak in 100% acetone for three minutes. This was then replaced with a 1:1 mixture of 100% acetone and resin for 30 min. Subsequently, 100% resin was added to the capsule for 12 h. The resin was replaced with fresh resin and incubated at 65 °C to polymerize. All transmission electron micrographs were taken on a Hitachi H-7650.

2.3.5 DNA extraction, amplification, and sequencing

For each species, seven trophozoites were isolated, washed three times with filtered seawater, and placed in separate 0.2 ml PCR tubes. Genomic DNA was extracted from the single-cell isolates using a QuickExtract FFPE RNA Extraction Kit (Epicentre, Madison, WI, USA).

SSU rDNA sequences were initially amplified by a polymerase chain reaction (PCR) using universal eukaryote primers PF1 5′ – CGCTACCTGGTTGATCCTGCC – 3′ and SSUR4 5′ – GATCCTTCTGCAGGTTCACCTAC – 3′ (Leander et al., 2003). Template DNA and primer pairs were added to Econotaq 29 Mastermix (Lucigen Corp. Middleton, WI). The following thermal cycle was used: initial denaturation at 94 °C for 2 min followed by 35 cycles of denaturation at 94 °C for 30 s, annealing at 52 °C for 30 s, extension at 72 °C for 2:00 min, and a final extension at 72 °C for 5 min. For both species, the product from this initial amplification was used as the template for a second round of nested PCRs using internal primers 18SRF 5′ – CCCGTGTTGAGTCAAATTAAG – 3′ (Mo et al., 2002) and SR4 5′ – AGGGCAAGTCTGGTGCCAG – 3′ (Yamaguchi and

Horiguchi, 2005). The products were screened on a 1% agarose gel and sequenced using the same primers as those used for the amplification and nested PCRs. Sequences were assembled using Geneious version 10.1.3 (Kearse et al., 2012) and initially identified by Basic Local Alignment and Search Tool (BLAST) analysis.

2.3.6 Molecular phylogenetic analyses

The phylogenetic positions of *Cuspisella ishikariensis* gen. nov., sp. nov. (1431 bp) and *L.* cf. *harmothoe* (1637 bp) were determined using a 78-taxon alignment of SSU rDNA sequences, including three dinoflagellate sequences (outgroup) and representatives from the major clades of apicomplexans. Sequences divergence between the single trophozoite isolations were 0.1% for *C. ishikariensis* gen. nov., sp. nov. and 2.8% for *L.* cf. *harmothoe*. Consensus sequences were used to represent *C. ishikariensis* gen. nov., sp. nov. and *L.* cf. *harmothoe* in the molecular phylogenetic analysis. The taxa included in the final phylogenetic analysis were based on preliminary trees that were made using alignments built from a comprehensive set of available gregarine sequences. Clades on long branches (e.g., crustacean gregarines and *Trichotokara*) with little relevance to the phylogenetic position of *C. ishikariensis* gen. nov., sp. nov. and *L. harmothoe* were excluded from the final analysis for clarity. Two environmental sequences (KT814188 and KT812852) were also included in the analysis to verify that the SSU rDNA sequence from *C. ishikariensis* gen. nov., sp. nov. was accurate and not a chimeric sequence or artefact of PCR. The SSU rDNA sequences were aligned using the MAFFT algorithm (Katoh et al., 2002) on Geneious version 10.1.3 (Kearse et al., 2012). The MAFFT algorithm was chosen over others for its ability to account for the secondary structure of ribosomal subunits. Ambiguously aligned regions and gaps were cut from the final alignment using Aliscore version 2.0 (Kück et al., 2010; Misof and Misof, 2009) and Alicut version 2.3. The resulting alignment included 1,464 unambiguously aligned sites.

The GTR+I+Γ model (proportion of invariable sites = 0.1780, gamma shape = 0.6940) was selected by jModelTest version 2.1.10 (Darriba et al., 2012; Guindon and

Gascuel, 2003) for maximum likelihood and Bayesian analyses under the Akaike information criterion (AIC). The maximum likelihood (ML) tree and ML bootstrap values were calculated using RAxML version 8.2.10 (Stamatakis, 2014) through the Cipres Science Gateway version 3.3 (Miller et al., 2010). Bayesian posterior probabilities were calculated using MrBayes version 3.2.6 (Ronquist et al., 2012) using the GTR substitution model with invariable sites over a gamma distribution (lset nst = 6, rates = invgamma) and Monte Carlo Markov Chains (MCMC) run with the following parameters: 10,000,000 generations (ngen = 10,000,000), 2 runs (nruns = 2), 4 chains (nchains = 4), temperature parameter at 0.2 (temp = 0.200), sample frequency of 100, prior burn-in of 0.25 of sampled trees, and a stop rule of 0.01 to terminate the program when the split deviation fell below 0.01.

2.4 Results

2.4.1 *Cuspisella ishikariensis* gen. nov., sp. nov.

Trophozoites were brass-coloured and roughly rhomboidal with an anterior region ending at an attachment apparatus covered in superficial spikes (n = 40; Fig. 2.1A,B). The attachment apparatus on some trophozoites was observed to decrease in volume on occasion leaving the trophozoite with a flattened anterior end (Fig. 2.1C). Cross sections of the attachment apparatus viewed under TEM did not reveal any invaginations of the membrane as might be seen if the attachment apparatus was being retracted as opposed to simply decreasing in volume. At its largest volume, the attachment apparatus measured 35 to 117 µm in length ($\bar{X}$ = 67 µm, n = 40) and 12 to 48 µm ($\bar{X}$ = 30 µm, n = 40) in width and possessed rows of uniform, superficial spikes that pointed posteriorly between longitudinal rows of epicytic folds (Fig. 2.1D). The cells ranged between 303 to 851 µm ($\bar{X}$ = 498 µm, n = 40) in length and 43 to 134 µm ($\bar{X}$ = 76 µm, n = 40) in width. The nucleus was oval with a major axis of 24 to 57 µm ($\bar{X}$ = 37 µm, n = 40) and a minor axis of 18 to 57 µm ($\bar{X}$ = 30 µm, n = 40). The trophozoites were covered by longitudinal epicytic folds

at a density of 4 to 5 folds/µl along the main body of the cell and 1 to 2 folds/µm along the attachment apparatus (Fig. 2.1E,F). No gliding motility was seen in the trophozoite stages and syzygy was observed to be lateral in one specimen under light microscopy. An attempt was made to isolate this pair of gregarines in syzygy, but the cells separated in the process and no micrographs could be taken.

Transmission electron microscopy revealed a cytoplasm containing mitochondria, Golgi bodies, amylopectin granules, and dense granules (Fig. 2.2). The mitochondria were large, often reaching lengths of approximately 10 µm (Fig. 2.2A–C), and branched in numerous places. Amylopectin granules and dense granules were distributed homogenously throughout the trophozoite. The spikes of the attachment apparatus appeared to form by inflation of a regular epicytic fold with cytosol (Fig. 2.2A). Some intermediary spikes were also observed adjacent to fully formed epicytic folds. At the posterior end, bacteria were found inhabiting the grooves between the epicytic folds (Fig. 2.2D). The grooves of the epicytic folds were also infrequently the site for cell inclusion (Fig. 2.2E). Microtubules were roughly arranged in rows and could only be found inside the attachment apparatus (Fig. 2.3A–C). Cross sections and longitudinal section posterior to the attachment apparatus did not reveal microtubules (Fig. 2.3D).

2.4.2 *Loxomorpha* cf. *harmothoe*

Trophozoite morphology was consistent with the original descriptions of *Loxomorpha harmothoe* (see Hoshide 1988; Simdyanov 1996). The cells were elongate and cylindrical, measuring approximately 150 µm in length, 40 µm in width, and syzygy was caudofrontal (Fig. 2.4A). *Loxomorpha* cf. *harmothoe* also possessed an attachment apparatus upon which only epicytic folds, and no apparent spikes, could be seen in TEM sections (Fig. 2.4B). No dense arrays of microtubules were found in the attachment apparatus, although it has been previously suggested that microtubules are present in the body of *L. harmothoe* (Simdyanov, 1996). Other organelles found within the cytoplasm included mitochondria, amylopectin granules, and dense granules (Fig. 2.4C–E).

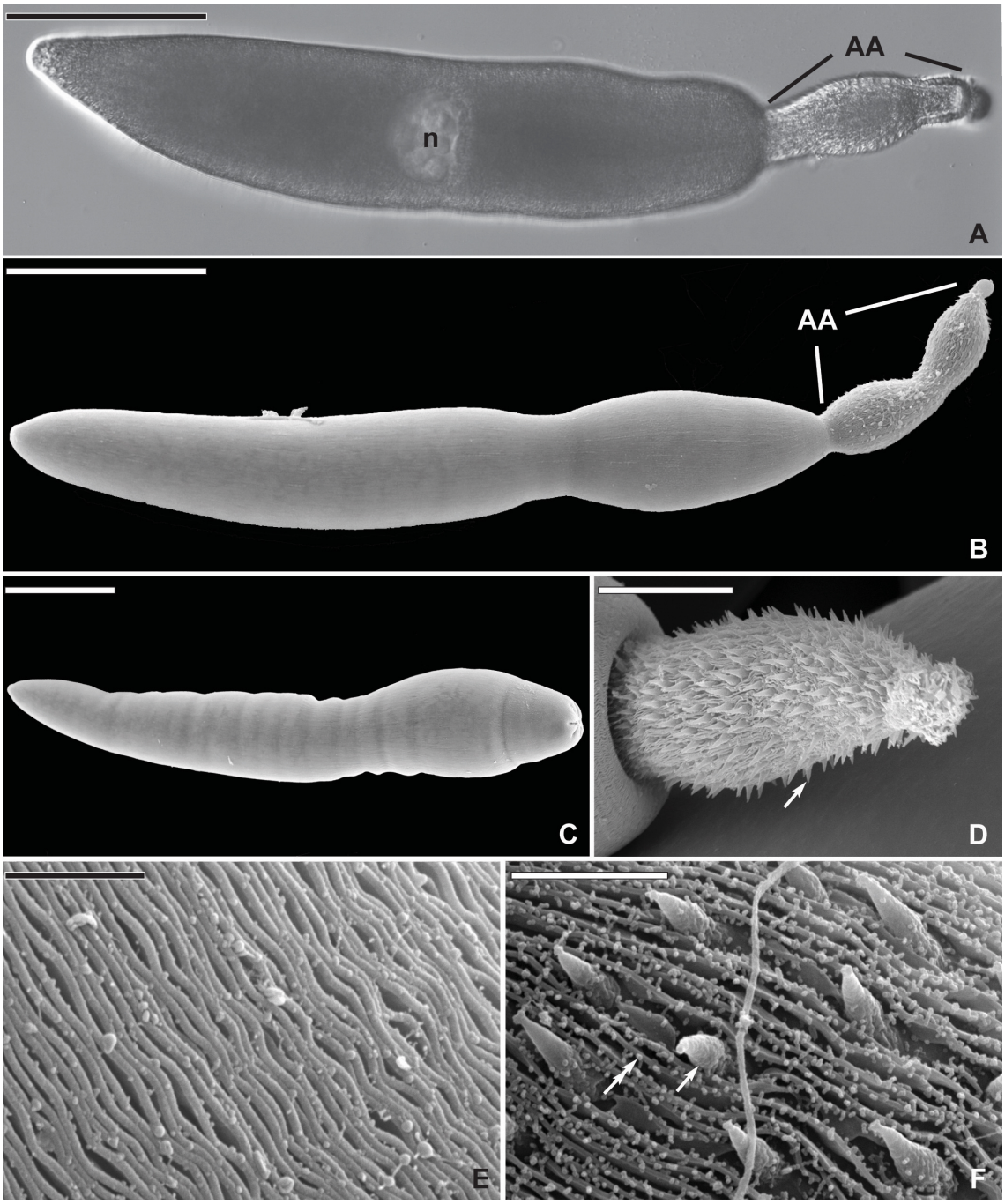

Figure 2.1: Light micrograph (LM) and scanning electron micrographs (SEM) of *Cuspisella ishikariensis* gen. nov., sp. nov. showing trophozoite morphology and ultrastructure. (A) LM of trophozoite taken in differential interference contrast (DIC). An oval nucleus (n) is visible located centrally within the cell. The attachment apparatus (Aa) is covered by spikes. (B) SEM of the trophozoite showing general trophozoite morphology and an attachment apparatus (Aa). (C) SEM of a trophozoite with a flattened anterior end due to the attachment apparatus having minimized in volume. (D) SEM close-up of the attachment apparatus. Superficial spikes (arrow) form longitudinal rows along the entire attachment apparatus in between epicytic folds. (E) SEM close-up of epicytic folds taken from the mid region of the trophozoite. (F) SEM close-up of the spikes (arrow) and epicytic folds (double-headed arrow) that line the attachment apparatus. Scale bars: A,B,C = 100 µm; D = 20 µm; E = 3 µm; F = 5 µm.

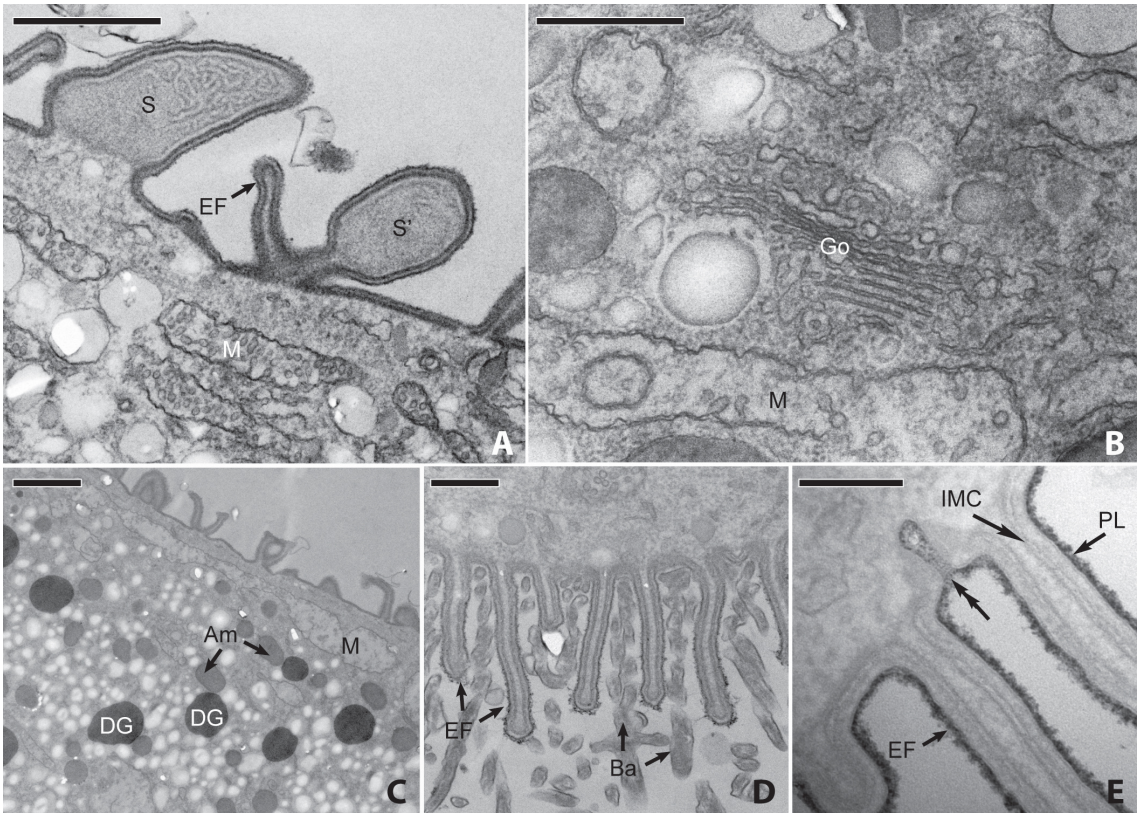

Figure 2.2: Transmission electron micrographs (TEM) of *Cuspisella ishikariensis* gen. nov., sp. nov. showing general subcellular morphology. Abbreviations: amylopectin granules (am), bacteria (Ba), dense granules (DG), epicytic fold (EF), Golgi body (Go), inner membrane complex (IMC), mitochondria (M), plasmalemma (PL), spike (S), developing/intermediary spikes (S'). (A) Longitudinal section showing the internal and surface morphology of the attachment apparatus. A fully formed spike (S) is seen next to one resembling an intermediary between a spike and an epicytic fold (S'). Inflation of an epicytic fold with cytosol may be the mechanism by which the spikes (S) form. (B) High magnification view of the organelles in the trophozoite body. (C) Longitudinal section showing a large mitochondrion near the periphery of the cell. (D) Longitudinal section taken from the most posterior end of the trophozoite. Bacteria are found in the grooves between the epicytic folds of the gregarine parasite. (E) High magnification view of the trophozoite plasmalemma and inner membrane complex. The open invagination of the plasma membrane through the IMC (double-headed arrows) is covered by a cell coat similar to that observed in Fig. 2.3C. Scale bars: A = 1 μm; B = 500 nm; C = 2 μm; D = 500 nm, E = 200 nm.

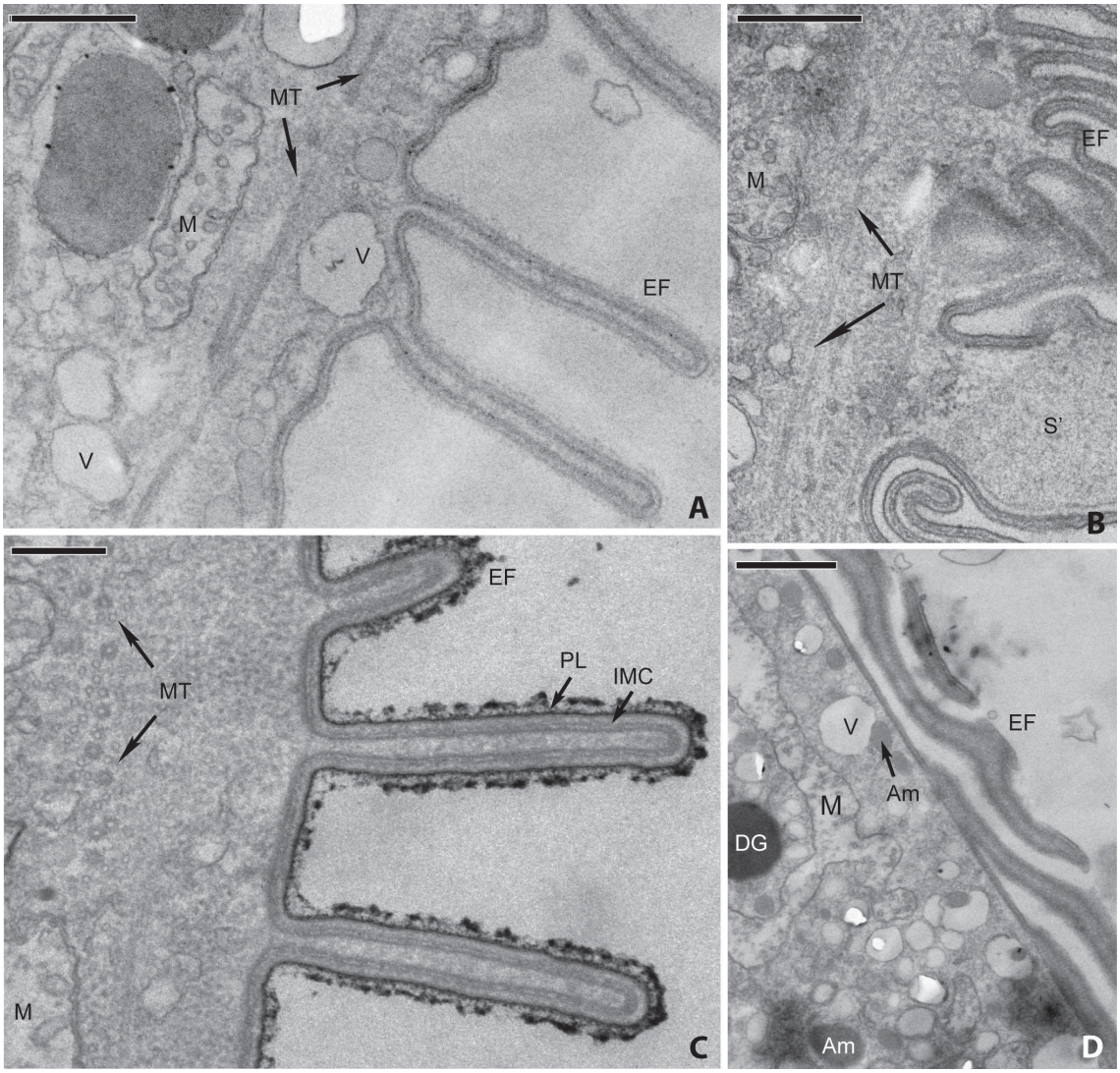

Figure 2.3: Transmission electron micrographs (TEM) of *Cuspisella ishikariensis* gen. nov., sp. nov. showing general subcellular morphology and microtubules. Abbreviations: amylopectin granules (Am), dense granules (DG), epicytic fold (EF), inner membrane complex (IMC), mitochondria (M), microtubules (MT), plasmalemma (PL), developing/intermediary spike (S'), and vacuoles (V). (A) Longitudinal section of an inflated attachment apparatus showing dense arrays of microtubules. (B) Longitudinal section taken from the anterior end of an inflated attachment apparatus showing microtubules beside a developing superficial spike. (C) Cross section of an inflated attachment apparatus showing a dense array of microtubules roughly arranged into rows. The plasmalemma and inner membrane complex are also visible. (D) Longitudinal section of trophozoite body posterior to the attachment apparatus. Subcellular components such as vacuoles, amylopectin granules, and dense granules are visible. Microtubules are not found in this region of the trophozoite. Scale bars: A,B = 500 nm; C = 250 nm; D = 1 µm.

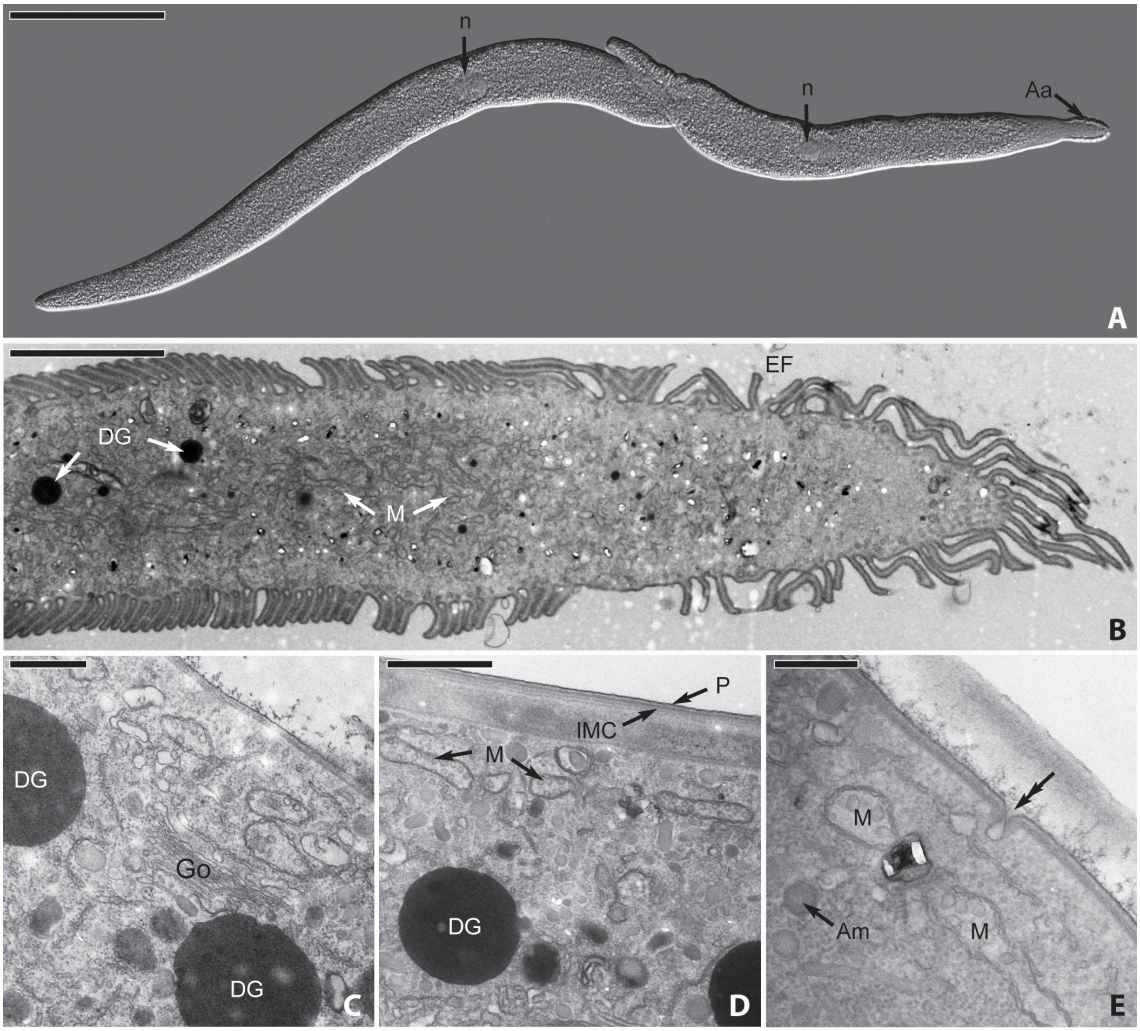

Figure 2.4: Light micrograph (LM) and transmission electron micrographs (TEM) of *Loxomorpha* cf. *harmothoe*.(A) LM of trophozoite taken in differential interference contrast (DIC). The cylindrical trophozoite possesses an oval nucleus (n) that is visible and located centrally within the cell. An attachment apparatus (Aa) is also apparent, but is not covered by spikes as seen in *Cuspisella ishikariensis* gen. nov., sp. nov. Syzygy is caudofrontal. (B) Longitudinal section taken through the attachment apparatus. Epicytic folds (EF) cover the outer surface of the cell and mitochondria (M) and dense granules (DG) are seen in the cytoplasm. There are no visible arrays of densely arranged microtubules. The attachment apparatus is also devoid of spikes and is instead covered exclusively in typical epicytic folds. (C) Longitudinal section of the trophozoite body posterior to the attachment apparatus with an apparent Golgi body (Go) and dense granules (DG). (D) Longitudinal section of the trophozoite body showing the plasmalemma (P) and inner membrane complex (IMC). Mitochondria (M) are arranged near the periphery of the cell and large dense granules (DG) are visible. (E) A cell inclusion (double-headed arrow), amylopectin granules (Am), and mitochondria (M). Scale bars:A = 100 µm; B = 4 µm; C = 2 µm; D = 1 µm; E = 500 nm.

2.4.3 Molecular phylogenetic analyses of SSU rDNA sequences

The 73-taxon alignment of SSU rDNA sequences yielded a strongly supported outgroup of dinoflagellates (93 maximum likelihood bootstrap [MLB], 1.00 Bayesian posterior probability [BPP]) and an ingroup of apicomplexans with a poorly resolved backbone (Fig. 2.5). Both maximum likelihood and Bayesian analyses recovered identical tree topologies. The apicomplexan backbone gave rise to piroplasmid, coccidian, rhytidocystid, cryptosporidian, and gregarine clades. The archigregarines were paraphyletic with *Platyproteum vivax* and *Filipodium phascolosomae* forming the earliest apicomplexan branch. Two distinct terrestrial gregarine clades were recovered: terrestrial gregarine clade I (74 MLB, 1.00 BPP) and terrestrial gregarine clade II (100 MLB, 1.00 BPP). Terrestrial gregarine clade I included environmental sequences (AF372779 and AY179988) acquired from marine environmental PCR surveys. Terrestrial gregarine clade II was comprised exclusively by gregarines described from terrestrial hosts. The marine gregarines include the capitellid gregarines, urosporids, lecudininds, *Difficilina*, *Veloxidium*, paralecudinids, *Selenidium*, polynoid gregarines, and sipunculid gregarines. Each group of marine gregarines was composed of members that infect similar hosts (e.g., capitellid gregarines and *Lankesteria* collected from tunicates).

Cuspisella ishikariensis gen. nov., sp. nov. (MF537615) was recovered on its own branch separate from a strongly supported lineage constituted by *Loxomorpha* cf. *harmothoe* (MF537616) and unidentified environmental sequences (KT814188 and KT812852). The two gregarine sequences and two environmental sequences grouped together on a branch distinct from previously established marine gregarine clades (67 MLB, 1.00 BPP).

2.5 Discussion

Molecular phylogenetic analyses of SSU rDNA sequences recovered a clade composed of two environmental sequences, *L.* cf. *harmothoe*, and *C. ishikariensis* gen. nov., sp. nov. The environmental sequences were used to verify that the SSU rDNA sequence used

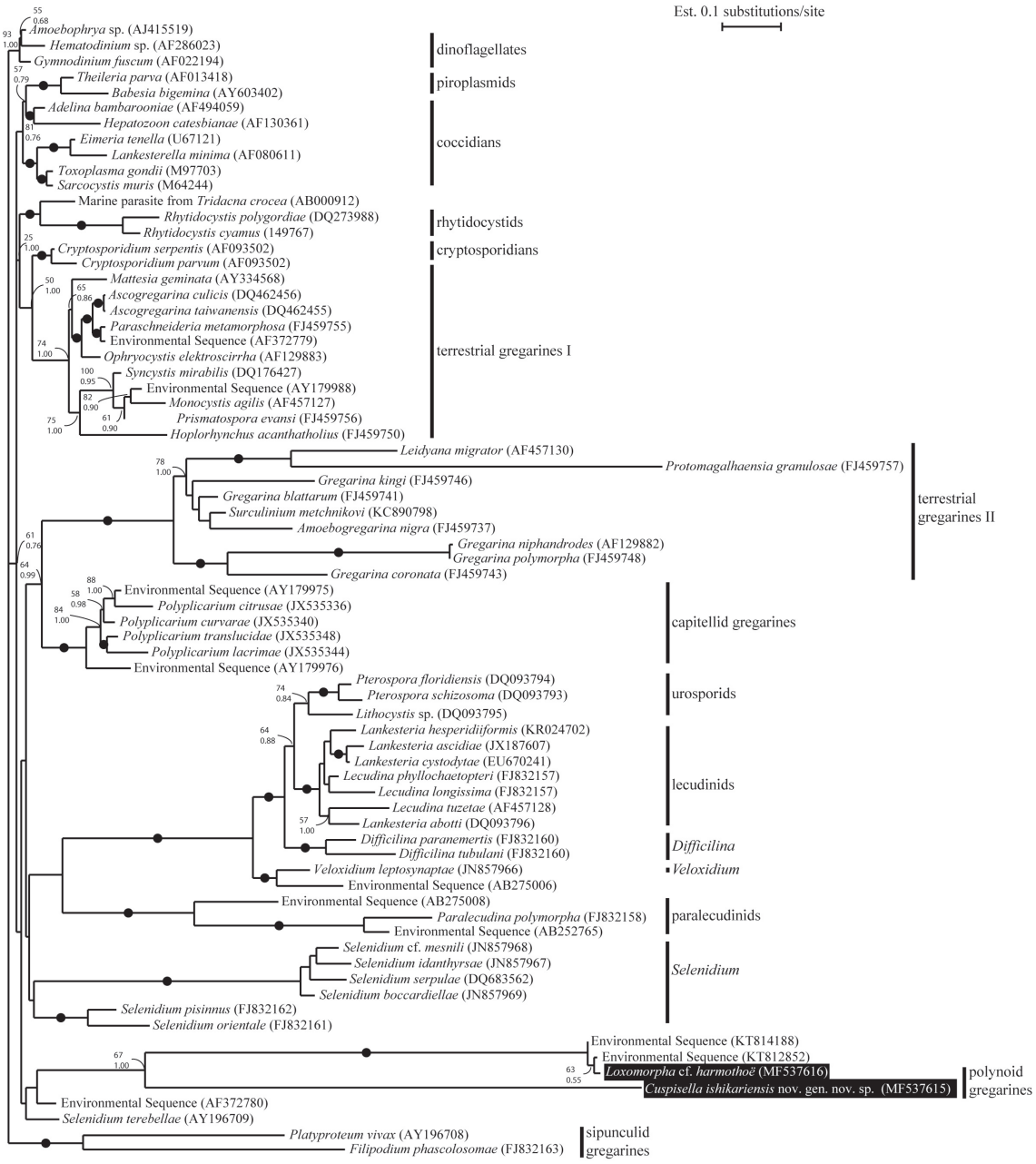

Figure 2.5: Maximum likelihood tree inferred from a 78 taxa dataset of SSU rDNA sequences with 1,464 unambiguously aligned sites using the GTR+I+Γ model of substitution (gamma shape = 0.6940, proportion of invariable sites = 0.1780). Numbers denote support values with the top values indicating bootstrap support and the bottom indicating Bayesian posterior probabilities. The black dots were used on branches when both bootstrap support and Bayesian posterior probabilities were equal to or $>$ 95 and 0.99 respectively. Support values were excluded from this tree when both bootstrap support and Bayesian posterior probabilities fell below 55 and 0.95 respectively for any given branch. The new species described in the current study as well as the sequence for *Loxomorpha* cf. *harmothoe* is highlighted with a black box.

for *C. ishikariensis* was accurate, and not a product of chimerism or an artefact of PCR. *Loxomorpha harmothoe* was originally described from the intestine of the polynoid host *Harmothoe imbricata* using light and electron microscopy (Hoshide, 1988; Simdyanov, 1996). The trophozoites of *L. harmothoe* are elongate and cylindrical (200 µm × 15 µm) ending in an anterior attachment apparatus and sexual reproduction occurs through caudofrontal syzygy. Due to the lack of genetic data in the original description of *L. harmothoe*, no comparison could be made between the SSU rDNA sequences of *L. harmothoe* (original description) and *L.* cf. *harmothoe* (this study). We have therefore continually distinguished the two throughout the text. *Cuspisella ishikariensis* gen. nov., sp. nov. was found in Hokkaido, Japan, the same locality as *L.* cf. *harmothoe*, from the intestine of the polynoid host *Lepidonotus helotypus*. Both species share basic morphological similarities such as an anterior region ending with an attachment apparatus as well as the lack of gliding motility in the trophozoite stages. A stark contrast, however, is the size difference between the trophozoites of *C. ishikariensis* gen. nov., sp. nov. (500 µm × 80 µm) and those of *L.* cf. *harmothoe* (150 µm × 40 µm). Syzygy in *C. ishikariensis* gen. nov., sp. nov. is also lateral and not caudofrontal. Intracellular differences are also clear whereby *C. ishikariensis* gen. nov., sp. nov. possesses large, branching mitochondria and a dense array of microtubules that support the attachment apparatus, whereas TEM sections of *L.* cf. *harmothoe* did not reveal any apparent microtubule arrays. Simdyanov (1996) reported the presence of microtubules in *L. harmothoe* through TEM micrographs, but they were more sparsely distributed than as seen in *C. ishikariensis* gen. nov., sp. nov. The attachment apparatus of *C. ishikariensis* gen. nov., sp. nov. was also covered by distinctive spikes arranged in rows, whereas the attachment apparatus of *L.* cf. *harmothoe* appeared to lack these spikes under thin sections viewed under TEM. The SEM photos taken by Simdyanov (1996) of *L. harmothoe* also did not show spikes projecting from the attachment apparatus, but I am unable to dismiss the possibility that the TEM sections and SEM micrograph by Simdyanov simply missed these structures due to rarity or small size.

The molecular phylogenetic analysis is consistent with the morphological differences in that the SSU rDNA sequences grouped the polynoid gregarines together, but clearly separated *C. ishikariensis* gen. nov., sp. nov. from *L.* cf. *harmothoe*. The combination of morphological and genetic differences, therefore, suggests that *C. ishikariensis* gen. nov., sp. nov. is a distinct species that also does not conform to the descriptions of *Loxomorpha* in general. Whether the grouping of *C. ishikariensis* gen. nov., sp. nov. and *L. harmothoe* in the current analysis suggests a clade of gregarines that infect polynoid hosts in nature is unclear. Until a more comprehensive set of polynoid gregarines are characterized, the possibility that multiple gregarine clades infect polynoid hosts remains open.

Many original descriptions of gregarines are based on line drawings and lack molecular data. However, gregarine trophozoites often take on a great deal of intraspecific variation (e.g., the diverse morphotypes of *Paralecudina polymorpha* and *Lecudina* cf. *tuzetae*; Leander and Keeling 2003; Rueckert et al. 2011b) associated with motility (e.g., *Pterospora schizosoma*; Leander et al. 2006) and morphology of different developmental stages. As such, morphological traits are sometimes difficult to interpret and their plasticity can confound gregarine systematics in the absence of molecular data. The distinctiveness of *L. harmothoe* from the genus *Lecudina* was previously brought into question (Clopton, 2000), but this study provides evidence based on SSU rDNA sequences that it does indeed belong to a separate genus. Comparative morphology and molecular phylogenetic analysis of SSU rDNA further suggest that *C. ishikariensis* gen. nov., sp. nov. is a novel species belonging to its own genus. Moreover, this study is the first to establish a molecular phylogenetic position for the *L.* cf. *harmothoe* and *C. ishikariensis* gen. nov., sp. nov.

The molecular phylogenetic pattern whereby closely related gregarines infect closely related hosts is seen consistently across marine gregarine taxa (Iritani et al., 2017; Rueckert et al., 2015; Wakeman and Leander, 2013a,b). Such phylogenetic association of gregarine parasites and their host set shows that gregarines have co-evolved with their inver-

tebrate hosts to yield a level of host specificity. In contrast to this pattern, some gregarine species have diversified sympatrically within a host as in the case of *Selenidium melongena* and *S. terebellae*; two sister species that simultaneously infect the coelom and intestinal lumen respectively. Co-evolutionary phylogenetic patterns in gregarine systematics are not evident from comparative morphology alone, which highlights the indispensable role molecular phylogenetic data play for further elucidating gregarine diversity and evolutionary history.

2.6 Taxonomic Summary

Phylum Apicomplexa Levine 1970

Order Eugregarinorida Léger 1900

Cuspisella gen. nov. Iritani, Horiguchi, and Wakeman 2017

Description. Trophozoites are long and roughly rhomboidal. A conspicuous attachment apparatus, which can decrease in volume, is uniformly covered in spikes arranged in longitudinal rows. Microtubules are present only in the attachment apparatus. Epicytic folds run along the length of the cell and become less dense on the attachment apparatus. Syzygy is lateral. Trophozoites do not display gliding motility.

Type Species. *Cuspisella ishikariensis*

Etymology. The genus name refers to the small (Latin: *-ella*) spike (Latin: *Cuspis-*) found on the attachment apparatus of the type species. The name is of feminine gender.

Cuspisella ishikariensis n. sp. Iritani, Horiguchi, and Wakeman 2017

Description. Trophozoites are brass-coloured and roughly rhomboidal ranging between 303 to 851 µm in length and 43 to 134 µm in width. Anterior region ends with attachment apparatus lined with superficial spikes. Attachment apparatus can decrease in volume leaving a flattened anterior end on some trophozoites. Attachment apparatus measures 35 to 117 µm in length and 12 to 48 µm in width and is supported by microtubules. Nucleus is oval with a major axis of 24 to 57 µm and a minor axis of 18 to 57

μm. Large and occasionally branching mitochondria distributed throughout cytoplasm. Longitudinal epicytic folds line the trophozoite at 4 to 5 folds/μm and 1 to 2 folds/μm along the attachment apparatus. Trophozoites display no gliding motility and syzygy is lateral.

DNA sequence. SSU rDNA sequence (GenBank MF537615).

Type locality. Ishikari Bay, Hokkaido, Japan (43°13′35.0″N 141°0′58.3″E). Host commonly found on the underside of large (∼1 m diameter) rocks in the low intertidal to subtidal zones.

Type habitat. Marine.

Type host. *Lepidonotus helotypus* Grube 1877 (Annelida, Polychaeta, Phyllodocida, Polynoidae).

Location in host. Intestinal lumen.

Iconotype. Fig. 2.1A Hapantotype. Trophozoites on SEM stubs with a gold/palladium alloy sputter coat have been stored in the algal and protist collection in the Hokkaido University Museum (DI – 1).

LSID. 69E7303B-03E0-480A-9250-965200061B6A.

Etymology. The species name refers to the type locality of Ishikari Bay.

2.7 Acknowledgements

This research was supported by a MEXT Doctoral Scholarship to Davis Iritani, as well as start-up funding from the International Institute for Collaboration at Hokkaido University and a joint JSPS/MBIE-RSZN provided to Kevin Wakeman.

3

Marine Gregarine Parasitism in Tunicates, Host Switching, and the Description of Four New Species

3.1 Abstract

The Apicomplexa are a diverse group of obligate parasites to a variety of animal species. In the present study, four new species of marine eugregarines (*Lecudina kaiteriteriensis* sp. nov., *L. dolabra* sp. nov., *L. savignyii* sp. nov., and *L. pollywoga* sp. nov.) that infect ascidian hosts were described using a combination of morphological and molecular data.

Phylogenetic analyses using SSU rDNA sequences suggested that gregarine parasitism in ascidians and polychaetes has a common origin as traditionally proposed by predecessors in the discipline. Furthermore, a taxonomic problem which evaded detection in previous studies, involving two major genera (*Lankesteria* and *Lecudina*), was examined through an emendation of *Lecudina* and a transfer of 49 *Lankesteria* species to *Lecudina* as new combinations. The species discovered and described in the current study provide new data for understanding gregarine systematics and evolution while also exploring parasitism in ascidians from New Zealand.

3.2 Introduction

The Apicomplexa are a widespread group of unicellular eukaryotes that parasitize a plethora of animal hosts. There are over 6000 named apicomplexans classified in ∼350 genera and select constituent members such as *Plasmodium*, *Toxoplasma*, and *Cryptosporidium* have attracted special attention due to their medical or veterinary impact. For example, there are still 219 million cases of malaria per year (WHO, 2019) and 30% of the global human population is chronically infected by *Toxoplasma* (Schlüter et al., 2014). Focused research of these apicomplexans, whose parasitism heavily impacts human life, has led to many advances in apicomplexan biology (e.g., Abrahamsen et al. 2004; Kim and Weiss 2004; Wilson et al. 1996). These well-studied taxa, however, represent only a portion of the total apicomplexan diversity, mostly undescribed, estimated at over one million species (Adl et al., 2007, 2019).

Marine gregarines are an understudied group that are of interest due to their ubiquity, diversity, and phylogenetically early branching position to all the Apicomplexa. They parasitize a wide range of phylogenetically and geographically distinct hosts and have retained key plesiomorphic characters (e.g., monoxeny, conspicuous feeding stages, and parasitism via myzocytosis) that are important for understanding apicomplexan diversification (Leander, 2008; Rueckert et al., 2011a; Sitnikova and Shirokaya, 2013; Wakeman and Leander, 2013b). The pathogenic effects of gregarines on invertebrates have not

been well studied, but are associated with decreased fecundity (Zuk, 1987a) as well as obstruction of the digestive tract (Mita et al., 2012) which is where most gregarine infections occur. The bulk of gregarine taxa remain wholly undiscovered or represented only as environmental sequences. Thus, a major task for gregarine biology is to further explore the uncharted diversity of gregarines and to better understand key character traits within a molecular phylogenetic framework.

Gregarines are broadly divided into three major groups: archigregarines, neogregarines, and eugregarines (Adl et al., 2012, 2019; Grassé, 1953; Leander, 2008). This classification scheme is rooted in morphology (e.g., cortical microtubules, attachment apparatuses, and cell shape), life history, and molecular phylogenies built on small subunit ribosomal DNA (SSU rDNA) data (Leander, 2006; Rueckert et al., 2013; Schrével et al., 2016; Simdyanov et al., 2017; Wakeman and Leander, 2012). The study of marine gregarines is especially concerned with the conspicuous feeding stage of the gregarine life cycle, known as the trophozoite, due to its more reliable or recognizable presence inside a host in contrast to the other stages such as the oocysts which can be challenging to recover once expelled into the environment.

Eugregarines (Eugregarinorida Léger 1900) represent the majority of marine gregarine taxa and are further divided into aseptate and septate groups. Most of the aseptate gregarines are classified within the poorly resolved family Lecudinidae Kamm 1922 (Levine, 1977). The two major genera in this family are *Lankesteria* and *Lecudina*. *Lankesteria* Mingazinni 1891 was originally a collection of gregarines isolated from various hosts including marine urochordates and terrestrial insects. Grassé (1953) removed the insect gregarines from *Lankesteria* and established *Ascocystis*; Ormières (1965) retained *Lankesteria* as a genus for gregarines that parasitize urochordates. *Lecudina* Mingazinni 1891, on the other hand, is a genus consisting of about 40 species that parasitize a variety of polychaete hosts (Levine, 1976).

In this study, I describe four new species of marine lecudinids that infect solitary sea squirts (Ascidiacea Blainville 1824) from New Zealand. The addition of these four novel

taxa corroborates a traditional conjecture which suggests that gregarine parasites of tunicates and polychaetes share a common origin (Théodoridès, 1967). My data also demonstrate the need for the two major lecudinid genera, *Lankesteria* and *Lecudina* (henceforth abbreviated as *La.* and *Le.* respectively) to be combined. The characterization of microbial pathogens in ascidians is important especially considering the serious biosecurity threats posed by ascidians as prolific invaders of marine ecosystems (Lambert, 2007; McKindsey et al., 2007; Zhan et al., 2015) and that gregarine parasitism of these hosts can be symptomatic and fatal (Mita et al., 2012). Fatal infections of ascidians would be significant for dense populations of both invaders and deliberately cultured populations meant as study material or food. The new species described in this study represent the first discovery of marine gregarines that parasitize ascidians in New Zealand.

3.3 Methods

3.3.1 Host collection and gregarine trophozoite isolation

Ascidians were collected from three locations around the South Island of New Zealand between March 1st and March 14th of 2019. *Pyura* sp. was collected from the underside of boulders exposed during low tide from Kaiteriteri Beach, Kaiteriteri, New Zealand (41°2′7.7″S 173°1′21.4″E). Both *Ciona savignyi* and *Molgula complanata* were collected from fouled ropes that hung submerged along the docks in Nelson Marina, Nelson, New Zealand (41°15′37.1″S 173°16′53.0″E). *Asterocarpa humilis* was similarly collected from a fouled rope in Waikawa Marina, Marlborough, New Zealand (41°16′2.8″S 174°2′18.4″E).

The ascidians were transported back to the laboratory and kept under running seawater. Each ascidian was dissected within two days of collection. The procedure involved removing the tunic and extracting the digestive tract from the posterior end of the pharyngeal basket to the anus. The entirety of the digestive tract was submerged in filtered seawater (0.45 μm) and split down its length using fine forceps to expose the contents of

the gut. Gregarine trophozoites were observed under an inverted light microscope and isolated individually using hand-drawn glass pipettes. The trophozoites from each individual host were then washed in filtered seawater (0.45 µm) and pooled together for subsequent use in light miscopy or scanning electron miscopy. Single-cell isolations were prepared for DNA extraction and sequencing.

3.3.2 Light microscopy

Trophozoite morphology was observed with an Olympus BX51 (Olympus, Tokyo, Japan) paired to an Olympus DP73. Light micrographs presented in the current dissertation are composites of multiple high magnification photos taken along the length of the entire cell subsequently stitched together using Panorama Stitcher Mini version 1.10 (Olga Kacher, Boltnev Studio). Micrographs were then refined with GIMP version 2.10.12 (GNU image manipulation program version; The GIMP Team).

3.3.3 Scanning electron microscopy

Trophozoites were pooled, separately for each individual host, and fixed with 2.5% glutaraldehyde for 30 min on ice. The fixative was washed out with chilled, filtered seawater. Fixation continued with the addition of 1% OsO_4 and the trophozoites were left for 30 min on ice. The fixative was again removed with filtered, chilled seawater. The trophozoites were then dehydrated in a graded series of ethanol for three minutes at each of the following concentrations: 50%, 70%, 80%, 90%, and 100%. A Leica EM CPD300 (Leica Microsystems, Wetzlar, Germany) was used for critical point drying. Each SEM stub was sputter coated with gold for 180 s at 15 µA. Scanning electron micrographs were taken on a Hitachi S3000N scanning electron microscope and placed on a black background using GIMP version 2.10.

3.3.4 DNA extraction, amplification and sequencing

For each gregarine species, trophozoites were individually isolated, washed three times with filtered seawater, and placed in separate 0.2 ml PCR tubes. Genomic DNA was extracted from the single-cell isolates using a QuickExtract FFPE RNA Extraction Kit (Epicentre, Wisconsin, USA). The SSU rDNA sequences were initially amplified by a polymerase chain reaction (PCR) using universal eukaryote primers PF1 5′ – CGCTAC-CTGGTTGATCCTGCC – 3′ and SSUR4 5′ – GATCCTTCTGCAGGTTCACCTAC – 3′ (Leander and Keeling, 2003) and TaKaRa Ex Taq (Takara Bio Inc., Otsu, Japan). The thermal cycler conditions used were as follows: initial denaturation at 94°C for 1 min followed by 35 cycles of denaturation at 94°C for 20 s, annealing at 56°C for 30 s, extension at 72°C for 1:40 min, and a final extension at 72°C for 7 min. The product from this initial amplification was diluted 1:100 in distilled water and used as template for nested PCRs using the primer pairs developed for this study: T74F 5′ – GTCTCGCAGATTAAGC-CATG – 3′ paired with T1140R 5′ – GAATACGAATGCCCTCAACC – 3’′ and T990F 5′ – GAGTGAATCGGCGTGTTC – 3′ paired with T1791R 5′ – CTCCGCCTAACTCAT-GATAC – 3′. The thermal cycler conditions used were as follows: initial denaturation at 94°C for 1 min followed by 35 cycles of denaturation at 94°C for 20 s, annealing at 52°C for 30 s, extension at 72°C for 1:40 min, and a final extension at 72°C for 7 min. The products were screened on a 1% agarose gel and subsequently sequenced using the same internal primers. The SSU rDNA sequences, from separate single-cell isolations, were assembled on MEGA version 7 (Kumar et al., 2016) for each gregarine species and initially identified using Basic Local Alignment and Search Tool (BLAST). Identification of the hosts were based on morphology using a species guide (Page et al., 2019) and with partial COI and SSU rDNA sequences amplified with Folmer primers (Folmer et al., 1994) or PF1 – 18SRF 5′ – CCCGTGTTGAGTCAAATTAAG – 3′ (Mo et al., 2002) and SR4 5′ – AGGGCAAGTCTGGTGCCAG – 3′ (Yamaguchi and Horiguchi, 2005) - SSUR4, respectively, with the following thermal cycler conditions: initial denaturation at 94°C for 1 min followed by 35 cycles of denaturation at 94°C for 20 s, annealing at 47°C or 50°C

for 30 s, extension at 72°C for 0:40 s, and a final extension at 72°C for 7 min.

3.3.5 Molecular phylogenetic analyses

The taxonomic affinities of *Lecudina pollywoga* sp. nov., *Le. savignyii* sp. nov., *Le. dolabra* sp. nov., and *Le. kaiteriteriensis* sp. nov. were recovered based on SSU rDNA data in two separate analyses. The first analysis consisted of a 90-taxon alignment including three dinoflagellate sequences to form the outgroup, and representative sequences from the major apicomplexan groups. Three separate sequences from *Le. pollywoga* nov. sp., *Le. savignyii* nov. sp., and *Le. dolabra* nov. sp., and two separate sequences for *Le. kaiteriteriensis* sp. nov. were included in the analysis. Clades which are known to be situated on long phylogenetic branches (e.g., crustacean gregarines and *Trichotokara*) that had little relevance to the analysis of the ascidian gregarines were excluded for the sake of clarity. The SSU rDNA sequences were aligned using MAFFT version 6 with the Q-INS-i option (Katoh et al., 2002) for its ability to account for the secondary structure of ribosomal subunits. Ambiguously aligned regions and gaps were cut from the final alignment using Aliscore version 2.0 (Kück et al., 2010; Misof and Misof, 2009) and Alicut version 2.31. The resulting alignment included 1,440 unambiguously aligned nucleotides.

The second phylogenetic analysis was performed using a smaller 48-taxon alignment that focused only on the taxa closely related to the ascidian gregarines. This phylogeny was built upon 11 archigregarine sequences that formed the outgroup and 37 lecudinid sequences that formed the ingroup. The alignment was constructed using identical methods to the first analysis and resulted in a final dataset with 1,444 unambiguously aligned nucleotides.

Maximum likelihood (ML) and Bayesian posterior probabilities were calculated using RAxML version 8.2.12 (Stamatakis, 2014) and Mr. Bayes version 3.2.6 (Ronquist et al., 2012) through the Cipres Science Gateway version 3.3 (Miller et al., 2010). The GTR+I+Γ model was suggested by jModelTest version 2.1.10 (Darriba et al., 2012; Guindon and Gascuel, 2003) both for the 90-taxon alignment (proportion of invariable sites =

0.1970, gamma shape = 0.6960) and 48-taxon alignment (proportion of invariable sites = 0.2000, gamma shape = 0.6130) for phylogenetic analysis. The parameters specified for MrBayes were as follows: lset nst = 6, rates = invgamma, and Monte Carlo Markov Chains (MCMC) run for 10,000,000 generations (ngen = 10 000 000), 2 runs (nruns = 2), 4 chains (nchains = 4), temperature parameter at 0.2 (temp = 0.200), sample frequency of 100, prior burn-in of 25% of sampled trees, and a stop rule of 0.01 to terminate the program when the split deviation fell below 0.01.

3.4 Results

3.4.1 *Lecudina kaiteriteriensis* sp. nov.

Cells were lanceolate and arched to an overall crescent whereby a narrow posterior gently curved and widened markedly towards the middle of the cell, near the nucleus, and ended in a stubbed, and conspicuous mucron (Fig. 3.1A,B). Trophozoites were darker near the periphery of the cell and at the posterior, which then turned to a light grey near the nucleus and ended at a silver or translucent mucron. The cells ranged between 165.3 to 405.7 µm ($\bar{X}$= 268.0 µm, n = 80) in length and 32.7 to 114.6 µm ($\bar{X}$ = 50.0 µm, n = 80) in width. An oval nucleus with a major axis between 38.5 to 71.7 µm ($\bar{X}$ = 56.3 µm, n = 20) and a minor axis between 35.7 to 66.0 µm ($\bar{X}$ = 49.6 µm, n = 20) was located in the anterior third of the cell. A distinct, ring-like nucleolus, measuring 14.8 to 31.6 µm ($\bar{X}$ = 25.4 µm, n = 20) by 17.2 to 29.7 µm ($\bar{X}$ = 23.7 µm, n = 80), was situated in the posterior half of the nucleus. The cell surface comprised of epicytic folds arranged longitudinally at a density of 4 folds/µm (Fig. 3.1C). The mucron was observed to be bent inwards (Fig. 3.1D). Gliding motility was observed.

3.4.2 *Lecudina dolabra* sp. nov.

The general shape of the trophozoites was subulate consisting of a rod-like body and a tapering posterior which ended in a sharp point (Fig. 3.2A,B). The posterior end of the

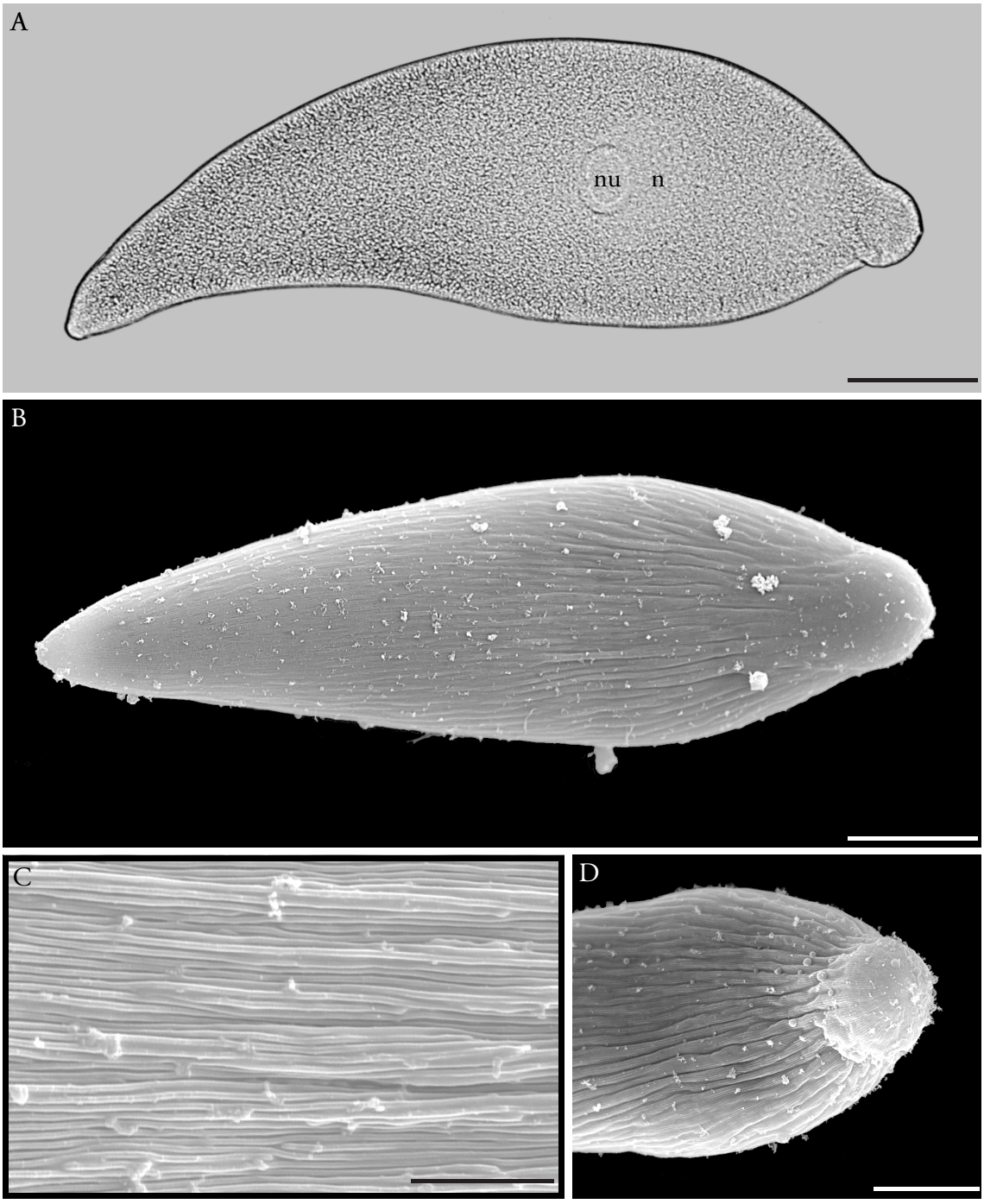

Figure 3.1: Light micrograph (LM) and scanning electron micrographs (SEM) of *Lecudina kaiteriteriensis* sp. nov. showing trophozoite morphology. Mucron oriented to the right. (A) LM of trophozoite taken in differential interference contrast (DIC). Lanceolate cell bent in a crescent shape with an oval nucleus (n) situated in the anterior third of the body with a distinct nucleolus (nu). The mucron is transparent and stubby. (B) SEM of the trophozoite showing overall shape and morphology. (C) SEM of epicytic folds forming a longitudinal array at a density of 4 folds/µm (D) SEM of the anterior portion of the cell including the mucron. Scale bars: A, B = 30 µm; C = 10 µm; D = 15 µm.

cell and the mucron were translucent, but the rest of the cell was a light golden brown. The cells ranged between 163.7 to 207.1 µm ($\bar{X}$ = 173.7 µm, n = 40) in length and 22.7 to 43.5 µm ($\bar{X}$= 32.6 µm, n = 40) in width. An inconspicuous nucleus with a major axis between 14.4 to 21.9 µm ($\bar{X}$= 18.3 µm, n = 10) and a minor axis between 6.0 µm to 16.4 µm ($\bar{X}$= 12.8 µm, n = 10) lay within the first fifth of the anterior portion of the trophozoite and could only be discerned by its marginally fainter colour compared to the rest of the cell. The cell surface had longitudinal arrays of epicytic folds at a density of 3 folds/µm (Fig. 3.2C). The mucron was triangular and formed an angled protrusion at the anterior (Fig. 3.2D). Gliding motility was observed.

3.4.3 *Lecudina savignyii* sp. nov.

The cells were roughly lanceolate with tapering posterior and anterior ends that flanked a fat center that bulged markedly in some individuals (Fig. 3.3A,B). The general coloration was gray to light brown with a translucent mucron. Trophozoite sizes ranged between 48.5 to 85.8 µm ($\bar{X}$= 68.7 µm, n = 40) in length and 14.9 to 35.0 µm ($\bar{X}$= 23.5 µm, n = 40) in width. The nucleus was oval and situated within the first sixth of the anterior of the cell with a major axis between 8.03 to 12.1 µm ($\bar{X}$= 9.4 µm, n = 20) and a minor axis between 6.1 to 10.4 µm ($\bar{X}$= 8.2 µm, n = 20). The cell surface comprised of epicytic folds arranged longitudinally at a density of 3 folds/µm (Fig. 3.3C). The mucron formed a protrusion that was capped by a small bump (Fig. 3.3B,D). Gliding motility was observed.

3.4.4 *Lecudina pollywoga* sp. nov.

The trophozoites were spatulate with a tapering, rod-like body beginning with a spherical anterior like a tadpole or roughly the overall shape of a medieval mace (Fig. 3.4A,B). The posterior end and mucron were translucent, but the remainder of the cell was a golden-brown. The cells ranged between 96.6 to 155.1 µm ($\bar{X}$= 118.4 µm, n = 40) in length and 25.2 to 43.6 µm ($\bar{X}$= 34.7 µm, n = 40) in width. A nearly circular nucleus that measured between 13.2 to 21.1 µm ($\bar{X}$= 18.4 µm, n = 20) by 12.7 to 19.4 µm ($\bar{X}$= 16.1 µm, n = 20)

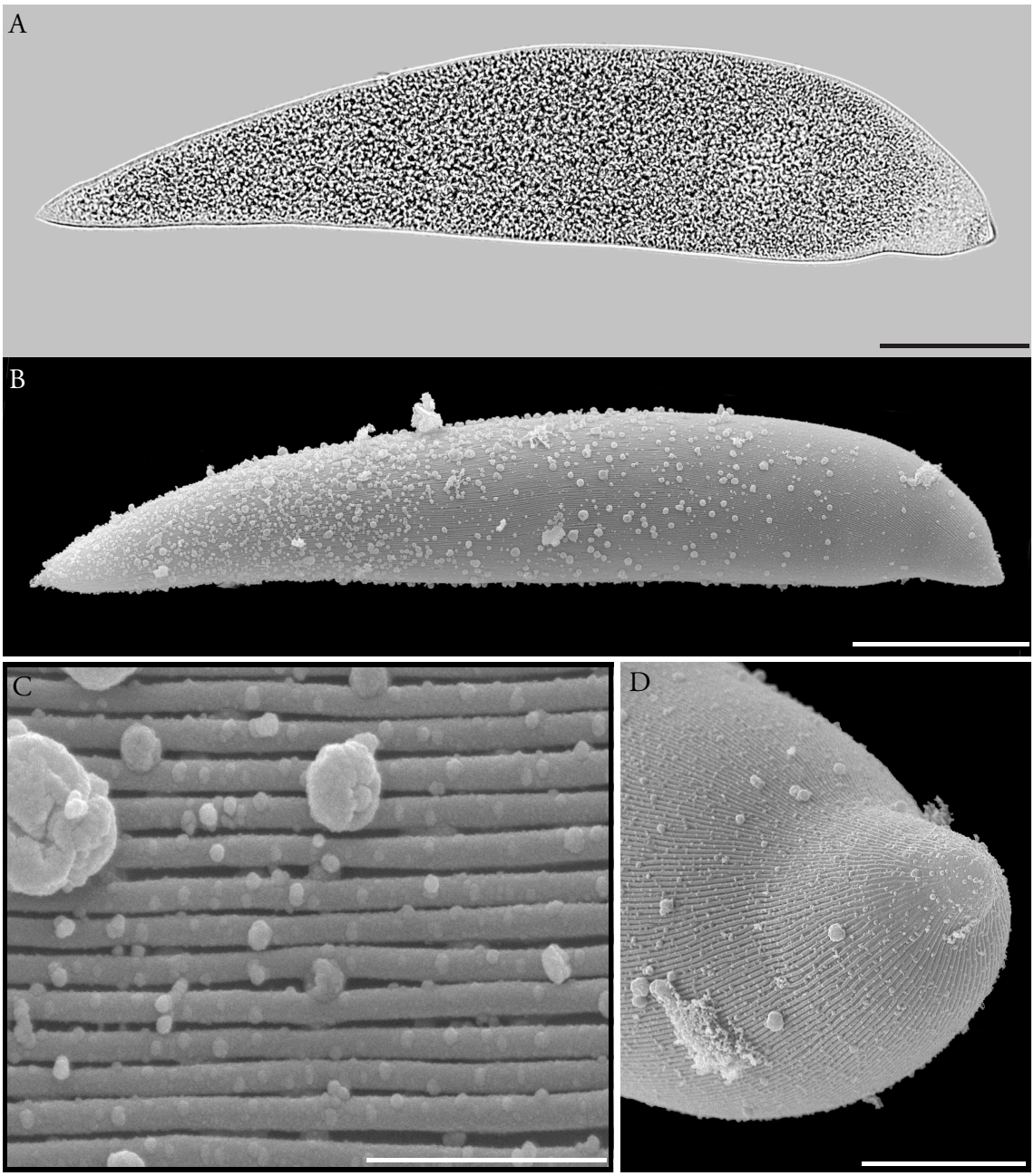

Figure 3.2: Light micrograph (LM) and scanning electron micrographs (SEM) of *Lecudina dolabra* sp. nov. showing trophozoite morphology. Mucron oriented to the right. (A) LM of trophozoite taken in differential interference contrast (DIC). Subulate cell with inconspicuous nucleus (n) situated in the anterior fifth of the body. (B) SEM of the trophozoite showing overall shape and morphology. (C) SEM of epicytic folds forming a longitudinal array at a density of 3 folds/µm (D) SEM of the anterior portion of the cell including the mucron which protrudes at an angle from the body. Scale bars: A, B = 30 µm; C = 2 µm; D = 10 µm.

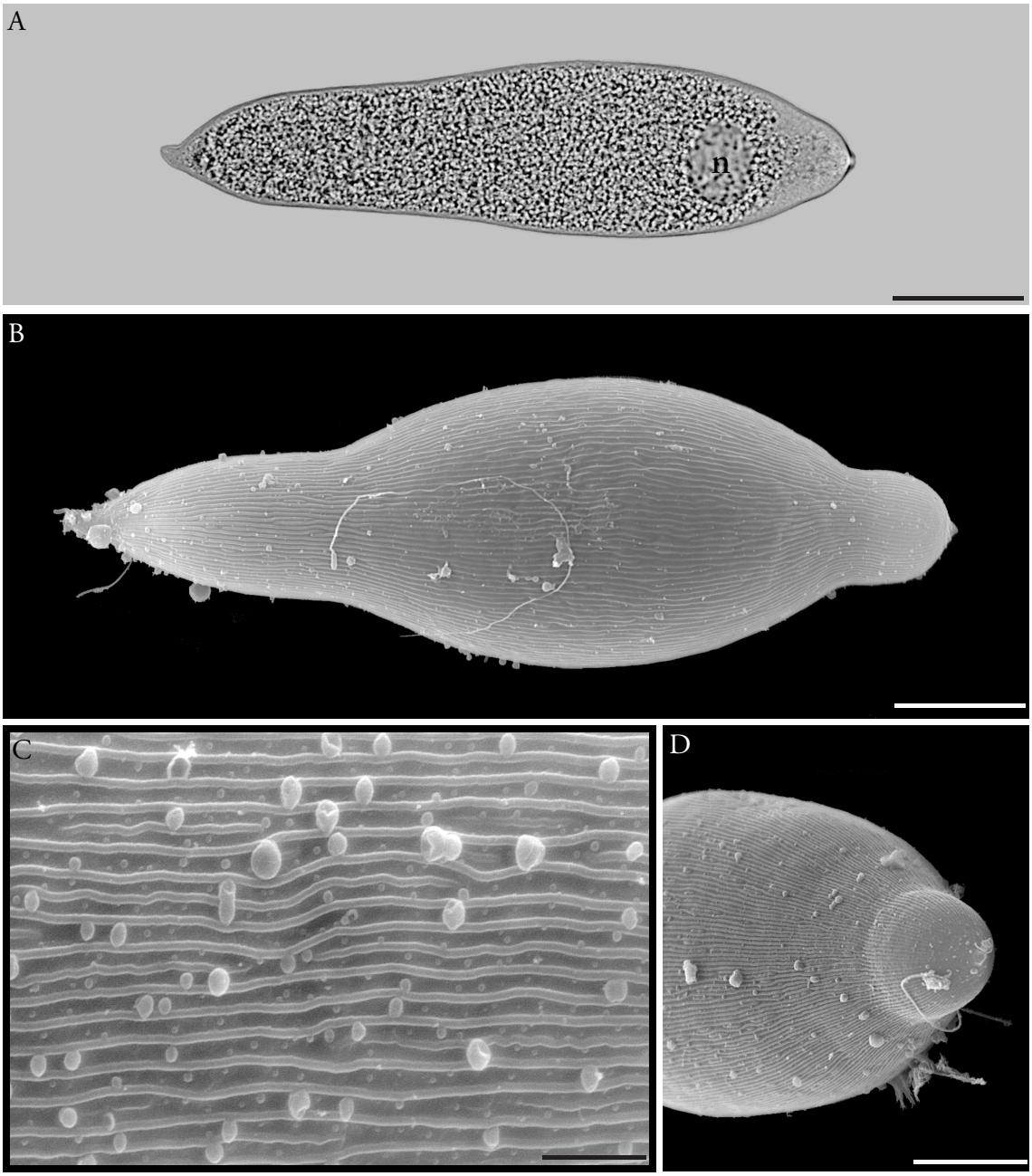

Figure 3.3: Light micrograph (LM) and scanning electron micrographs (SEM) of *Lecudina savignyii* sp. nov. showing trophozoite morphology. Mucron oriented to the right. (A) LM of trophozoite taken in differential interference contrast (DIC). Lanceolate cell with oval nucleus (n) situated in the anterior sixth of the body. (B) SEM of the trophozoite showing overall shape and morphology. (C) SEM of epicytic folds forming a longitudinal array at a density of 3 folds/µm (D) SEM of the anterior portion of the cell including the small mucron. Scale bars: A, B = 10 µm; C = 2 µm; D = 10 µm.

was located approximately one fifth of the total body length from the anterior of the cell. The nucleolus, placed at the anterior end of the nucleus, was also circular and measured between 4.2 to 11.9 µm ($\bar{X}$= 7.3 µm, n = 20) in diameter. The cell surface comprised of epicytic folds arranged longitudinally at a density of 3–4 folds/µm (Fig. 3.4C). The mucron consisted of a protrusion that bent ventrally which could be clearly seen from a lateral view (Fig. 3.4D). Gliding motility was observed.

3.4.5 SSU rDNA sequences and phylogenetic analyses

The 90-taxon alignment of SSU rDNA sequences yielded the dinoflagellates (98% Maximum likelihood bootstrap [MLB], 1.00 Bayesian posterior probability [BPP]) and an ingroup of apicomplexans sorted into broad groups situated on a poorly resolved backbone (Fig. 3.5). Both maximum likelihood and Bayesian analyses recovered identical tree topologies. The deepest apicomplexan nodes found piroplasmid, coccidian, rhytidocystid, cryptosporidian, and gregarine clades. Two terrestrial gregarine clades were recovered: terrestrial gregarine clade I (94 MLB, 1.00 BPP) and terrestrial gregarine clade II (100 MLB, 1.00 BPP). The marine eugregarines (69 MLB, 0.99 BPP) formed a sister clade to terrestrial gregarine Clade I and included the capitellid gregarines, urosporids, lecudininds, *Difficilina*, *Veloxidium*, and paralecudinids. Archigregarines were unresolved with *Selenidium* forming three separate branches and sipunculid gregarines forming a fourth archigregarine branch.

The SSU rDNA sequences that were obtained for each of the novel species included in this study formed distinct branches within the lecudinids (Figs. 3.5, 3.6). The 90-taxon phylogeny placed *Le. pollywoga* sp. nov. at the base of the lecudinids in contrast to the 48-taxon phylogeny which placed *Le. longissimi* and *Le. phyllochaetopteri* at the base with *Le. pollywoga* sp. nov. diverging from the rest of the lecudinids on a shallower node. The individual sequences for *Le. pollywoga* sp. nov., in both cases, clustered with each other with strong support (100 MLB, 1.00 BPP). *Lecudina savignyii* sp. nov. formed a sister lineage to *Le. ascidiae* comb. nov. (90-taxon: 100 MLB, 1.00 BPP; 48-taxon: 98

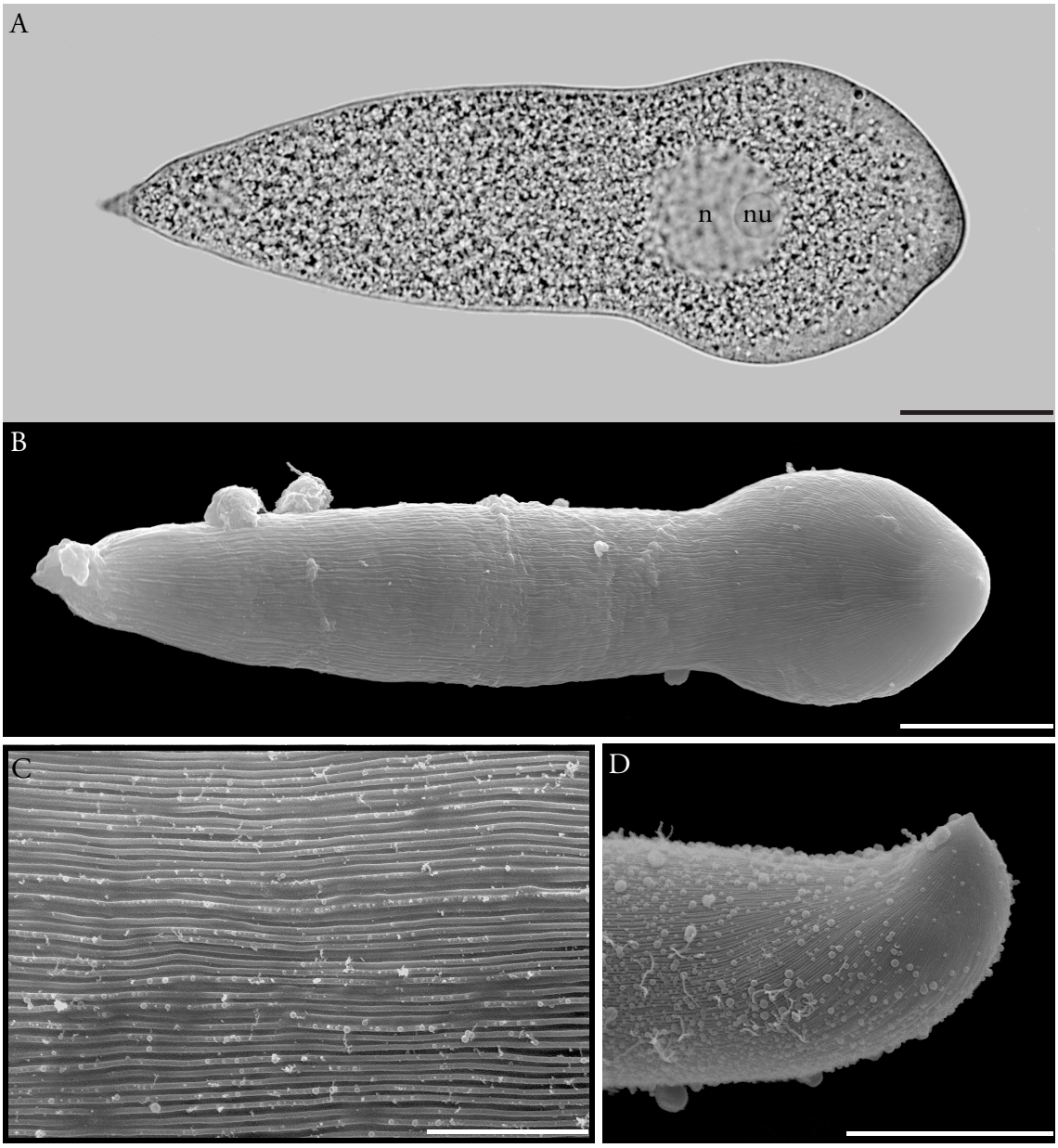

Figure 3.4: Light micrograph (LM) and scanning electron micrographs (SEM) of *Lecudina pollywoga* sp. nov. showing trophozoite morphology. Mucron oriented to the right. (A) LM of trophozoite taken in differential interference contrast (DIC). Spatulate, tadpole-shaped cell with nucleus (n) and nucleolus (nu) situated in the anterior fifth of the body. (B) SEM of the trophozoite showing overall shape and morphology. (C) SEM of epicytic folds forming a longitudinal array at a density of 3–4 folds/µm (D) SEM of the anterior portion of the cell including an inconspicuous mucron that bends ventrally and is most observable from a lateral view. Scale bars: A, B = 20 µm; C = 5 µm; D = 20 µm.

MLB, 1.00 BPP), the type species for ex. *Lankesteria*, and these two species formed a clade with *Le. cystodytae* comb. nov. (90-taxon: 90 MLB, 1.00 BPP; 48-taxon: 98 MLB, 1.00 BPP). *Lecudina dolabra* sp. nov. and *Le. kaiteriteriensis* sp. nov. were recovered as sister taxa to each other (90-taxon: 94 MLB, 1.00 BPP; 48-taxon: 74 MLB, 0.79 BPP), but the phylogenetic position of these two species in the context of the lecudinid topology is uncertain (90-taxon: 94 MLB, 1.00 BPP; 48-taxon: 74 MLB, 0.79 BPP).

Lecudina spp. and *Lecudina* spp. comb. nov. (ex. *Lankesteria*) did not form two separate clades. Instead, the overall topology of the lecudinids consisted of a highly supported clade comprised of *Lecudina* spp. and *Lecudina* spp. comb. nov. (ex. *Lankesteria*) mixed together (90-taxon: 100 MLB, 1.00 BPP; 48-taxon: 100 MLB, 1.00 BPP; Fig. 3.6, Key node 1). The type species of *Lecudina*, *Le. pellucida*, was sister to *Le. caspera* (90-taxon: 91 MLB, 1.00 BPP; 48-taxon: 80 MLB, 1.00 BPP) and was nested within a strongly supported clade of *Lecudina* spp. comb. nov. (ex. *Lankesteria*) (90-taxon: 99 MLB, 1.00 BPP; 48-taxon: 100 MLB, 1.00 BPP; Fig 3.6, Key node 2).

3.5 Discussion

3.5.1 Systematics and evolutionary history of *Lankesteria* and *Lecudina*

Lankesteria was a poorly defined genus that encompassed taxonomically dissimilar species including gregarines that infect ascidians, chaetognaths, turbellarians, and insects (Levine, 1977). Following the removal of the insect gregarines from *Lankesteria* and into *Ascocystis* by Grassé (1953), Ormières (1965) proposed that *Lankesteria* be kept solely for the gregarines that parasitize urochordates. *Lecudina* is closely related to *Lankesteria* and consists of gregarine taxa that infect a variety of polychaete hosts. Théodoridès (1967) suggested that *Lankesteria* and *Lecudina* share a common evolutionary origin and diverged into two genera that infect distinct hosts (i.e., ascidians and polychaetes). There are indeed morphological similarities between *Lankesteria* and *Lecudina* such as

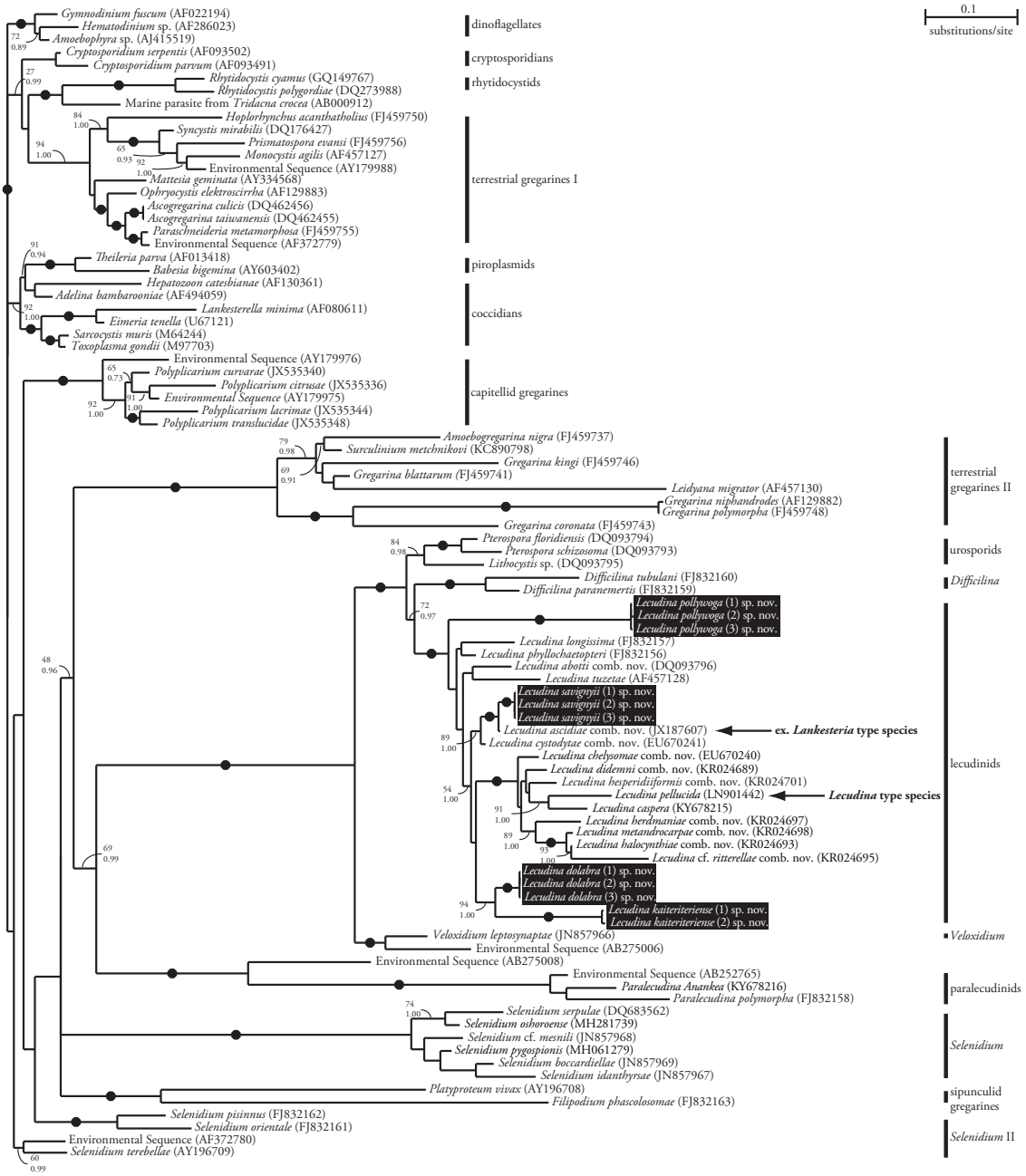

Figure 3.5: Maximum likelihood phylogeny inferred from a 90 taxa dataset of SSU rDNA sequences with 1,440 unambiguously aligned sites using the GTR+I+Γ model of substitution (proportion of invariable sites = 0.1970, gamma shape = 0.6960). Numbers above the branches indicate bootstrap support and numbers below indicate Bayesian posterior probabilities. Black dots on branches denote when both bootstrap support and Bayesian posterior probabilities were equal to or $>$ 95 and 0.99 respectively. Branches without support values had bootstrap support and Bayesian posterior probabilities below 60 and 0.95 respectively. The new species described in the current study are highlighted with black boxes. Black dots to the right of taxon names denote polychaete hosts and asterisks denote ascidian hosts.

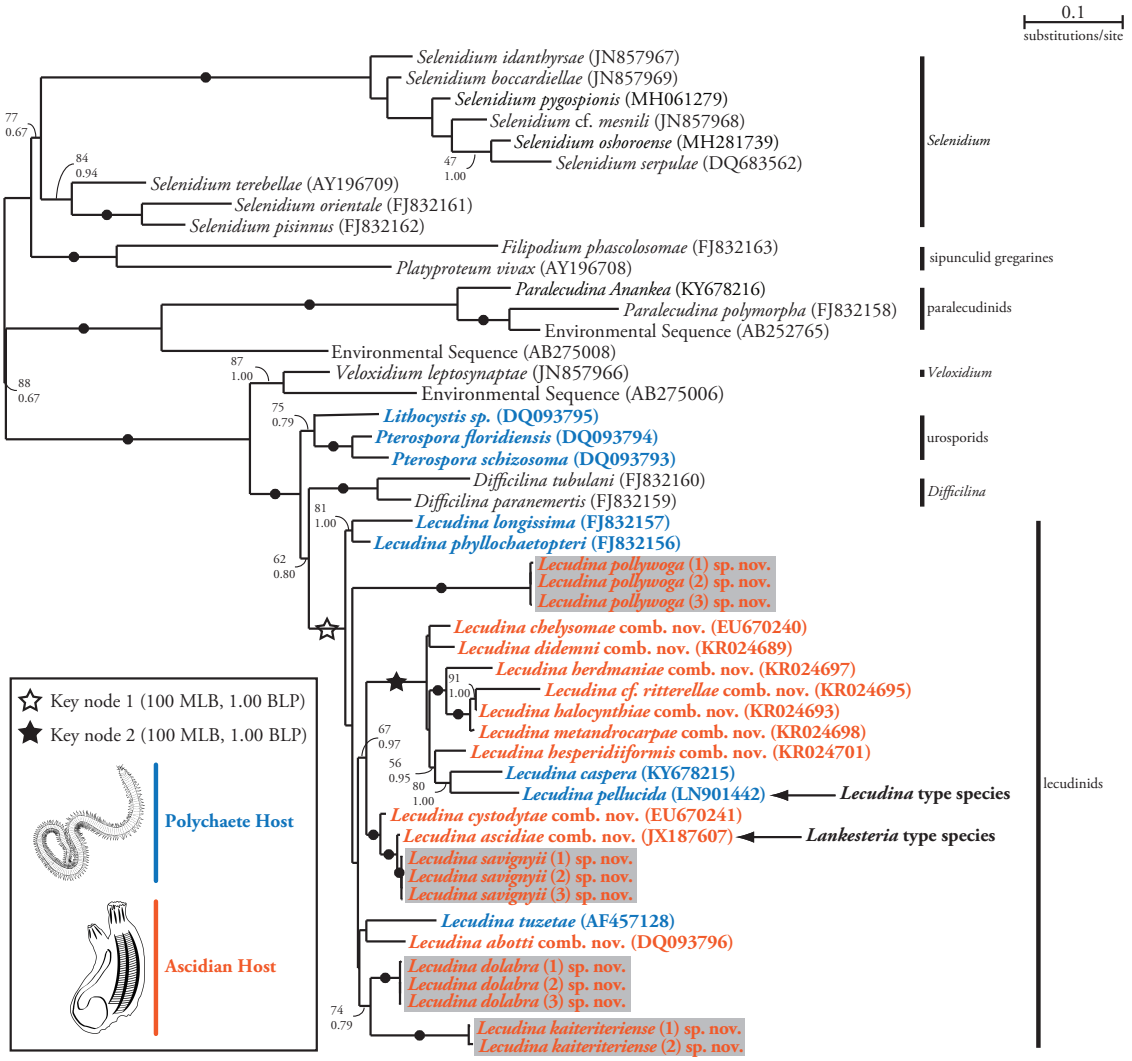

Figure 3.6: Maximum likelihood tree inferred from a 48 taxa dataset of SSU rDNA sequences with 1,444 unambiguously aligned sites using the GTR+I+Γ model of substitution (proportion of invariable sites = 0.2000, gamma shape = 0.6130). Numbers above the branches indicate bootstrap support and numbers below indicate Bayesian posterior probabilities. Black dots on branches denote when both bootstrap support and Bayesian posterior probabilities were equal to or $>$ 95 and 0.99 respectively. Branches without support values had bootstrap support and Bayesian posterior probabilities below 60 and 0.95 respectively. White star (key node 1) marks the *Lecudina* spp. and *Lecudina* spp. comb. nov. (ex. *Lankesteria*) clade. The black star (key node 2) marks the clade comprised of the *Lecudina* type species nested within ex. *Lankesteria*. Taxa in blue are parasites of polychaete hosts whereas taxa in orange are parasites of ascidian hosts. The new species described in the current study are highlighted with gray boxes.

unsegmented intracellular development, an elongated morphology that ends anteriorly at a mucron, and head-to-head syzygy (Levine, 1977), and overall lifecycle (Desportes and Schrével, 2013). Early molecular phylogenetic studies supported distinct *Lankesteria* and *Lecudina* lineages and revealed three subclades comprised of (1) *La. abbotti* and *La.* sp.; (2) *Le. tuzetae* and an environmental sequence; and (3) *La. chelysomae* and *La. cystodytae* (Desportes and Schrével, 2013). Moreover, Desportes and Schrével (2013) elaborate that the above-mentioned subclades (1) and (3) not clustering together to form a clade is a situation which requires additional molecular data to address. The molecular phylogenetic analyses from the present study do not recover these same subclades and they reveal a taxonomic problem whereby *Lecudina* species are scattered and distributed within *Lankesteria* clades.

My data corroborate the notion of a common origin between *Lankesteria* and *Lecudina*, but fail to recover either as separate monophyletic groups. Rather, both genera are bound together in one clade (Fig. 3.6, Key node 1) with *Lecudina* species scattered amongst *Lankesteria* as follows: *Le. longissima* and *Le. phyllochaetopteri* as early branching sister taxa within the lecudinids; *Le. pellucida*, the type species of *Lecudina*, is sister to *Le. caspera* and is nested within a highly supported clade of *Lankesteria* species; and *Le. tuzetae* is sister to *L. abbotti* on their own branch flanked by *Lankesteria* species. The placement of *Le. pellucida* within a strongly supported clade of *Lankesteria* species (Fig. 3.6, Key node 2) offers evidential support for the refutation of *Lecudina* and *Lankesteria* as distinct genera. From an evolutionary standpoint, it can be inferred that the most recent ancestor to the lecudinids was a parasite of polychaetes based on how other gregarines that infect polychaetes (e.g., paralecudinids, *Pterospora*, *Selenidium*) occupy deeper nodes. The switch to ascidian parasitism was then made at the base of the *Lecudina* clade (Fig. 3.6, Key node 1) although the precise topology remains unresolved. Morphological resemblance between *Lecudina* parasites of polychaete hosts deep in the phylogeny to those species nested within ascidian parasites is perhaps due to convergence following a secondary switch to polychaete hosts.

Phylogenetic evidence for evolutionary mechanisms such as host switching is in contrast to the convention that gregarines are highly host specific (Perkins et al., 2002) and the use of host species as a major factor in delimiting gregarine species (Levine, 1979). The discovery of new gregarines in past studies has shown that closely related gregarines infect closely related hosts (e.g., Iritani et al. 2018; Rueckert et al. 2015; Simdyanov et al. 2015; Wakeman and Leander 2013a). This observation has also contributed to the view that gregarines are host specific. Detwiler and Janovy (2008), however, demonstrated that gregarines can infect species other than their natural hosts under the right experimental conditions. The scattered phylogenetic distribution of *Lecudina* species that parasitize polychaetes and ascidians further shows that host switching has likely played a role in gregarine evolution. The co-evolutionary relationship between gregarines and their hosts, diversification through mechanisms such as host switching, and the phylogenetic congruence between gregarine parasites and their hosts are all aspects of gregarine biology that deserve further study.

Previously published marine eugregarine phylogenies (e.g., Iritani et al. 2017; Rueckert et al. 2015; Rueckert and Leander 2008; Schrével et al. 2016) likely did not detect the problematic distribution of *Lecudina* species simply because these studies employed datasets that were comprehensive for a specific clade of concern, but were not inclusive of all comparable data for *Lankesteria* and *Lecudina*. The nested placement of *Le. pellucida* within a clade of *Lankesteria*, as seen in the present study, suggests that *Lankesteria* and *Lecudina* require taxonomic revision. The diagnostic morphological criteria for *Lankesteria* include: a mucron, of variable complexity, present although not always apparent; more or less spatulate trophozoites; head-to-head or scissors-like syzygy; spherical gametocysts; anisogamy present; ellipsoidal oocysts, often with a plug at each end; and parasitism of ascidians (Levine, 1977). Other characteristics that are often included in the description of new *Lankesteria* species are a brownish coloration associated with the accumulation of amylopectin granules in the cytoplasm, the infection occurring within the host intestine or stomach, and gliding motility (Desportes and Schrével 2013; Levine

1981; Mita et al. 2012; Rueckert et al. 2015; Rueckert and Leander 2008).

In contrast, the diagnostic criteria for *Lecudina* include: a simple mucron without hooks or exfoliations, trophozoites without myonemes, ovoid oocysts which are thickened at one end, and parasitism of polychaetes and other marine invertebrates (Levine, 1976). These morphological diagnostics for *Lankesteria* and *Lecudina* are subjective and lack quantitative characteristics that can conclusively classify a given species within either genus. Thus, retaining *Lankesteria* by establishing a new genus for *Le. longissimi* and *Le. phyllochaetopteri*, a new monotypic genus for *Le. tuzetae*, and emending *Lecudina* to only include *Le. pellucida* and *Le. caspera* would be taxonomically undesirable especially in unison with the lack of distinguishing morphological characteristics. I instead commit to an alternative taxonomic act whereby *Lankesteria* is combined with *Lecudina* into the emended genus *Lecudina* (Mingazinni 1891) Iritani, Horiguchi, Wakeman 2019 (Table 3.1).

3.5.2 Systematic and taxonomic considerations for *Le. pollywoga* sp. nov., *Le. savignyii* sp. nov., *Le. dolabra* sp. nov., *Le. kaiteriteriensis* sp. nov.

Lecudina pollywoga sp. nov. was recovered with low statistical support in two different positions in the 90-taxon phylogeny and the 48-taxon phylogeny. The 90-taxon phylogeny places *Le. pollywoga* sp. nov. diverging at the base within the lecudinids. In contrast, the 48-taxon phylogeny suggests that *Le. longissimi* and *Le. phyllochaetopteri* are the earliest branching taxa with a subsequent divergence giving rise to *Le. pollywoga* sp. nov. and the rest of the *Lecudina* species. Morphologically, *Le. pollywoga* sp. nov. shares general similarities with the line drawings of *La. diaphanis* and *La. pittendrighi* (Levine, 1981). The trophozoite stage of *Lankesteria diaphanis* is described as being brownish overall with an elongated body ending in a mucron which often bears a small knob at the anterior end. Although *Le. pollywoga* sp. nov. shares the overall shape and brownish colouration, *La diaphanis* is smaller measuring 78 µm long by 17-30 µm wide compared

to *Le. pollywoga* sp. nov. which measures 118 µm long by 35 µm on average. Moreover, *La. diaphanis* is capable of metabolic movement, which was not observed in *Le. pollywoga* sp. nov. The hosts are also different as *La. diaphanis* was isolated from the colonial ascidian *Eudistoma diaphanes* in California. *Lankesteria pittendrighi* trophozoites are described as being brownish with a broadly lanceolate body or with an anterior swelling starting near the anteriorly positioned nucleus (Levine, 1981). *Lankesteria pittendrighi* is, however, smaller than *Le. pollywoga* sp. nov., measuring 52–60 µm long by 23–31 µm. Additionally, the hosts are different as *Lankesteria pittendrighi* was isolated from the solitary sea squirt *Ascidia ceratodes* in California.

Lecudina pollywoga sp. nov., therefore, is distinguishable from previously described species in terms of size, host species, and the lack of metabolic movement. Furthermore, although the position of the *Le. pollywoga* sp. nov. lineage is uncertain on the molecular phylogeny, there is high support for *Le. pollywoga* sp. nov. sequences clustering amongst each other to the exclusion of other known sequences. These data, therefore, strongly suggests that *Le. pollywoga* sp. nov. is a new species of *Lecudina*.

Lecudina savignyii sp. nov. and *Le. ascidiae* were robustly supported as sister species in both the 90 and 48-taxon phylogenies. Interestingly, *Ciona savignyi* and *C. intestinalis*, the hosts for both gregarine taxa, are also sister species (Stach and Turbeville, 2002; Turon and López-Legentil, 2004). The most significant morphological difference between *Le. savignyii* sp. nov. and *Le. ascidiae* is limited to the general trophozoite shape whereby *Le. savignyii* sp. nov. is lanceolate with a fat, bulging center that tapers to a narrow anterior whereas *Le. ascidiae* is either described, hand-drawn, or photographed as a clavate cell with a round anterior (Ciancio et al., 2001; Levine, 1981; Mita et al., 2012). The sizes of the two species overlap: *Le. savignyii* sp. nov. measured 69 µm long and 23 µm wide on average compared to *Le. ascidiae* which measures 50–99 µm long, 20–30 µm wide (Levine, 1981) or 62 µm long, 19 µm wide (Mita et al., 2012). Furthermore, both species were found in the intestine of their respective hosts and were capable of gliding motility.

The molecular phylogenetic analyses, however, suggest that *Le. savignyii* sp. nov. represents a unique lineage and the sequences from individual isolates cluster together and exclude the *Le. ascidiae* sequences. Additionally, *Le. savignyii* sp. nov. infects *C. savignyi* and has not been observed in previous investigations of *C. intestinalis* by other authors. Therefore, these data suggest that *Le. savignyii* sp. nov. is a new species.

Le. kaiteriteriensis sp. nov. and *Le. dolabra* sp. nov. were recovered as sister species based on the molecular phylogenetic data. The two species are morphologically dissimilar with *Le. kaiteriteriensis* sp. nov. trophozoites possessing a lanceolate shape that arches to an overall crescent shape whereas *Le. dolabra* sp. nov. trophozoites are subulate and taper to a sharp point at both the posterior and anterior ends. Their size ranges also do not overlap; *Le. kaiteriteriensis* sp. nov. was 268 µm long and 27 µm wide on average in contrast to *Le. dolabra* sp. nov. which measured 174 µm long and 33 µm wide. Furthermore, each species was isolated from different hosts from separate localities.

Molecular phylogenetics also showed that the species cluster with their respective single isolate sequences in the molecular phylogenies. Therefore, both *Le. kaiteriteriensis* sp. nov. and *Le. dolabra* sp. nov. represent new species of *Lecudina*.

3.5.3 Emended description of *Lecudina*

A mucron is present although not always conspicuous. Mucron can be simple or complex, but without hooks or exfoliations. Oocysts are ovoid to ellipsoidal with a plug or thickening at one end. Gliding motility is often observed, but not always. Coloration is brownish or golden due to the accumulation of amylopectin granules in the cytoplasm. Parasitism in polychaetes, ascidians, and other marine invertebrates.

3.5.4 Taxonomic summary

Phylum Apicomplexa Levine 1970

Order Eugregarinorida Léger 1900

Family Lecudinidae Kamm 1922

Lecudina Mingazinni 1891

3.5.5 *Lecudina kaiteriteriensis* sp. nov.

Description. Lanceolate trophozoites bend to an overall crescent shape and ranged between 165.3 to 405.7 µm ($\bar{X}$ = 268.0 µm, n = 80) in length and 32.7 to 114.6 µm ($\bar{X}$ = 50.0 µm, n = 80) in width. Dark brown posterior gradually turns light gray near the nucleus. Silver to translucent mucron is conspicuous and stubby. Oval nucleus with a major axis 38.5 to 71.7 µm ($\bar{X}$ = 56.3 µm, n = 20) and a minor axis between 35.7 to 66.0 µm ($\bar{X}$ = 49.6 µm, n = 20) situated in the first anterior third of the cell body. Distinct nucleolus forms a ring measuring 14.8 to 31.6 µm ($\bar{X}$ = 25.4 µm, n = 20) by 17.2 to 29.7 µm ($\bar{X}$ = 23.7 µm, n = 80). Longitudinal epicytic folds line the cell surface at 4 folds/µm. Gliding motility.

DNA sequence. SSU rDNA sequence (GenBank xxxxxx).

Type locality. Kaiteriteri Beach, Kaiteriteri, New Zealand (41°2′7.7″S 173°1′21.4″E). Host commonly found on the underside or cracks of large (∼1 m diameter) rocks in the low intertidal to subtidal zones.

Type habitat. Marine.

Type host. *Pyura* sp. Molina 1782 (Chordata, Tunicata, Ascidiacea, Stolidobranchia, Pyuridae).

Location in host. Intestinal lumen.

Iconotype. Figure 3.1A.

Hapantotype. Trophozoites on SEM stubs with a gold/palladium alloy sputter coat have been stored in the algal and protist collection in the Hokkaido University Museum (DI – 2).

LSID. xxxxxx.

Etymology. Species name refers to the type locality of Kaiteriteri, New Zealand.

3.5.6 *Lecudina dolabra* sp. nov.

Description. Subulate trophozoites consisting of rod-like body and tapering posterior ending in a sharp point. Both posterior end and mucron are transparent; cell body is light golden brown. Trophozoites range between 163.7 to 207.1 µm ($\bar{X}$ = 173.7 µm, n = 40) in length and 22.7 to 43.5 µm ($\bar{X}$ = 32.6 µm, n = 40) in width. Faint, inconspicuous nucleus with a major axis between 14.4 to 21.9 µm ($\bar{X}$ = 18.3 µm, n = 10) and a minor axis between 6.0 µm to 16.4 µm ($\bar{X}$ = 12.8 µm, n = 10) situated in the first anterior fifth of trophozoite body. Mucron is translucent, bent, and ends in point. Cell surface constituted by longitudinal epicytic folds at a 3 folds/µm density. Gliding motility.

DNA sequence. SSU rDNA sequence (GenBank xxxxxx).

Type locality. Waikawa Marina, Marlborough, New Zealand (41°15′37.1″S 173°16′53.0″E). Host commonly found on fouled ropes submerged off the side of docks.

Type habitat. Marine.

Type host. *Asterocarpa humilis* Heller 1878 (Chordata, Tunicata, Ascidiacea, Stolidobranchia, Styelidae).

Location in host. Intestinal lumen.

Iconotype. Figure 3.2A.

Hapantotype. Trophozoites on SEM stubs with a gold/palladium alloy sputter coat have been stored in the algal and protist collection in the Hokkaido University Museum (DI – 3).

LSID. xxxxxx.

Etymology. Species name refers to the morphological resemblance of the trophozoite to the head of a pickaxe or dolabra.

3.5.7 *Lecudina savignyii* sp. nov.

Description. Trophozoites roughly lanceolate with a tapering posterior and anterior. Body is fat and bulges markedly in some individuals. Gray to light brown with a translucent mucron. Trophozoites range between 48.5 to 85.8 µm ($\bar{X}$ = 68.7 µm, n = 40) in length

and 14.9 to 35.0 µm ($\bar{X}$ = 23.5 µm, n = 40) in width. Oval nucleus situated within the first sixth of the cell from the anterior with a major axis between 8.0 to 12.1 µm ($\bar{X}$ = 9.4 µm, n = 20) and a minor axis between 6.1 to 10.4 µm ($\bar{X}$ = 8.2 µm, n = 20). Translucent mucron capped with small bump. Cell surface comprised of longitudinal epicytic folds at a 3 folds/µm density. Gliding motility.

DNA sequence. SSU rDNA sequence (GenBank xxxxxx).

Type locality. Nelson Marina, Nelson, New Zealand (41°15′37.1″S 173°16′53.0″E) on fouled ropes hanging from the docks.

Type habitat. Marine.

Type host. *Ciona savignyi* Herdman 1882 (Chordata, Tunicata, Ascidiacea, Phlebobranchia, Cionidae).

Location in host. Intestinal lumen.

Iconotype. Figure 3.3A.

Hapantotype. Trophozoites on SEM stubs with a gold/palladium alloy sputter coat have been stored in the algal and protist collection in the Hokkaido University Museum (DI – 4).

LSID. xxxxxx.

Etymology. Species name refers to the name of the host: *Ciona savignyi*.

3.5.8 *Lecudina pollywoga* sp. nov.

Description. Spatulate trophozoites with elongated, rod-like body ending in a spherical anterior. Golden-brown overall with translucent posterior and mucron. Trophozoites between 96.6 to 155.1 µm ($\bar{X}$ = 118.4 µm, n = 40) in length and 25.2 to 43.6 µm ($\bar{X}$ = 34.7 µm, n = 40) in width. Circular nucleus between 13.2 to 21.1 µm ($\bar{X}$ = 18.4 µm, n = 20) by 12.7 to 19.4 µm ($\bar{X}$ = 16.1 µm, n = 20) located one fifth of the total body length from anterior. Circular nucleolus measures between 4.2 to 11.9 µm ($\bar{X}$ = 7.3 µm, n = 20) in diameter and is situated at the anterior portion of nucleus. Translucent mucron bends ventrally and is seen clearly from a lateral view. Cell surface comprised of longitudinal

epicytic folds at a 3-4 folds/μm density. Gliding motility.

DNA sequence. SSU rDNA sequence (GenBank xxxxxx).

Type locality. Nelson Marina, Nelson, New Zealand (41°16′2.8″S 174°2′18.4″E) on fouled ropes hanging from the docks.

Type habitat. Marine.

Type host. *Molgula complanata* Alder & Hancock 1870 (Chordata, Tunicata, Ascidiacea, Stolidobranchia, Molgulidae).

Location in host. Intestinal lumen.

Iconotype. Figure 3.4A.

Hapantotype. Trophozoites on SEM stubs with a gold/palladium alloy sputter coat have been stored in the algal and protist collection in the Hokkaido University Museum (DI – 5).

LSID. xxxxxx.

Etymology. Species name refers to the morphological resemblance of the trophozoite to both a tadpole and a stage two Demogorgon (i.e., pollywog in both cases) from the hit Netflix series Stranger Things (Season 2, Episode 3).

Table 3.1: New combinations of *Lecudina* with basionyms, synonyms, and reference to original literature.

New Combinations: *Lecudina* (Mingazinni 1891) Iritani, Horiguchi, & Wakeman 2019	**Basionym; Synonym**	**Literature**
Lecudina aplidii (Levine 1981) Iritani, Horiguchi, & Wakeman comb. nov.	*Lankesteria aplidii* Levine 1981	Levine, 1981

Lecudina diaphanis (Levine 1981) Iritani, Horiguchi, & Wakeman comb. nov.	*Lankesteria diaphanis* Levine 1981	Levine, 1981
Lecudina montereyensis (Levine 1981) Iritani, Horiguchi, & Wakeman comb. nov.	*Lankesteria montereyensis* Levine 1981	Levine, 1981
Lecudina psammii (Levine 1981) Iritani, Horiguchi, & Wakeman comb. nov.	*Lankesteria psammii* Levine 1981	Levine, 1981
Lecudina ritterii (Levine 1981) Iritani, Horiguchi, & Wakeman comb. nov.	*Lankesteria ritterii* Levine 1981	Levine, 1981
Lecudina pittendrighi (Levine 1981) Iritani, Horiguchi, & Wakeman comb. nov.	*Lankesteria pittendrighi* Levine 1981	Levine, 1981
Lecudina ascidiae (Lankester 1872) Iritani, Horiguchi, & Wakeman comb. nov.	*Monocystis ascidiae* Lankester 1872; *Gregarina cionae* Frenzel 1885; *Urospora cionae* Parona 1886 and *U. cionae* Gruber 1886	Frenzel, 1885; Gruber, 1886; Lankester, 1872; Parona, 1886
Lecudina abbotti (Levine 1981) Iritani, Horiguchi, & Wakeman comb. nov.	*Lankesteria abbotti* Levine 1981	Levine, 1981

Lecudina ritterellae (Levine 1981) Iritani, Horiguchi, & Wakeman comb. nov.	*Lankesteria ritterellae* Levine 1981	Levine, 1981
Lecudina euherdmaniae (Levine 1981) Iritani, Horiguchi, & Wakeman comb. nov.	*Lankesteria euherdmaniae* Levine 1981	Levine, 1981
Lecudina pescaderoensis (Levine 1981) Iritani, Horiguchi, & Wakeman comb. nov.	*Lankesteria pescaderoensis* Levine 1981	Levine, 1981
Lecudina synoici (Levine 1981) Iritani, Horiguchi, & Wakeman comb. nov.	*Lankesteria synoici* Levine 1981	Levine, 1981
Lecudina ormieresi (Levine 1977) Iritani, Horiguchi, & Wakeman comb. nov.	*Lankesteria ormieresi* Levine 1977	Levine, 1977
Lecudina chelyosomae (Rueckert & Leander 2008) Iritani, Horiguchi, & Wakeman comb. nov.	*Lankesteria chelyosomae* Rueckert and Leander 2008	Rueckert and Leander, 2008
Lecudina cystodytae (Rueckert & Leander 2008) Iritani, Horiguchi, & Wakeman comb. nov.	*Lankesteria cystodytae* Rueckert and Leander 2008	Rueckert and Leander, 2008

Lecudina hesperidiiformis (Rueckert, Wakeman, & Leander 2015) Iritani, Horiguchi, & Wakeman comb. nov.	*Lankesteria hesperidiiformis* Rueckert, Wakeman, & Leander 2015	Rueckert et al., 2015
Lecudina metandrocarpae (Rueckert, Wakeman, & Leander 2015) Iritani, Horiguchi, & Wakeman comb. nov.	*Lankesteria metandrocarpae* Rueckert, Wakeman, & Leander 2015	Rueckert et al., 2015
Lecudina halocynthiae (Rueckert, Wakeman, & Leander 2015) Iritani, Horiguchi, & Wakeman comb. nov.	*Lankesteria halocynthiae* Rueckert, Wakeman, & Leander 2015	Rueckert et al., 2015
Lecudina herdmaniae (Rueckert, Wakeman, & Leander 2015) Iritani, Horiguchi, & Wakeman comb. nov.	*Lankesteria herdmaniae* Rueckert, Wakeman, & Leander 2015	Rueckert et al., 2015
Lecudina didemni (Rueckert, Wakeman, & Leander 2015) Iritani, Horiguchi, & Wakeman comb. nov.	*Lankesteria didemni* Rueckert, Wakeman, & Leander 2015	Rueckert et al., 2015

Lecudina parascidiae (Duboscq & Harant 1923) Iritani, Horiguchi, & Wakeman comb. nov.	*Lankesteria parascidiae* Duboscq & Harant 1923	Duboscq and Harant, 1923
Lecudina ascidiarum (Duboscq & Harant 1923) Iritani, Horiguchi, & Wakeman comb. nov.	*Lankesteria ascidiarum* Duboscq & Harant 1923	Duboscq and Harant, 1923
Lecudina siedleckii (Duboscq & Harant 1923) Iritani, Horiguchi, & Wakeman comb. nov.	*Lankesteria siedleckii* Duboscq & Harant 1923	Duboscq and Harant, 1923
Lecudina ascidiellae (Duboscq & Harant 1923) Iritani, Horiguchi, & Wakeman comb. nov.	*Lankesteria ascidiellae* Duboscq & Harant 1923	Duboscq and Harant, 1923
Lecudina tuzetae (Ormières 1965) Iritani, Horiguchi, & Wakeman comb. nov.	*Lankesteria tuzetae* Ormières 1965	Ormières, 1965
Lecudina striata (Ormières 1965) Iritani, Horiguchi, & Wakeman comb. nov.	*Lankesteria striata* Ormières 1965	Ormières, 1965
Lecudina acutissima (Ormières 1965) Iritani, Horiguchi, & Wakeman comb. nov.	*Lankesteria acutissima* Ormières 1965	Ormières, 1965
Lecudina botrylli (Ormières 1965) Iritani, Horiguchi, & Wakeman comb. nov.	*Lankesteria botrylli* Ormières 1965	Ormières, 1965

Lecudina zonata (Ormières 1965) Iritani, Horiguchi, & Wakeman comb. nov.	*Lankesteria zonata* Ormières 1965	Ormières, 1965
Lecudina monstrosa (Ormières 1965) Iritani, Horiguchi, & Wakeman comb. nov.	*Lankesteria monstrosa* Ormières 1965	Ormières, 1965
Lecudina globosa (Ormières 1965) Iritani, Horiguchi, & Wakeman comb. nov.	*Lankesteria globosa* Ormières 1965	Ormières, 1965
Lecudina perophoropsis (Ormières 1965) Iritani, Horiguchi, & Wakeman comb. nov.	*Lankesteria perophoropsis* Ormières 1965	Ormières, 1965
Lecudina molgulidarum (Ormières 1965) Iritani, Horiguchi, & Wakeman comb. nov.	*Lankesteria molgulidarum* Ormières 1965	Ormières, 1965
Lecudina morchellii (Ormières 1965) Iritani, Horiguchi, & Wakeman comb. nov.	*Lankesteria morchellii* Ormières 1965	Ormières, 1965
Lecudina gracilis (Ormières 1965) Iritani, Horiguchi, & Wakeman comb. nov.	*Lankesteria gracilis* Ormières 1965	Ormières, 1965
Lecudina maculata (Ormières 1965) Iritani, Horiguchi, & Wakeman comb. nov.	*Lankesteria maculata* Ormières 1965	Ormières, 1965

Lecudina gigantea (Ormières 1965) Iritani, Horiguchi, & Wakeman comb. nov.	*Lankesteria gigantea* Ormières 1965	Ormières, 1965
Lecudina gyriniformis (Ormières 1965) Iritani, Horiguchi, & Wakeman comb. nov.	*Lankesteria gyriniformis* Ormières 1965	Ormières, 1965
Lecudina styelae (Ormières 1965) Iritani, Horiguchi, & Wakeman comb. nov.	*Lankesteria styelae* Ormières 1965	Ormières, 1965
Lecudina diazonae (Mingazzini 1891) Iritani, Horiguchi, & Wakeman comb. nov.	*Lankesteria diazonae* Mingazzini 1891	Mingazzini, 1891
Lecudina distapliae (Mingazzini 1891) Iritani, Horiguchi, & Wakeman comb. nov.	*Lankesteria distapliae* Mingazzini 1891	Mingazzini, 1891
Lecudina butschlii (Mingazzini 1891) Iritani, Horiguchi, & Wakeman comb. nov.	*Lankesteria butschlii* Mingazzini 1891	Mingazzini, 1891
Lecudina amaroucii (Giard 1873) Iritani, Horiguchi, & Wakeman comb. nov.	*Lankesteria amaroucii* Giard 1873	Giard, 1873

Lecudina clavellinae (Labbé1899) Iritani, Horiguchi, & Wakeman comb. nov.	*Lankesteria clavellinae* von Kölliker 1849; Labbé 1899	Labbé 1899; von Kölliker, 1845
Lecudina tethyi (Bogolepova 1953) Iritani, Horiguchi, & Wakeman comb. nov.	*Lankesteria tethyi* Bogolepova 1953	Bogolepova, 1953

3.6 Acknowledgements

This research was supported by a MEXT doctoral scholarship to Davis Iritani, and a joint JSPS/MBIE-RSZN (PG6R180004) provided to Kevin Wakeman, Steve Webb, and Jonathan Banks. We are grateful to the Electron Microscope Laboratory, Research Faculty of Agriculture, Hokkaido University for sharing their critical point dryer, and to Dr. Katrina-Kay Alaimo for providing her expertise in classical Latin and Greek.

4

Description of *Platyproteum* sp. and Reconstruction of the Flagellar Apparatus

4.1 Abstract

The Apicomplexa are a diverse group of obligate parasites to a variety of animal species. *Platyproteum* is an enigmatic, monotypic genus formerly assigned to the Apicomplexa, until a recent phylogenomic study demonstrated that it diverged from the base of the chromerid and colpodellid (chrompodellid) taxa and apicomplexan clade. In the present study, a species of *Platyproteum* is described using a combination of morphological and molecular data. Moreover, a reconstruction of the flagellar apparatus is presented to characterize the presence of flagella which was, until this study, an unknown trait for this

genus. Phylogenetic analyses using SSU rDNA sequences suggested that *P.* sp. is a sister species of *P. vivax* diverging from the base of the chrompodellids and apicomplexans. This study provides new morphological data that corroborates the position of *Platyproteum* amongst other biflagellate species and contributes to an improved definition of *Platyproteum*.

4.2 Introduction

The Apicomplexa are obligate parasites of numerous animal hosts with over 6000 named species classified in 350 genera (Adl et al., 2019). Included in this group are infamous taxa such as *Plasmodium*, *Toxoplasma*, and *Cryptosporidium* that have attracted special attention due to their medical or veterinary impact. Despite the parasitic nature of extant apicomplexan taxa, the ancestor to the group was a free-living, biflagellate organism (Cavalier-Smith, 2004; Leander, 2008; Leander and Keeling, 2003). This evolutionary transition to parasitism has been a topic of great interest and is reflected in retained ancestral traits such as the apicoplast - a modified plastid of red algal origin (Arisue and Hashimoto, 2015; Fichera and Roos, 1997; Kim and Weiss, 2004; Lim and McFadden, 2010; Sato, 2011). Cilia and flagella, on the other hand, are infrequently seen in the apicomplexan life cycle and their presence is generally limited to the male, microgametes of certain taxa (Adl et al., 2019).

Apicomplexans and their closest relatives are included in a group known as the Myzozoa Cavalier-Smith & Chao 2004. Dinoflagellates represent a major myzozoan lineage with species classified in over 300 genera that employ various modes of life including autotrophy, heterotrophy, and parasitism (Adl et al., 2019). Dinoflagellates and other non-apicomplexan myzozoans such as chromerids and colpodellids are characteristically biflagellate (Cavalier-Smith, 2004; Moore et al., 2008; Simpson and Patterson, 1996). The discovery and understanding of these close apicomplexan relatives have greatly informed the understanding of apicomplexan evolutionary history (Cavalier-Smith, 2004; Janouškovec et al., 2015; Kuvardina et al., 2002). Specifically, identifying and character-

izing fundamental traits are necessary to gain an accurate view of apicomplexan phylogenetics which is hindered greatly by poor taxon sampling (Morrison, 2009). Cytoskeletal components, such as the flagellar apparatus, have been studied in apicomplexan relatives as an informative trait for understanding myzozoan evolution (Francia and Striepen, 2014; Leander and Keeling, 2003; Okamoto and Keeling, 2014; Portman et al., 2014).

Platyproteum is a genus of single-celled parasites found in the intestinal tract of sipunculid hosts (Gunderson and Small, 1986; Leander and Keeling, 2003; Leander, 2006; Rueckert and Leander, 2009). The type species for the genus, *Platyproteum vivax* (ex. *Selenidium vivax*), was discovered from the host *Phascolosoma agassizii* (Gunderson and Small, 1986). This first report on *P. vivax* emphasized morphological observation and classified the new species into an existing genus of marine gregarines, *Selenidium*, while noting that there are differences to its congeners in terms of size, plasticity in cell shape, and the lack of permanent superficial striations at the light miscroscope level (Gunderson and Small, 1986). The authors also noted a "small, refractile body" that was visible at the tip of living cells, but not in stained specimens. A subsequent ultrastructural analysis was conducted that observed both internal and external morphology in great detail (Leander and Keeling, 2003; Leander, 2006). Interestingly, the presence of pores and vermiform structures protruding from these pores were noted in these ultrastructural observations. The SSU rDNA for *P. vivax* was sequenced by Rueckert and Leander (2009) and a molecular phylogenetic analysis showed that *P. vivax* should be removed from *Selenidium*. *Platyproteum* was suggested as a new genus to accommodate this taxonomic act. Most recently, a transcriptomic analysis of several eukaryotic groups including a *Platyproteum* sp. showed that *Platyproteum* falls outside of the apicomplexan phylogeny and is instead an early diverging myzozoan lineage near the Apicomplexa and chrompodellids (Mathur et al., 2019).

In the present study, I characterize an undescribed species of *Platyproteum* discovered from the northwestern coast of Hokkaido, Japan. The presence of flagella in the adult stages is shown using both scanning and transmission electron microscopy. Serial

sections of the flagellar apparatus and a schematic reconstruction are also presented in the hopes of further characterizing this enigmatic genus. Finally, a molecular phylogenetic analysis of SSU rDNA sequences shows that *P.* sp. forms a sister relationship with *P. vivax* branching from the base of the chromerid and colpodellid (chrompodellid) taxa and apicompexan clade. The discovery and characterization of these early myzozoan lineages are crucial to informing the evolutionary history of apicomplexan parasitism. This study contributes to that effort by presenting the first characterization of the flagellar apparatus in this formerly apicomplexan genus.

4.3 Methods

4.3.1 Host collection and parasite isolation

Phascolosoma noduliferum Stimpson 1855 was collected from Oshoro, Hokkaido, Japan (43°12′55.2″N 140°51′17.2″E) during the summer of 2019. The animals were found inhabiting the spaces between the roots of seagrass. The worms were transported back to the laboratory and dissected within 48 hours of collection. The procedure involved carefully extracting the digestive tract from the base of the proboscis to the anus. The entire digestive tract was split down its length using fine forceps to expose the contents of the gut in filtered seawater (0.45 µm). Parasites were observed under an inverted light microscope and isolated using hand-drawn glass pipettes. Individual parasites from each host were then washed multiple times in filtered seawater (0.45 µm) and pooled together for subsequent use in light miscopy or scanning electron miscopy. Single-cell isolations were prepared for DNA extraction and sequencing.

4.3.2 Light microscopy

Trophozoite morphology was observed with a Zeiss Axioskop 2 Plus microscope (Carl-Zeiss, Göttingen, Germany) paired to a Canon EOS Kiss X8i digital camera (Canon, Tokyo, Japan). Light micrographs presented in the current dissertation are composites of

multiple high magnification photos taken along the length of the entire cell subsequently stitched together using Panorama Stitcher Mini version 1.10 (Olga Kacher, Boltnev Studio). Micrographs were then refined with GIMP version 2.10.12 (GNU image manipulation program version; The GIMP Team).

4.3.3 Scanning electron microscopy

Trophozoites were pooled and fixed with 2.5% glutaraldehyde for 30 mins on ice. The fixative was washed out with chilled, filtered seawater. Fixation continued with 1% OsO_4 and the trophozoites were left for 30 min on ice. The fixative was removed again with filtered, chilled seawater. The trophozoites were then dehydrated in a graded series of ethanol for 3 min at each of the following concentrations: 50%, 70%, 80%, 90%, and 100%. A Leica EM CPD300 (Leica Microsystems, Wetzlar, Germany) was used for critical point drying. Each SEM stub was sputter coated with gold for 180 s at 15 µA. Scanning electron micrographs were taken on a Hitachi S3000N (Hitachi Ltd., Tokyo, Japan) scanning electron microscope and placed on a black background using GIMP version 2.10.

4.3.4 Transmission electron microscopy

Trophozoites were pooled into a polypropylene dish pre-coated with poly-L-lysine and filled with a mixture of 2% glutaraldehyde and 0.5% OsO_4 in 0.1 M Na-cacodylate buffer. The cells were left in the fixative for 30 min and rinsed three times with seawater. Post-fixation was done with 1% OsO_4 in 0.1 M Na-cacodylate buffer at pH 7.4 for 1.5 hr. Dehydration involved a graded series of acetone for 10 min at each of the following concentrations: 30%, 50%, 80%, 90%, and 95%. Final dehydration was done by keeping the trophozoites in 100% acetone for 30 min twice. Cells were infiltrated with 100% resin overnight which was polymerized at 65 °C for 24 hr. Samples were sectioned using a diamond knife on an EM-Ultracut S ultramicrotome (Leica Microsystems, Wetzlar, Germany). Sections were placed on formvar-coated one-slot grids and observed with a

Hitachi H-7650 TEM.

4.3.5 DNA extraction, amplification and sequencing

Parasites were individually isolated, washed three times with filtered seawater, and placed in separate 0.2 ml PCR tubes. Genomic DNA was extracted from the single-cell isolates using a QuickExtract FFPE RNA Extraction Kit (Epicentre, Wisconsin, USA). The SSU rDNA sequences were initially amplified by a polymerase chain reaction (PCR) using universal eukaryote primers PF1 5′ – CGCTACCTGGTTGATCCTGCC – 3′ and SSUR4 5′ – GATCCTTCTGCAGGTTCACCTAC – 3′ (Leander and Keeling, 2003) and TaKaRa Ex Taq (Takara Bio Inc., Otsu, Japan). The thermal cycler conditions used were as follows: initial denaturation at 94°C for 1 min followed by 35 cycles of denaturation at 94°C for 20 s, annealing at 52°C for 30 s, extension at 72°C for 1:20 min, and a final extension at 72°C for 7 min. The product from this initial amplification was diluted 1:100 in distilled water and used as template for nested PCRs using the primer pairs PF1 – 18SRF 5′ – CCCGTGTTGAGTCAAATTAAG – 3′ (Mo et al., 2002) and SR4 5′ – AGGGCAAGTCTGGTGCCAG – 3′ (Yamaguchi and Horiguchi, 2005) – SSUR4 with the following thermal cycler conditions: initial denaturation at 94°C for 30 s followed by 35 cycles of denaturation at 94°C for 20 s, annealing at 52°C for 30 s, extension at 72°C for 0:40 s, and a final extension at 72°C for 7 min. The products were screened on a 1% agarose gel and subsequently sequenced using the same internal primers. The SSU rDNA sequences, from separate single-cell isolations, were assembled on MEGA version 7 (Kumar et al., 2016) for each gregarine species and initially identified using Basic Local Alignment and Search Tool (BLAST). Identification of the hosts was based on morphology using a species guide (Cutler et al., 1984) and with partial SSU rDNA sequences.

4.3.6 Molecular phylogenetic analysis

The phylogenetic position of *Platyproteum* sp. was recovered based on SSU rDNA data. The analysis consisted of a 53-taxon alignment of representative myzozoan taxa includ-

ing dinoflagellates, chrompodellids, and apicomplexans. The SSU rDNA sequences were aligned using MAFFT version 6 with the Q-INS-i option (Katoh et al., 2002) for its ability to account for the secondary structure of ribosomal subunits. Ambiguously aligned regions and gaps were cut from the final alignment using Aliscore version 2.0 (Kück et al., 2010; Misof and Misof, 2009) and Alicut version 2.31. The resulting alignment included 1,563 unambiguously aligned nucleotides.

Maximum likelihood (ML) and Bayesian posterior probabilities were calculated using RAxML version 8.2.12 (Stamatakis, 2014) and MrBayes version 3.2.6 (Ronquist et al., 2012) through the Cipres Science Gateway version 3.3 (Miller et al., 2010). The GTR+I+Γ model was suggested by jModelTest version 2.1.10 (Darriba et al., 2012; Guindon and Gascuel, 2003) for the 53-taxon alignment phylogenetic analysis (proportion of invariable sites = 0.190, gamma shape = 0.698). The parameters specified for MrBayes were as follows: lset nst = 6, rates = invgamma, and Monte Carlo Markov Chains (MCMC) run for 10,000,000 generations (ngen = 10 000 000), 2 runs (nruns = 2), 4 chains (nchains = 4), temperature parameter at 0.2 (temp = 0.200), sample frequency of 100, prior burn-in of 25% of sampled trees, and a stop rule of 0.01 to terminate the program when the split deviation fell below 0.01.

4.4 Results

4.4.1 Morphology and flagellar apparatus

The trophozoites were roughly elliptic with a general shape resembling that of a crescent or a leaf (Fig. 4.1A,B). Significant contortions in cell shape, however, were continuously observed in live specimens as the trophozoites actively contracted and expanded. A typical trophozoite would be observed undergoing repeated cycles of starting from a flattened, leaf-life shape, then stretching along the anteroposterior axis creating a constriction near the middle of the cell body, followed by a steady contraction along the same axis to form a nearly spherical shape, and then finally relaxing back to initial flattened and leaf-like

shape. No gliding motility or directional locomotion was observed.

The nucleus was oval, measuring 16–17 μm along the major axis and 10–13 μm along the minor axis, and situated just posterior to the transverse midline of the cell (n = 40). Although the size of the trophozoite was never constant, the length generally ranged between 111–121 μm and 29–43 μm in width. Longitudinal striations could be seen at the posterior end at the light microscope level. The anterior differed in shape from the posterior end in that it was more flattened, and flagella could be seen beating in a whip-like motion. Although the movement of the flagella were perceptible under light microscopy, the continuous movement of the trophozoite made consistent observation of the anterior difficult. However, two flagella roughly 5–7 μm long were clearly seen protruding from the anterior under SEM (Fig. 4.1B,C). Epicytic striations consisted of both longitudinal and transverse striations that formed a criss-cross lattice of 2 by 2 folds/μm.

Transmission electron microscopy revealed a cytoplasm containing mitochondria, Golgi bodies, amylopectin granules, and dense granules (Fig. 4.2). The mitochondria were particularly prevalent around the periphery of the cell in contrast to the amylopectin granules that congregated closer to the center of the cell body (Fig. 4.2A). Longitudinal arrays of microtubules were seen subtending the plasma membrane in both cross-section (Fig. 4.2B,C) and longitudinal section (Fig. 4.2D,E). Epicytic folds were also present in both sections as protrusions of the plasma membrane and cytoplasm. Dense granules, golgi bodies, and vacuoles were observed in the cytoplasm (Fig. 4.2F).

The flagellar apparatus was located at the apical end of the cell and consisted of two flagella, two corresponding basal bodies, a posterior root, two anterior roots, and a fibrous connective material that spanned between the posterior and anterior roots (Fig. 4.3). The flagella themselves were comprised of nine doublets around a central doublet (Fig. 4.4A). Each basal body was constituted in similar fashion with nine doublets, but the central doublet was not observed (Fig. 4.4B). The two basal bodies were roughly parallel to each other and placed about 1 μm apart. Each of the basal bodies were approximately 100 μm in length (Fig 4.4C,D). Serial TEM cross-sections suggested that the right basal body is

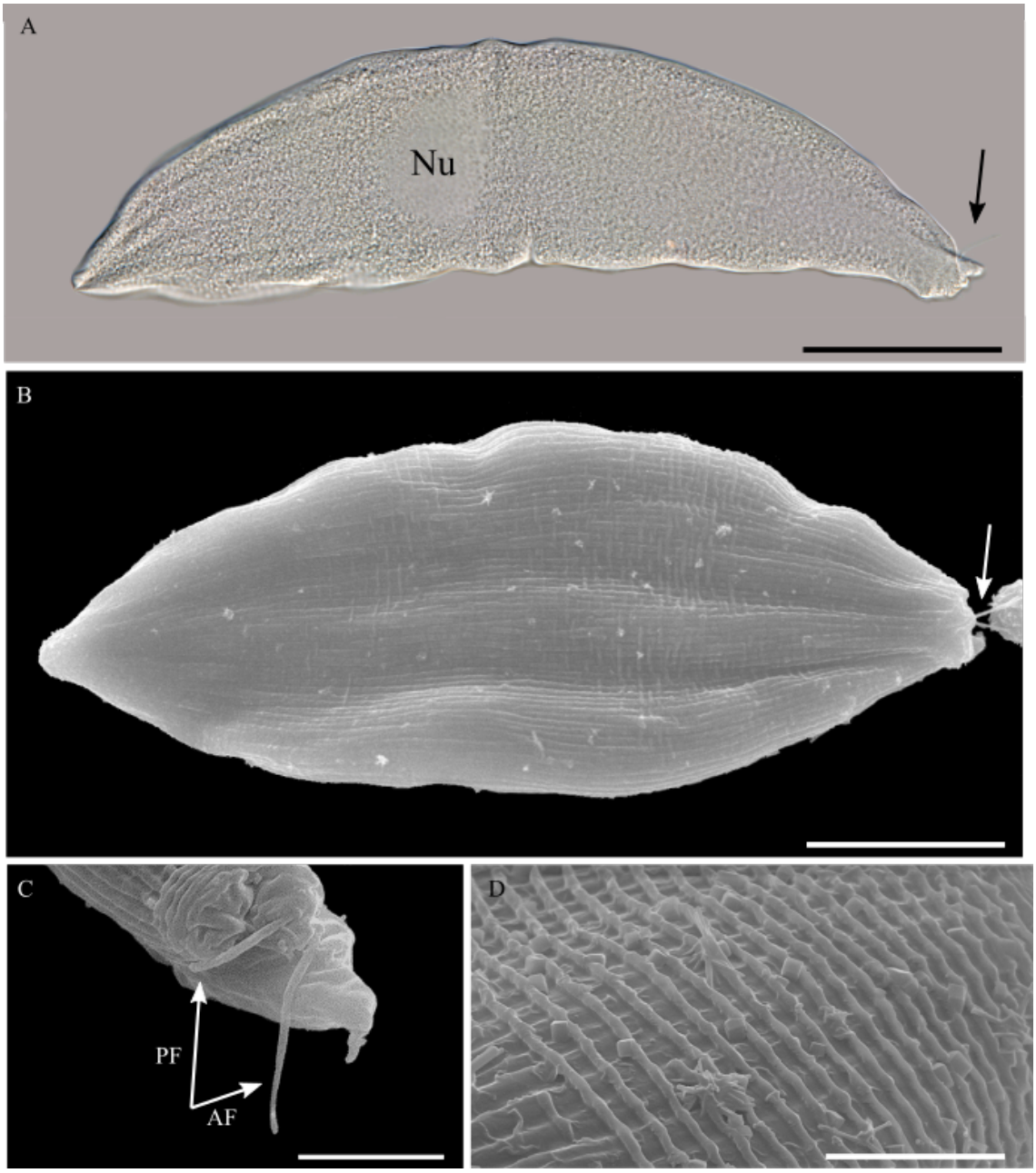

Figure 4.1: Light micrograph (LM) and scanning electron micrographs (SEM) of *Platyproteum* sp. showing trophozoite morphology. Mucron oriented to the right. (A) LM of trophozoite taken in differential interference contrast (DIC). Crescent shaped cell halfway through a constant contortion involving extreme stretching and contracting. An oval nucleus (Nu) situated just posterior to the transverse midline of the cell. Flagella are seen as rough refractions (arrow). (B) SEM of the trophozoite showing overall leaf-life shape. Two flagella protrude from the apical end of the cell (arrow) (C) SEM apical view of the anterior (AF) and posterior (PF) flagella (arrows) (D) SEM of longitudinal and transverse epicytic striations forming a criss-cross pattern at a density of 2 folds/µm Scale bars: A, B = 25 µm; C, D = 6 µm.

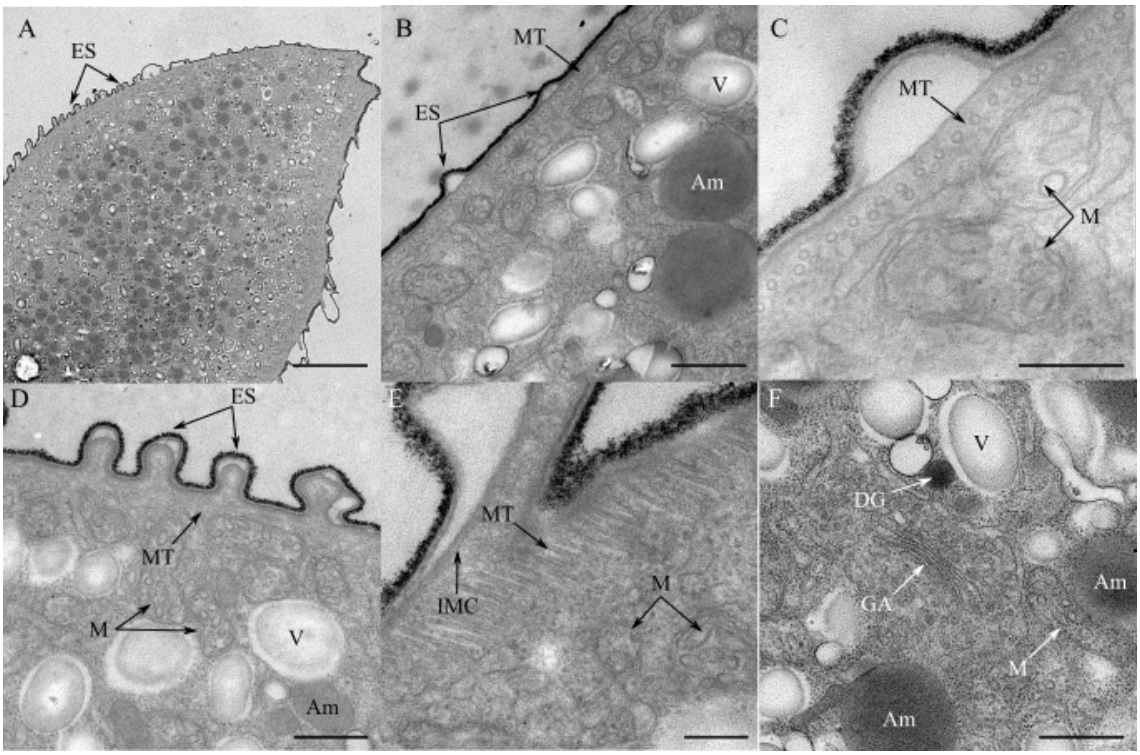

Figure 4.2: Transmission electron micrographs (TEM) of *Platyproteum* sp. showing general subcellular morphology. Abbreviations: amylopectin granules (Am), dense granules (DG), epicytic striation (ES), Golgi apparatus (GA), inner membrane complex (IMC), mitochondria (M), microtubules (MT), and vacuoles (V). (A) Longitudinal section of the apical end of a trophozoite showing epicytic striations and the general distribution of organelles (B) Cross section showing epicytic striations, cortical microtubules, amylopectin granules, and vacuoles. (C) High magnification cross section of an array of cortical microtubules. Mitochondria are also visible. (D) Longitudinal section showing epicytic striations, cortical microtubules, mitochondria and vacuoles. (E) High magnification longitudinal section showing an array of cortical microtubules. The inner membrane complex is seen below an epicytic fold. (F) Subcellular organelles in the trophozoite body including amylopectin granules, dense granules, a Golgi apparatus, mitochondria, and vacuoles. Scale bars: A = 5 µm; B, D, F = 500 nm; C, E = 200 nm.

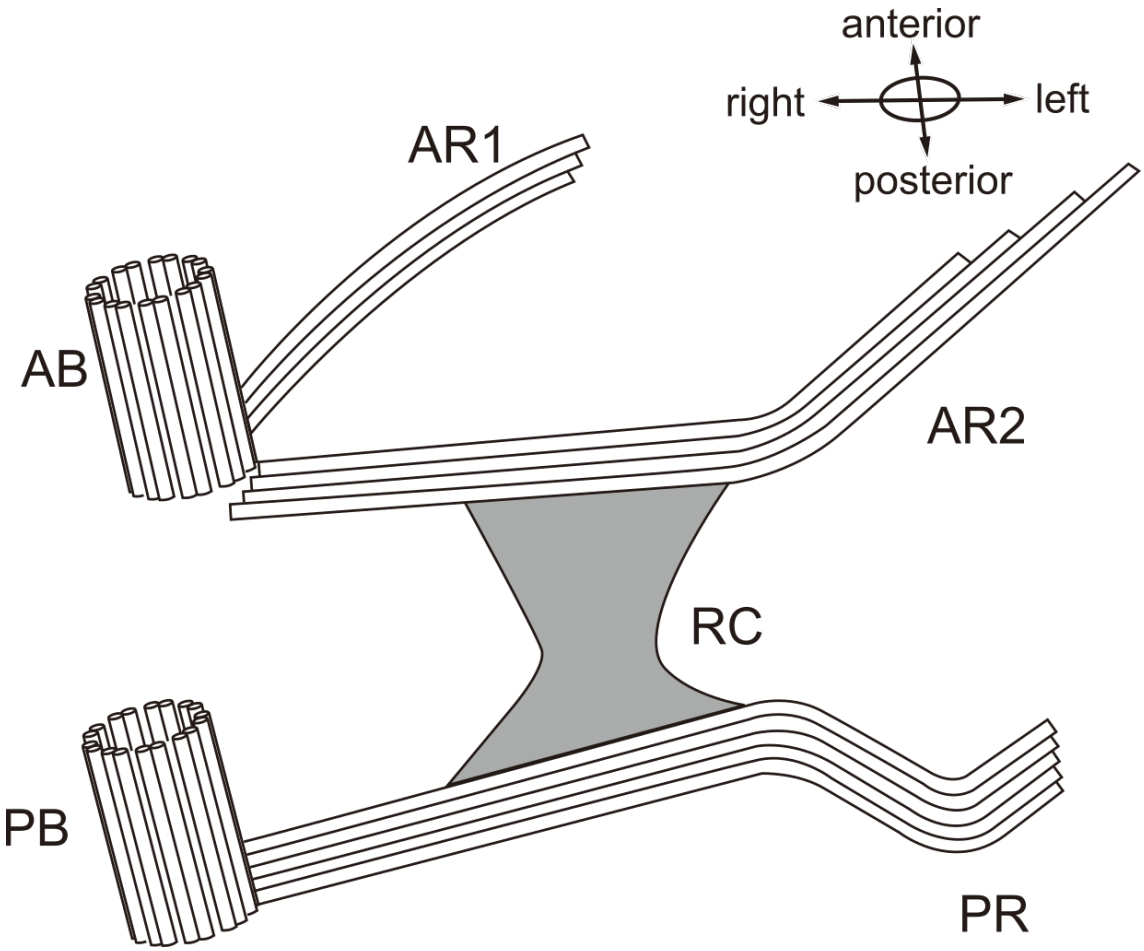

Figure 4.3: Schematic reconstruction of the flagellar apparatus of *Platyproteum* sp. Abbreviations: anterior basal body (AB); anterior root 1 and 2 (AR1 and 2); posterior basal body (PB); posterior root (PR); root connective (RC).

attached to two flanking roots (Fig. 4.4C,D). Anterior root 2 was connected by a fibrous connective material that reached the posterior root associated with a posterior basal body. (Fig. 4.4E, F). The basal bodies inserted into the cell vertically to the cell membrane, whereas the roots run along the periphery of the cell (Fig 4.4P-S). Anterior roots 1 and 2 and the posterior root were made of three, four, and five microtubules respectively (Fig 4.4F,Q,S).

4.4.2 SSU rDNA phylogenetic analysis

The 53-taxon alignment of SSU rDNA sequences yielded the dinoflagellates and perkinsids at the base (94% Maximum likelihood bootstrap [MLB], 0.88 Bayesian posterior

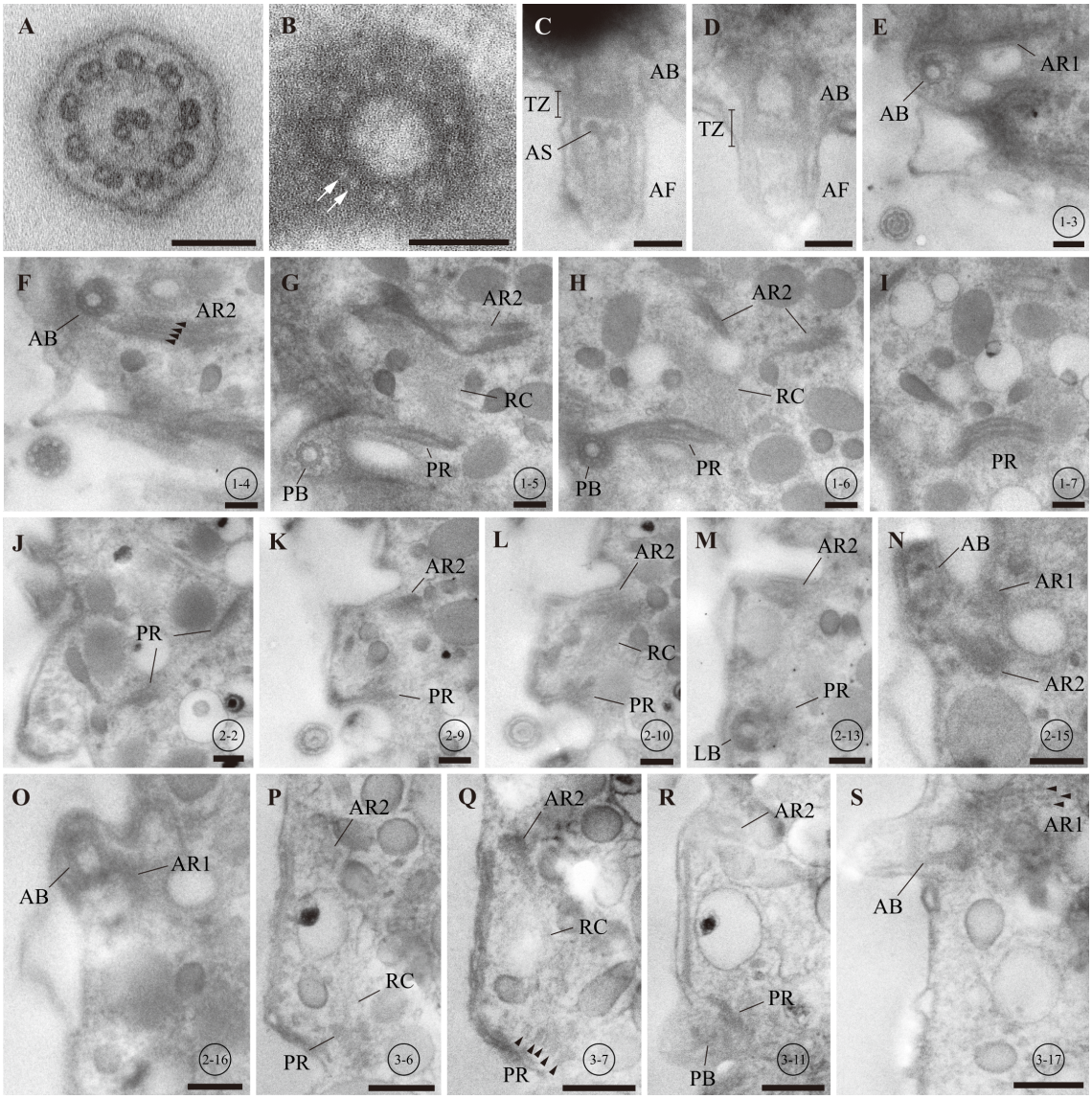

Figure 4.4: Transmission electron micrographs of *Platyproteum* sp. flagella and flagellar apparatus in serial sections. Abbreviations: anterior basal body (AB); anterior flagellum (AF); anterior root 1 (AR1); anterior root 2 (AR2); axosome (AS); posterior basal body (PB); posterior root (PR); root connective material (RC); transition zone (TZ) (A) cross section of a posterior flagellum comprising of nine sets of doublet microtubules and two central microtubules. (B) a posterior basal body comprising of nine sets of doublet microtubules (arrows). (C,D) longitudinal sections of an anterior basal body, an anterior flagellum with an axosome and their transition zone. (E-S) Serial sections of a flagellar apparatus showing anterior basal body, anterior root 1 comprising of four microtubules (F; arrowheads), anterior root 2 comprising of four microtubules (S; arrowheads), posterior basal body, posterior root comprising of five microtubules (Q; arrowheads) and root connective material. (E-I), (J-O), and (P-S) show serial sections of the same flagellar apparatuses, respectively. Section numbers are indicated in circles. Directions of sectioning are from the anterior to the posterior (E-I), ventral to dorsal (J-O), and from left to right (P-S). Scale bars: A-D = 100 nm; E-S = 200 nm.

probability [BPP]) and an ingroup of chrompodellids and apicomplexans sorted into broad groups situated on a poorly resolved backbone (Fig. 4.5). The maximum likelihood and Bayesian phylogenies recovered similar tree topologies with *P.* sp. (Oshoro isolate 1), *P. vivax*, and *Filipodium phascolosomae* forming the deepest branch in the ingroup. These species were followed by colpodellids and chromerids forming basal lineages to the major apicomplexan groups including the piroplasmid, coccidian, rhytidocystid, cryptosporidian, and gregarine clades. The SSU rDNA sequence that was obtained for *P.* sp. was recovered as a sister species of *P. vivax* (100% [MLB], 1.00 [BPP]) and was 18.4% divergent. The two *Platyproteum* species and *F. phascolosomae* formed a monophyletic group (100% MLB, 1.00 BPP) at the base of the chrompodellid and apicomplexan taxa (33% MLB, 0.65 BPP).

4.5 Discussion

Platyproteum sp. possesses morphological and behavioural characteristics that are similar to *P. vivax*. The most remarkable of these similarities include the overall flattened shape, the extreme contortions of the cell body in live specimens, and the mix of both longitudinal and transverse epicytic folds. *Platyproteum* sp. was observed to reach approximately 120 µm when fully stretched whereas *P. vivax* has been observed around 550 µm (Gunderson and Small, 1986), 150 to 425 µm (Leander and Keeling, 2003), and 120 to 500 µm (Leander, 2006). The host for *P.* sp. nov is *Phascolosoma noduliferum* whereas the host for *P. vivax* is *Phascolosoma agassizii*. *Platyproteum* is currently a monotypic genus, thus, has a limited set of diagnostic traits. However, the tape-like cell with dynamic movements, transverse striations, and parasitism in sipunculid hosts are all consistent with diagnostic traits that were suggested at the inception of this genus (Rueckert and Leander, 2009). Morphologically, therefore, *P.* sp. is similar to *P. vivax*. The only noteworthy differences between *P.* sp. and *P. vivax* are size and host species.

Although the presence of flagella in *P. vivax* has not been explicitly discussed in previous ultrastructural studies, Leander (2006) clearly mentions apical pores, “thread-

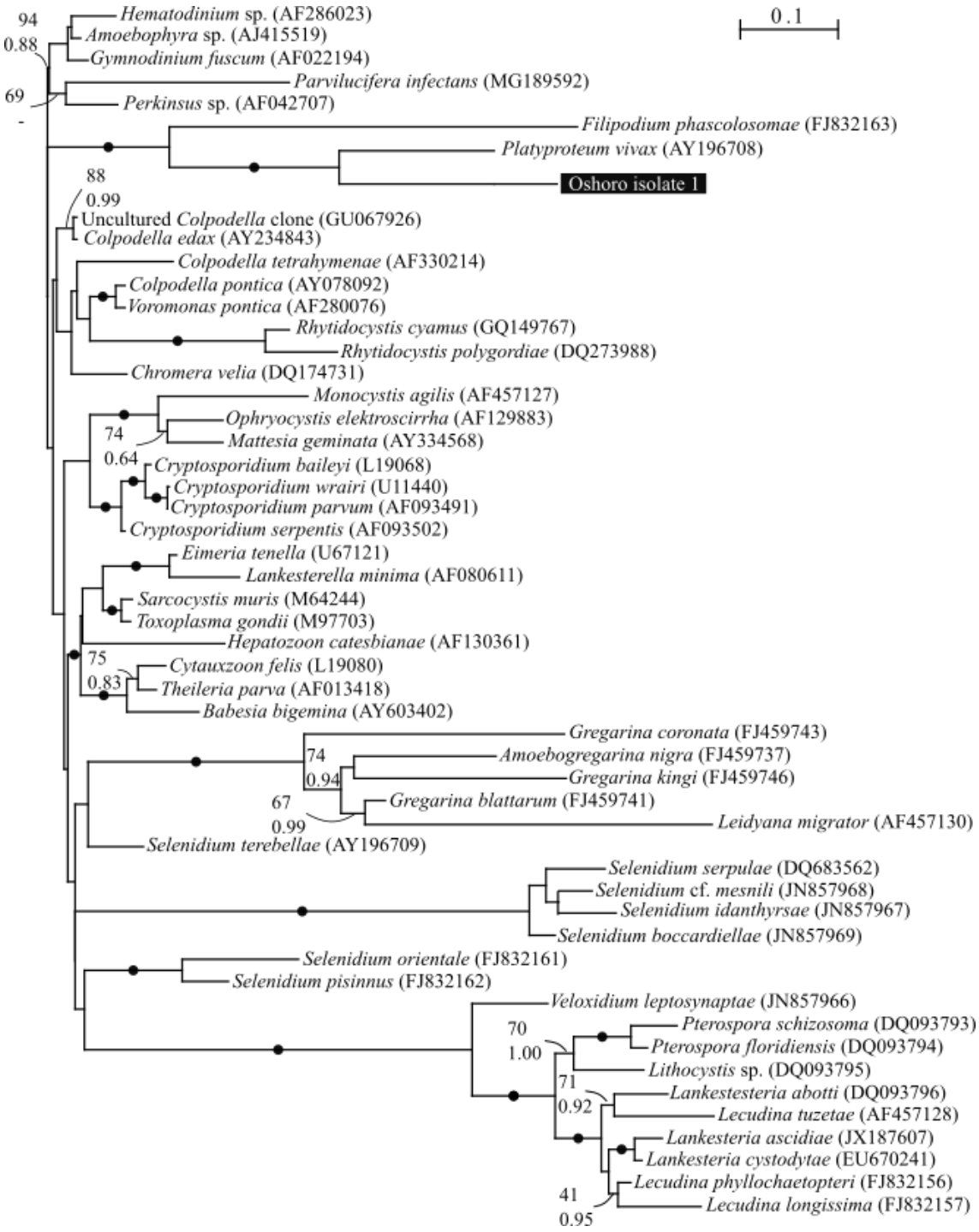

Figure 4.5: Maximum likelihood phylogeny inferred from a 53 taxa dataset of SSU rDNA sequences with 1,563 unambiguously aligned sites using the GTR+I+Γ model of substitution (proportion of invariable sites = 0.190, gamma shape = 0.698). Numbers indicate bootstrap support. Black dots on branches denote when bootstrap support and Bayesian posterior probability was higher than or equal to 95% and 0.99 respectively. Branches without support values have bootstrap support and Bayesian probability lower than or equal to 60% and 0.95 respectively. The new species described in the current study is highlighted with a black box.

shaped structures" protruding from these pores, and an "unidentified linear structure" which appears to be a part of a root at the apical end of the cell under TEM. Our study reconstructed the flagellar apparatus of a member of *Platyprotuem* and revealed that each basal body is comprised of nine doublets of microtubules, which is in contrast to other major eukaryotes with basal bodies comprised of nine triplets. This nine-doublet structure of the basal body has also been described in *Colpodella vorax* (Brugerolle, 2002), which perhaps indicates that this construction is common amongst early branching myzozoans including the chrompodellids. In addition, the *P.* sp. basal bodies are similar in length ($\sim$100 µm) to those found in *C. vorax* (150 µm) and in that they are distantly separated from one another. On the other hand, the root system revealed by our observation of *P.* sp. is novel. It is difficult to designate the flagella of *P* sp. as number 1 and 2 as according to the convention suggested by Moestrup (2000) or as the longitudinal and transverse flagella as for dinoflagellates. Considering their positions in the cell however, the posterior flagellum likely corresponds to the number 1 flagellum and the anterior flagellum corresponds to the number 2 flagellum. According to this convention, the posterior root and the anterior roots 1 and 2 would be interpreted as root 1, 3, and 4, respectively (Moestrup, 2000). Eukaryotes, including *C. vorax*, have basal bodies that are linked directly by a connective (Okamoto and Keeling, 2014; Yubuki and Leander, 2013), but no such basal body connective was found in *P.* sp. Instead, the basal bodies are associated indirectly via a posterior root, anterior root 2, and a root connective which is possibly homologous to the striated root connective (SRC) that links roots 1 and 4 widely observed in dinoflagellates (Okamoto and Keeling, 2014). In retrospective consideration of the structures observed in *P. vivax* by Leander (2006), the mentioned apical pores and thread-shaped structures share a striking resemblance to flagella protruding from the apical end of the trophozoite. The unidentified linear structure seen under TEM is likely a portion of the flagellar apparatus, possibly a flagellar root, that was unintentionally sectioned.

The molecular phylogenetic analysis of SSU rDNA sequences recovered *P.* sp. as a sister species to *P. vivax*. The maximum likelihood tree (Fig. 4.5) shows that *P.* sp., *P.*

vivax, and *F. phascolosomae* branch at the base of the chrompodellids and apicomplexans which is consistent with the contemporary understanding of *Platyproteum* phylogenetics provided by Mathur and et al. (2019). In their transcriptomic analysis of an unidentified *Platyproteum* species, they also showed that the genus falls outside of the Apicomplexa altogether and instead forms a distinct lineage at the base of both the chrompodellids and apicomplexans. The *Platyproteum* and *Filipodium* clade infects sipunculid hosts as does the *Selenidium orientale* and *S. pisinnus* gregarine clade. Moreover, *Platyproteum vivax*, *F. phascolosomae*, and *S. pisinnus* can all be found as co-infections in *P. agassizii* (Rueckert and Leander, 2009). It appears, therefore, that this particular sipunculid host has been infected independently numerous times which hints at the possibility of many more myzozoan and apicomplexan parasites yet to be discovered from sipunculids.

Taking into consideration the morphological and behavioural characteristics of *P.* sp., the diagnostic criteria for *Platyproteum*, and the divergence of the SSU rDNA sequences of *P.* sp. nov from *P. vivax*, *P.* sp. likely represents an distinct, undescribed species. The presence of transverse striations, the distinct contortions of the cell body, and the overall tape-like, flattened morphology adhere to the diagnostic traits of *Platyproteum*. Furthermore, the flagella and flagellar apparatus characterized for *P.* sp. in this study resemble the apical features that were seen in the ultrastructural study of *P. vivax* (Leander, 2006). Differences, however, include the overall smaller size of *P.* sp. compared to *P. vivax*, the host species, and the SSU rDNA sequences (18.4%). The continued discovery and characterization of additional myzozoan taxa, especially from sipunculids, is key to earning an improved understanding of *Platyproteum* and the construction of a taxonomy that accurately reflects the phylogeny of taxa that diverged from the base of the Apicomplexa and chrompodellids.

5

Conclusions

At the heart of taxonomy is the elegant implication that all life on Earth is related to one another. The systematic application of categorical names relies on similarities among species as a result of common descent. Simultaneously, taxonomy also acknowledges the uniqueness of each lineage and their elegant adaptations to the specific ecological challenges that led to the evolution of apomorphic traits. The result is a system of naming life based on shared characteristics while, at the same time, drawing boundaries between groups of life that are sufficiently different.

The creation of names and classifications is a fundamental exercise in constructing a lexicon for biology. Having this universally accepted set of vocabulary provides a means for interdisciplinary communication. For instance, a botanist who first discovers an obscure plant in the tropics is able to assign to it a two-part, binomial name which carries

with it all the information needed for a future biochemist to understand exactly what plant is being referred to. Taxonomy and its endeavour to categorize the immense biodiversity of the planet is both indispensable and compelling as a classical branch of biology.

The current dissertation aimed to contribute to the efforts of taxonomy by engaging with an enigmatic group of parasitic eukaryotes known as the Apicomplexa and its relatives. Given the disparity between the devastating effects of apicomplexan parasites across the globe and the disproportionately poor understanding of the group as a whole, the Apicomplexa offered unique opportunities for discovery. As such, presented in the body of the current dissertation are a new genus, five new species of apicomplexan parasites, a characterization of an undescribed myzozoan isolated from various animal hosts. This work further aimed to highlight the importance of reconciling the traditional body of morphological knowledge with the ever-expanding body of molecular phylogenetics. Above all else, the most important objective for taxonomy is to create a classification that reflects phylogeny (i.e., evolutionary history) and not simply convenience or utility.

The first chapter of this dissertation outlined an overview of apicomplexan biology, taxonomy, and systematics. It provided a general introduction to the discipline as well as the many challenges that need to be addressed for future progress. Summarizing the conclusions from many of the accomplished authors in the past, the major obstacles to apicomplexan biology include poor taxon sampling, a lack of literature on non-medically significant species, and the mismatch between existing taxonomy and phylogenetics. In light of these problems, the second chapter described the discovery of a new species of marine apicomplexan from scale worm hosts found in Hokkaido, Japan. These novel findings led to the addition of a unique genus in the marine gregarine phylogeny with associated characters described through morphology and molecular analysis. The third chapter presented four new species of marine gregarines found in ascidian hosts from New Zealand. These data unveiled a history of host switching in these parasites and led to the emendation of a major, traditional genus to more accurately reflect the new understanding of gregarine evolutionary history. The fourth chapter discussed a species

found from a sipunculid host in Hokkaido, Japan. This enigmatic organism belonged to a genus diverging from the base of the apicomplexan and chrompodellid phylogeny. Moreover, flagella and the associated flagellar apparatus were characterized for the first time in this genus. These studies have hopefully added a humble amount of momentum to ever so slightly push the frontier of apicomplexan biology.

The future of biology, and by extension apicomplexan taxonomy and systematics, will undoubtedly be shaped by the generation of large molecular datasets. Phylogenomic approaches to hypothesis testing are becoming increasingly accessible and will greatly accelerate the understanding of enigmatic groups such as the Apicomplexa. Challenges associated with parasites such as uncultivability, low prevalence, and morphological plasticity can all be potentially overcome with the use of comprehensive DNA data. Furthermore, surveying the genomes of basal organisms for signs of ancestral genes, photosynthesis-related genes in apicomplexans for instance, will be crucial for the accurate reconstruction of ancient evolutionary changes. New data should be reconciled with the existing body of literature and taxonomic changes should be applied to reflect the understanding of phylogeny at the time. For as long as there are species yet to be discovered and life continues to radiate in unison with the continuous fluctuations of environmental niches, taxonomy will continue to be a fundamental component of biology.

Bibliography

Abrahamsen, M. S., T. J. Templeton, S. Enomoto, J. E. Abrahante, G. Zhu, C. A. Lancto, M. Deng, C. Liu, G. Widmer, S. Tzipori, G. A. Buck, P. Xu, A. T. Bankier, P. H. Dear, B. A. Konfortov, H. F. Spriggs, L. Iyer, V. Anantharaman, L. Aravind, and V. Kapur, 2004. Complete genome sequence of the apicomplexan, *Cryptosporidium parvum*. Science 304:441–445.

Adl, S. M., D. Bass, C. E. Lane, J. Lukeš, C. L. Schoch, A. Smirnov, S. Agatha, C. Berney, M. W. Brown, F. Burki, P. Cárdenas, I. Čepička, L. Chistyakova, J. del Campo, M. Dunthorn, B. Edvardsen, Y. Eglit, L. Guillou, V. Hampl, A. A. Heiss, M. Hoppenrath, T. Y. James, A. Karnkowska, S. Karpov, E. Kim, M. Kolisko, A. Kudryavtsev, D. J. Lahr, E. Lara, L. Le Gall, D. H. Lynn, D. G. Mann, R. Massana, E. A. Mitchell, C. Morrow, J. S. Park, J. W. Pawlowski, M. J. Powell, D. J. Richter, S. Rueckert, L. Shadwick, S. Shimano, F. W. Spiegel, G. Torruella, N. Youssef, V. Zlatogursky, and Q. Zhang, 2019. Revisions to the classification, nomenclature, and diversity of eukaryotes. Journal of Eukaryotic Microbiology 66:4–119.

Adl, S. M., B. S. Leander, A. G. B. Simpson, J. M. Archibald, O. R. Anderson, D. Bass, S. S. Bowser, G. Brugerolle, M. a. Farmer, S. Karpov, M. Kolisko, C. E. Lane, D. J. Lodge, D. G. Mann, R. Meisterfeld, L. Mendoza, Ø. Moestrup, S. E. Mozley-Standridge, A. V. Smirnov, and F. Spiegel, 2007. Diversity, nomenclature, and taxonomy of protists. Systematic Biology 56:684–689.

Adl, S. M., A. G. B. Simpson, M. A. Farmer, R. A. Andersen, O. R. Anderson, J. R. Barta, S. S. Bowser, G. Brugerolle, R. A. Fensome, S. Fredericq, T. Y. James, S. Karpov, P. Kugrens, J. Krug, C. E. Lane, L. A. Lewis, J. Lodge, D. H. Lynn, D. G. Mann, R. M. Mccourt, L. Mendoza, j. Moestrup, S. E. Mozley-Standridge, T. A. Nerad, C. A. Shearer, A. V. Smirnov, F. W. Spiegel, and M. F. J. R. Taylor, 2005. The new higher level classification of eukaryotes with emphasis on the taxonomy of protists. Journal of Eukaryotic Microbiology 52:399–451.

Adl, S. M., A. G. B. Simpson, C. E. Lane, J. Lukeš, D. Bass, S. S. Bowser, M. W. Brown, F. Burki, M. Dunthorn, V. Hampl, A. Heiss, M. Hoppenrath, E. Lara, L. L. Gall, D. H. Lynn, H. McManus, E. A. D. Mitchell, S. E. Mozley-Stanridge, L. W. Parfrey, J. Pawlowski, S. Rueckert, L. Shadwick, C. L. Schoch, A. Smirnov, and F. W. Spiegel, 2012. The revised classification of eukaryotes. Journal of Eukaryotic Microbiology 59:429–493.

Agar, H. D., P. V. Gustafson, and D. I. Cramer, 1954. An electron microscope study of *Toxoplasma*. The American Journal of Tropical Medicine and Hygiene 3:1008–1022. URL http://www.ajtmh.org/content/journals/10.4269/ajtmh.1954.3.1008.

Aikawa, M., 1971. Parasitological review. *Plasmodium*: the fine structure of malarial parasites. Experimental Parasitology 30:284–320. URL http://www.ncbi.nlm.nih.gov/pubmed/4399774.

Allen, K. E., E. M. Johnson, and S. E. Little, 2011. *Hepatozoon* spp infections in the United States. Veterinary Clinics of North America - Small Animal Practice 41:1221–1238. URL http://dx.doi.org/10.1016/j.cvsm.2011.08.006.

Altizer, S. M. and K. S. Oberhauser, 1999. Effects of the protozoan parasite *Ophryocystis elektroscirrha* on the fitness of monarch butterflies (*Danaus plexippus*). Journal of Invertebrate Pathology 74:76–88.

Anderson-White, B. R., F. D. Ivey, K. Cheng, T. Szatanek, A. Lorestani, C. J. Beckers, D. J. Ferguson, N. Sahoo, and M. J. Gubbels, 2011. A family of intermediate filament-like proteins is sequentially assembled into the cytoskeleton of *Toxoplasma gondii*. Cellular Microbiology 13:18–31.

Archibald, J. M., 2012. The evolution of algae by secondary and tertiary endosymbiosis. Advances in Botanical Research 64:87–118.

Arisue, N. and T. Hashimoto, 2015. Phylogeny and evolution of apicoplasts and apicomplexan parasites. Parasitology International 64:254–259. URL http://dx.doi.org/10.1016/j.parint.2014.10.005.

Babes, V., 1888. Sur l'hémoglobinurie bactérienne du bœuf. Comptes rendus de l'Académie des Sciences 107:692–694.

Bannister, L. H., J. M. Hopkins, R. E. Fowler, S. Krishna, and G. H. Mitchell, 2000. A brief illustrated guide to the ultrastructure of *Plasmodium falciparum* asexual blood stages. Parasitology Today 16:427–433.

Barta, J. R., 1989. Phylogenetic analysis of the class Sporozoea (Phylum Apicomplexa Levine, 1970): evidence for the independent evolution of heteroxenous life cycles. The Journal of Parasitology 75:195–206. URL http://www.jstor.org/stable/3282766.

———, 2001. Molecular approaches for inferring evolutionary relationships among protistan parasites. Veterinary Parasitology 101:175–186.

Barta, J. R., J. D. Ogedengbe, D. S. Martin, and T. G. Smith, 2012. Phylogenetic position of the adeleorinid coccidia (myzozoa, Apicomplexa, coccidia, eucoccidiorida, Adeleorina) inferred using 18s rDNA sequences. Journal of Eukaryotic Microbiology 59:171–180.

Baum, J., T. W. Gilberger, F. Frischknecht, and M. Meissner, 2008. Host-cell invasion by

malaria parasites: insights from *Plasmodium* and *Toxoplasma*. Trends in Parasitology 24:557–563.

Betancourt, W. Q. and J. B. Rose, 2004. Drinking water treatment processes for removal of *Cryptosporidium* and *Giardia*. Veterinary Parasitology 126:219–234.

Bhattacharya, D. and L. Medlin, 1995. The phylogeny of plastids: a review based on comparisons of small-subunit ribosomal RNA coding regions. Journal of Phycology 31:489–498.

Bishop, R., A. Musoke, S. Morzaria, M. Gardner, and V. Nene, 2004. *Theileria*: intracellular protozoan parasites of wild and domestic ruminants transmitted by ixodid ticks. Parasitology 129:S271–S283.

Bodył, A., 2005. Do plastid-related characters support the chromalveolate hypothesis? Journal of Phycology 41:712–719.

Bodył, A., P. Mackiewicz, and J. W. Stiller, 2009a. Early steps in plastid evolution: Current ideas and controversies. BioEssays 31:1219–1232.

Bodył, A., J. W. Stiller, and P. Mackiewicz, 2009b. Chromalveolate plastids: direct descent or multiple endosymbioses? Trends in Ecology and Evolution 24:119–121.

Bogolepova, I., 1953. Gregariny iz Zaliva Petra Velikogo (in Russian). Les Grégarines de la Baie Pierre-le-Grand. Trudy Zoologicheskogo Instituts. Akademiià Nauk Gruzinskol SSR 13:38–55.

Boisard, J. and I. Florent, 2020. Why the –omic future of Apicomplexa should include Gregarines. Biology of the Cell 112:173–185.

Borst, P., J. P. Overdulve, P. J. Weijers, F. Fase-Fowler, and M. Van den Berg, 1984. DNA circles with cruciforms from *Isospora* (*Toxoplasma*) *gondii*. BBA - Gene Structure and Expression 781:100–111.

Brasil, L., 1907. Recherches sur le cycle évolutif des Selenidiidae, Grégarines parasites d'Annélides polychètes. I. La schizogonie et la croissance des gamétocytes chez Selenidium caulleryi n.sp. Archiv für Protistenkunde 16:370–397.

Brugerolle, G., 2002. *Colpodella vorax*: Ultrastructure, predation, life-cycle, mitosis, and phylogenetic relationships. European Journal of Protistology 38:113–125.

Burki, F., K. Shalchian-Tabrizi, and Pawlowski, 2008. Phylogenomics reveals a new megagroup including most photosynthetic eukaryotes. Biology Letters 4:366–9. URL http://www.pubmedcentral.nih.gov/articlerender.fcgi?artid=PMC2610160.

Cacciò, S. M., 2005. Molecular epidemiology of human cryptosporidiosis. Parassitologia 47:185–192. URL http://europepmc.org/abstract/MED/16252472.

Caullery, M. and F. Mesnil, 1899. Sur quelques parasites internes des Annélides. I. Grégarines nématoides des annélides. Travaux de la Station zoologique de Wimereux 80–99:80–99.

———, 1900. Sur un mode particulier de division nucléaire chez les Grégarines. Archives d'Anatomie Microscopique 3:1460167.

———, 1901. Le parasitisme et la reproduction asexuée des Grégarines. Journal de la Société de biologie Paris 52:84–87.

Cavalier-Smith, T., 1999. Principles of protein and lipid targeting in secondary symbiogenesis: euglenoid, dinoflagellate, and sporozoan plastid origins and the eukaryote family tree. The Journal of Eukaryotic Microbiology 46:347–366.

———, 2000. Membrane heredity and early chloroplast evolution. Trends in Plant Science 5:174–182.

———, 2004. Only six kingdoms of life. Proceedings of the Royal Society B: Biological Sciences 271:1251–1262.

———, 2014. Gregarine site-heterogeneous 18S rDNA trees, revision of gregarine higher classification, and the evolutionary diversification of Sporozoa. European Journal of Protistology 50:472–495. URL http://dx.doi.org/10.1016/j.ejop.2014.07.002.

Cavalier-Smith, T., M. Van Der Giezen, W. Martin, A. Wilkins, W. F. Doolittle, J. F. Allen, C. J. Leaver, F. R. Whatley, and C. J. Howe, 2003. Genomic reduction and evolution of novel genetic membranes and protein-targeting machinery in eukaryote-eukaryote chimaeras (meta-algae). Philosophical Transactions of the Royal Society B: Biological Sciences 358:109–134.

Centers for Disease Control and Prevention, 2015. *Cryptosporidium* (also known as "Crypto"). URL https://www.cdc.gov/parasites/crypto/pathogen.html.

Cesbron-Delauw, M. F., C. Gendrin, L. Travier, P. Ruffiot, and C. Mercier, 2008. Apicomplexa in mammalian cells: trafficking to the parasitophorous vacuole. Traffic 9:657–664.

Chapman, H. D., 2014. Milestones in avian coccidiosis research: a review. Poultry Science 93:501–511. URL http://dx.doi.org/10.3382/ps.2013-03634.

Chartier, C. and C. Paraud, 2012. Coccidiosis due to *Eimeria* in sheep and goats, a review. Small Ruminant Research 103:84–92. URL http://dx.doi.org/10.1016/j.smallrumres.2011.10.022.

Checkley, W., A. C. White, D. Jaganath, M. J. Arrowood, R. M. Chalmers, X. M. Chen, R. Fayer, J. K. Griffiths, R. L. Guerrant, L. Hedstrom, C. D. Huston, K. L. Kotloff, G. Kang, J. R. Mead, M. Miller, W. A. Petri, J. W. Priest, D. S. Roos, B. Striepen, R. C. Thompson, H. D. Ward, W. A. Van Voorhis, L. Xiao, G. Zhu, and E. R. Houpt, 2015. A review of the global burden, novel diagnostics, therapeutics, and vaccine targets for *Cryptosporidium*. The Lancet Infectious Diseases 15:85–94.

Ciancio, A., S. Scippa, and M. Cammarano, 2001. Ultrastructure of trophozoites of the gregarine *Lankesteria ascidiae* (Apicornplexa: Eugregarinida) parasitic in the ascidian *Ciona intestinalis* (protochordata). European Journal of Protistology 37:327–336.

Clopton, R. E., 2000. Phylum Apicomplexa Levine, 1970: Order Eugregarinorida Léger, 1900. *in* J. Lee, G. F. Leedale, and P. Bradbury, eds. Illustrated Guide to the Protozoa, 2 ed. Society of Protozoologists, Lawrence, Kansas.

———, 2004. Standard nomenclature and metrics of plane shapes for use in gregarine taxonomy. Comparative Parasitology 71:130–140. URL http://www.bioone.org/doi/abs/10.1654/4151.

Clopton, R. E., J. Janovy, and T. J. Percival, 1992. Host stadium specificity in the gregarine assemblage parasitizing *Tenebrio molitor*. The Journal of Parasitology 78:334–337.

Corso, P. S., M. H. Kramer, K. A. Blair, D. G. Addiss, J. P. Davis, and A. C. Haddix, 2003. Cost of illness in the 1993 waterborne *Cryptosporidium* outbreak, Milwaukee, Wisconsin. Emerging Infectious Diseases 9:426–431.

Cowley, J. M., 1989. Effect of disease caused by a neogregarine protozoan (*Mattesia* sp.) on the population dynamics of a hill country sod webworm (*Eudonia sabulosella*, Pyralidae: Scopariinae). Journal of Invertebrate Pathology 53:159–163. URL http://www.sciencedirect.com/science/article/pii/0022201189900037.

Craun, G. F., R. L. Calderon, and M. F. Craun, 2005. Outbreaks associated with recreational water in the United States. International Journal of Environmental Health Research 15:243–262.

Criado-Fornelio, A., 2007. A review of nucleic acid-based diagnostic tests for *Babesia* and *Theileria*, with emphasis on bovine piroplasms. Parassitologia 49:39.

Criado-Fornelio, A., C. Verdú-Expósito, T. Martin-Pérez, I. Heredero-Bermejo, J. Pérez-Serrano, L. Guàrdia-Valle, and M. Panisello-Panisello, 2017. A survey for gregarines

(Protozoa: Apicomplexa) in arthropods in Spain. Parasitology Research 116:99–110. URL http://dx.doi.org/10.1007/s00436-016-5266-0.

Cummings, C. A., R. J. Panciera, K. M. Kocan, J. S. Mathew, and S. A. Ewing, 2005. Characterization of stages of *Hepatozoon americanum* and of parasitized canine host cells. Veterinary Pathology 42:788–796.

Current, W. L., N. C. Reese, J. V. Ernst, W. S. Bailey, M. B. Heyman, and W. M. Weinstein, 1983. Human cryptosporidiosis in immunocompetent and immunodeficient persons: studies of an outbreak and experimental transmission. New England Journal of Medicine 308:1252–1257.

Cutler, E. B., N. J. Cutler, and T. Nishikawa, 1984. The Sipuncula of Japan : their systematics and distribution. Publications of the Seto Marine Biological Laboratory 29:249–322.

Darriba, D., R. Taboada, Guillermo L Doallo, and D. Posada, 2012. jModelTest 2: more models, new heuristics and parallel computing. Nature Methods 9:772.

Davies, A. J., N. J. Smit, P. M. Hayes, A. M. Seddon, and D. Wertheim, 2004. *Haemogregarina bigemina* (Protozoa: Apicomplexa: Adeleorina) - past, present and future. Folia Parasitologica 51:99–108.

Desportes, I. and J. Schrével, 2013. The Gregarines. Koninklijke Brill NV, Leiden.

Detwiler, J. and J. Janovy, 2008. The role of phylogeny and ecology in experimental host specificity: insights from a eugregarine–host system. Journal of Parasitology 94:7–12.

Devetak, D., K. Mihelak, and I. Kos, 2019. Gregarines (Apicomplexa: Eugregarinida) of Chilopoda and Diplopoda in Slovenia. Acta Zoologica Bulgarica 71:121–128.

Doganci, T., E. Araz, A. Ensari, M. Tanyuksel, and L. Doganci, 2002. Detection of *Cryptosporidium parvum* infection in childhood using various techniques. Medical Science Monitor 8:223–227.

Dubey, J. P., 2009. History of the discovery of the life cycle of *Toxoplasma gondii*. International Journal for Parasitology 39:877–882. URL http://dx.doi.org/10.1016/j.ijpara.2009.01.005.

———, 2020. The history and life cycle of *Toxoplasma gondii*. 1909. LTD. URL http://dx.doi.org/10.1016/B978-0-12-815041-2.00001-3.

Dubremetz, J. F., N. Garcia-Réguet, V. Conseil, and M. N. Fourmaux, 1998. Apical organelles and host-cell invasion by Apicomplexa. International Journal for Parasitology 28:1007–1013.

Fayer, R., J. M. Trout, and M. C. Jenkins, 1998. Infectivity of *Cryptosporidium parvum* oocysts stored in water at environmental temperatures. The Journal of Parasitology 84:1165–1169. URL http://www.jstor.org/stable/3284666.

Fichera, M. E. and D. S. Roos, 1997. A plastid organelle as a drug target in apicomplexan parasites. Nature 390:407–409.

Field, S. G. and N. K. Michiels, 2005. Parasitism and growth in the earthworm *Lumbricus terrestris*: fitness costs of the gregarine parasite *Monocystis* sp. Parasitology 130:397–403. URL http://www.journals.cambridge.org/abstract{_}S0031182004006663.

Flegr, J., J. Prandota, M. Sovičková, and Z. H. Israili, 2014. Toxoplasmosis - A global threat. Correlation of latent toxoplasmosis with specific disease burden in a set of 88 countries. PLoS ONE 9:e90203.

Folmer, O., M. Black, W. Hoeh, R. Lutz, and R. Vrijenhoek, 1994. DNA primers for amplification of mitochondrial cytochrome c oxidase subunit I from diverse metazoan invertebrates. Molecular Marine Biology and Biotechnology 3:294–9. URL http://www.ncbi.nlm.nih.gov/pubmed/7881515.

Foth, B. J. and G. I. McFadden, 2003. The apicoplast: A plastid in *Plasmodium falciparum* and other apicomplexan parasites. International Review of Cytology 224:57–110.

Francia, M. E. and B. Striepen, 2014. Cell division in apicomplexan parasites. Nature Reviews Microbiology 12:125–136.

Freund, D., S. S. Wheeler, A. K. Townsend, W. M. Boyce, H. B. Ernest, C. Cicero, and R. N. Sehgal, 2016. Genetic sequence data reveals widespread sharing of *Leucocytozoon* lineages in corvids. Parasitology Research 115:3557–3565. URL `http://dx.doi.org/10.1007/s00436-016-5121-3`.

Galen, S. C., J. Borner, E. S. Martinsen, J. Schaer, C. C. Austin, C. J. West, and S. L. Perkins, 2018. The polyphyly of *Plasmodium*: comprehensive phylogenetic analyses of the malaria parasites (Order Haemosporida) reveal widespread taxonomic conflict. Royal Society Open Science 5:171780.

Gardner, M. J., D. H. Williamson, and R. J. Wilson, 1991. A circular DNA in malaria parasites encodes an RNA polymerase like that of prokaryotes and chloroplasts. Molecular and Biochemical Parasitology 44:115–123.

Giard, A., 1884. Note sur un nouveau groupe de protozoaires parasites de annélides polychétes et sur quelques points de l'histoire des grégarines (*Selenidium pendula*). Compte Rendu de la Association Française pour l'Avancement des Sciences P. 192.

Gleeson, M. T., 2000. The plastid in Apicomplexa: What use is it? International Journal for Parasitology 30:1053–1070.

Gould, S. B., R. F. Waller, and G. I. McFadden, 2008. Plastid evolution. Annual Review of Plant Biology 59:491–517.

Grassé, P., 1953. Classe des grégarinomorphes (gregarinomorpha, N. nov., gregarinae Haeckel, 1866; gregarinidea Lankester, 1885; grégarines des auteurs). In Traité de Zoologie. Publications de la Société Linnéenne de Lyon, Paris.

Gubbels, M. J. and M. T. Duraisingh, 2012. Evolution of apicomplexan secretory organelles. International Journal for Parasitology 42:1071–1081. URL `http://dx.doi.org/10.1016/j.ijpara.2012.09.009`.

Guindon, S. and O. Gascuel, 2003. A simple, fast, and accurate algorithm to estimate large phylogenies by maximum likelihood. Systematic Biology 52:696–704.

Gunderson, J. and E. B. Small, 1986. *Selenidium vivax* n. sp. (Protozoa, Apicomplexa) from the sipunculid *Phascolosoma agassizii* Keferstein, 1867. The Journal of Parasitology 72:107–110.

Harper, J. T., E. Waanders, and P. J. Keeling, 2005. On the monophyly of chromalveolates using a six-protein phylogeny of eukaryotes. International Journal of Systematic and Evolutionary Microbiology 55:487–496.

Hoshide, K., 1988. Two gregarines found in polychaetes from the Hokkaido coast of Japan. Proceeding of the Japanese Society of Systematic Zoology 37:47–53.

Hu, K., J. Johnson, L. Florens, M. Fraunholz, S. Suravajjala, C. DiLullo, J. Yates, D. S. Roos, and J. M. Murray, 2006. Cytoskeletal components of an invasion machine - the apical complex of *Toxoplasma gondii*. PLoS Pathogens 2:0121–0138.

Imura, T., S. Sato, Y. Sato, D. Sakamoto, T. Isobe, K. Murata, A. A. Holder, and M. Yukawa, 2014. The apicoplast genome of *Leucocytozoon caulleryi*, a pathogenic apicomplexan parasite of the chicken. Parasitology Research 113:823–828.

Inagaki, Y., J. B. Dacks, W. Ford Doolittle, K. I. Watanabe, and T. Ohama, 2000. Evolutionary relationship between dinoflagellates bearing obligate diatom endosymbionts: Insight into tertiary endosymbiosis. International Journal of Systematic and Evolutionary Microbiology 50:2075–2081.

Iritani, D., T. Horiguchi, and K. C. Wakeman, 2018. Molecular phylogenetic positions and ultrastructure of marine gregarines (Apicomplexa) *Cuspisella ishikariensis* n. gen.,

n. sp. and *Loxomorpha* cf. *harmothoe* from Western Pacific scaleworms (Polynoidae). Journal of Eukaryotic Microbiology 65:637–647. URL http://doi.wiley.com/10.1111/jeu.12509.

Iritani, D., K. Wakeman, and B. S. Leander, 2017. Molecular phylogenetic positions of two new marine gregarines (Apicomplexa) – *Paralecudina anankea* n. sp. and *Lecudina caspera* n. sp. – from the intestine of *Lumbrineris inflata* (Polychaeta) show patterns of co-evolution. Journal of Eukaryotic Microbiology 65:211–219. URL http://doi.wiley.com/10.1111/jeu.12462.

Janouškovec, J., D. V. Tikhonenkov, F. Burki, A. T. Howe, M. Kolísko, A. P. Mylnikov, and P. J. Keeling, 2015. Factors mediating plastid dependency and the origins of parasitism in apicomplexans and their close relatives. Proceedings of the National Academy of Sciences of the United States of America 112:10200–10207.

Janouškovec, J., D. V. Tikhonenkov, K. V. Mikhailov, T. G. Simdyanov, V. V. Aleoshin, A. P. Mylnikov, and P. J. Keeling, 2013. Colponemids represent multiple ancient alveolate lineages. Current Biology 23:2546–2552.

Jouvenaz, D. and D. Anthony, 1979. *Mattesia geminata* sp. n. (Neogregarinida: Ophrocystidae) a Parasite of the Tropical Fire Ant, *Solenopsis geminata* (Fabricius)*. The Journal of Protozoology 26:354–356. URL https://onlinelibrary.wiley.com/doi/abs/10.1111/j.1550-7408.1979.tb04636.x.

Kain, K. C. and J. S. Keystone, 1998. Malaria in travelers: epidemiology, disease, and prevention. Infectious Disease Clinics 12:267–284.

Katoh, K., K. Misawa, K. Kuma, and T. Miyata, 2002. MAFFT: a novel method for rapid multiple sequence alignment based on fast Fourier transform. Nucleic Acids Research 30:3059–3066.

Katris, N. J., G. G. van Dooren, P. J. McMillan, E. Hanssen, L. Tilley, and R. F. Waller,

2014. The apical complex provides a regulated gateway for secretion of invasion factors in *Toxoplasma*. PLoS Pathogens 10:e1004074.

Kearse, M., R. Moir, A. Wilson, S. Stones-Havas, M. Cheung, S. Sturrock, S. Buxton, A. Cooper, S. Markowitz, C. Duran, T. Thierer, B. Ashton, P. Meintjes, and A. Drummond, 2012. Geneious Basic: an integrated and extendable desktop software platform for the organization and analysis of sequence data. Bioinformatics 28:1647–1649.

Keeling, P. J., 2009. Chromalveolates and the evolution of plastids by secondary endosymbiosis. Journal of Eukaryotic Microbiology 56:1–8.

———, 2010. The endosymbiotic origin, diversification and fate of plastids. Philosophical Transactions of the Royal Society of London. Series B, Biological Sciences 365:729–48. URL http://www.researchgate.net/publication/41399433.

———, 2013. The number, speed, and impact of plastid endosymbioses in eukaryotic evolution. Annual Review of Plant Biology 64:583–607.

Keeton, S. T. N. and C. B. Navarre, 2018. Coccidiosis in large and small ruminants. Veterinary Clinics of North America - Food Animal Practice 34:201–208. URL https://doi.org/10.1016/j.cvfa.2017.10.009.

Kilejian, A., 1975. Circular mitochondrial DNA from the avian malarial parasite *Plasmodium lophurae*. BBA Section Nucleic Acids And Protein Synthesis 390:276–284.

Kim, K. and Y. Tsuda, 2010. Seasonal changes in the feeding pattern of *Culex pipiens pallens* govern the transmission dynamics of multiple lineages of avian malaria parasites in Japanese wild bird community. Molecular Ecology 19:5545–5554. URL https://onlinelibrary.wiley.com/doi/abs/10.1111/j.1365-294X.2010.04897.x.

Kim, K. and L. M. Weiss, 2004. *Toxoplasma gondii*: The model apicomplexan. International Journal for Parasitology 34:423–432.

Kjemtrup, A. M. and P. A. Conrad, 2006. A review of the small canine piroplasms from California: *Babesia conradae* in the literature. Veterinary Parasitology 138:112–117.

Kopečná, J., M. Jirků, M. Oborník, Y. S. Tokarev, J. Lukeš, and D. Modrý, 2006. Phylogenetic analysis of coccidian parasites from invertebrates: search for missing links. Protist 157:173–183.

Kück, P., K. Meusemann, J. Dambach, B. Thormann, B. M. von Reumont, J. W. Wägele, and B. Misof, 2010. Parametric and non-parametric masking of randomness in sequence alignments can be improved and leads to better resolved trees. Frontiers in Zoology 7:10.

Kumano, N., N. Iwata, T. Kuriwada, K. Shiromoto, D. Haraguchi, C. Yasunaga-Aoki, and T. Kohama, 2010. The neogregarine protozoan *Farinocystis* sp. reduces longevity and fecundity in the West Indian sweet potato weevil, *Euscepes postfasciatus* (Fairmaire). Journal of Invertebrate Pathology 105:298–304. URL http://dx.doi.org/10.1016/j.jip.2010.08.003.

Kumar, S., G. Stecher, and K. Tamura, 2016. MEGA7: Molecular Evolutionary Genetics Analysis version 7.0 for bigger datasets. Molecular Biology and Evolution 33:1870–1874. URL http://www.ncbi.nlm.nih.gov/pubmed/27004904.

Kuvardina, O. N., B. S. Leander, V. V. Aleshin, A. P. Myl'nikov, P. J. Keeling, and T. G. Simdyanov, 2002. The phylogeny of colpodellids (Alveolata) using small subunit rRNA gene sequences suggests they are the free-living sister group to apicomplexans. Journal of Eukaryotic Microbiology 49:498–504.

Lambert, G., 2007. Invasive sea squirts: a growing global problem. Journal of Experimental Marine Biology and Ecology 342:3–4.

Leander, B. S., 2006. Ultrastructure of the archigregarine *Selenidium vivax* (Apicomplexa) – a dynamic parasite of sipunculid worms (host: *Phascolosoma agassizii*). Ma-

rine Biology Research 2:178–190. URL http://www.tandfonline.com/doi/abs/10.1080/17451000600724395.

———, 2007. Molecular phylogeny and ultrastructure of *Selenidium serpulae* (Apicomplexa, Archigregarinia) from the calcareous tubeworm *Serpula vermicularis* (Annelida, Polychaeta, Sabellida). Zoologica Scripta 36:213–227.

———, 2008. Marine gregarines: evolutionary prelude to the apicomplexan radiation? Trends in parasitology 24:60–7. URL http://www.ncbi.nlm.nih.gov/pubmed/18226585.

Leander, B. S., R. E. Clopton, and P. J. Keeling, 2003. Phylogeny of grenarines (Apicomplexa) as inferred from a small-subunit rDNA and β-tubulin. International Journal of Systematic and Evolutionary Microbiology 53:345–354.

Leander, B. S. and P. J. Keeling, 2003. Morphostasis in alveolate evolution. Trends in Ecology and Evolution 18:395–402.

Leander, B. S., S. A. J. Lloyd, W. Marshall, and S. C. Landers, 2006. Phylogeny of marine gregarines (apicomplexa) - *Pterospora*, *Lithocystis* and *Lankesteria* - and the origin(s) of coelomic parasitism. Protist 157:45–60.

Leclerc, A., J.-M. Chavatte, I. Landau, G. Snounou, and T. Petit, 2014. Morphologic and molecular study of hemoparasites in wild corvids and evidence of sequence identity with *Plasmodium* DNA detected in captive black-footed penguins (*Spheniscus demersus)*. Journal of Zoo and Wildlife Medicine 45:577–588.

Lee, R. E. and P. Kugrens, 1992. Relationship between the flagellates and the ciliates. Microbiological Reviews 56:529–542.

Léger, L., 1892. Recherches sur les Grégarines. Tablettes Zoologiques 3:1–182.

Levine, N. D., 1971. Taxonomy of the Archigregarinorida and Selenidiidae (Protozoa, Apicomplexa). The Journal of Protozoology 18:704–717.

———, 1976. Revision and checklist of the species of the aseptate gregarine genus *Lecudina*. Transactions of the American Microscopical Society 95:695–702.

———, 1977. Checklist of the species of the aseptate gregarine family Urosporidae. International Journal for Parasitology 7:101–108.

———, 1979. New genera and higher taxa of septate gregarines (Protozoa, Apicomplexa). Journal of Protozoology 26:532–536.

———, 1981. New species of *Lankesteria* (Apicomplexa, Eugregarinida) from ascidians on the Central California Coast. Journal of Protozoology 28:363–370.

———, 1984. Taxonomy and review of the coccidian genus *Cryptosporidium* (Protozoa, Apicomplexa). The Journal of Protozoology 31:94–98.

Lim, L. and G. I. McFadden, 2010. The evolution, metabolism and functions of the apicoplast. Philosophical Transactions of the Royal Society B: Biological Sciences 365:749–763.

MacKenzie, W., 1994. A massive outbreak in milwaukee of *Cryptosporidium* infection transmitted through the public water-supply. New England Journal of Medicine 331:1035–1035.

Mackinnon, D. L. and H. N. Ray, 1933. The life cycle of two species of "*Selenidium*" from the polychaete worm *Potamilla reniformis*. Parasitology 25:143–162.

Mans, B. J., R. Pienaar, and A. A. Latif, 2015. A review of *Theileria* diagnostics and epidemiology. International Journal for Parasitology: Parasites and Wildlife 4:104–118. URL `http://dx.doi.org/10.1016/j.ijppaw.2014.12.006`.

Margulis, L., 1970. Origin of Eukaryotic Cells. Yale University Press, New Haven.

Mathur, V., M. Kolísko, E. Hehenberger, N. A. Irwin, B. S. Leander, Á. Kristmundsson, M. A. Freeman, and P. J. Keeling, 2019. Multiple independent origins of apicomplexan-like parasites. Current Biology 29:2936–2941.e5.

McFadden, G. I., 2011. The apicoplast. Protoplasma 248:641–650.

McFadden, G. I. and E. Yeh, 2016. The apicoplast: now you see it, now you don't. International Journal for Parasitology 47:137–144.

McKindsey, C. W., T. Landry, F. X. O'Beirn, and I. M. Davis, 2007. Bivalve aquaculture and exotic species: a review of ecological considerations and management issues. Journal of Shellfish Research 26:281–294.

Mehlhorn, H. and E. Schein, 1985. The piroplasms: life cycle and sexual stages. Advances in Parasitology 23:37 – 103.

Mercier, C., K. D. Adjogble, W. Däubener, and M. F. C. Delauw, 2005. Dense granules: are they key organelles to help understand the parasitophorous vacuole of all apicomplexa parasites? International Journal for Parasitology 35:829–849.

Miller, M. A., W. Pfeiffer, and T. Schwartz, 2010. Creating the CIPRES Science Gateway for inference of large phylogenetic trees. 2010 Gateway Computing Environments Workshop, GCE 2010 .

Mingazzini, P., 1891. Gregarine monocistidee, nuove o poco conosciute, del Golfo di Napoli. Rendiconti dell'Academia di Lincei. Roma 4:229–35.

Misof, B. and K. Misof, 2009. A Monte Carlo approach successfully identifies randomness in multiple sequence alignments: a more objective means of data exclusion. Systematic Biology 58:21–34.

Mita, K., N. Kawai, S. Rueckert, and Y. Sasakura, 2012. Large-scale infection of the ascidian *Ciona intestinalis* by the gregarine *Lankesteria ascidiae* in an inland culture system. Diseases of Aquatic Organisms 101:185–195.

Mo, C., J. Douek, and B. Rinkevich, 2002. Development of a PCR strategy for thraustochytrid identification based on 18S rDNA sequence. Marine Biology 140:883–889.

Moestrup, Ø., 2000. The flagellate cytoskeleton. Introduction of a general terminology for microtubular flagellar roots in protists. The Flagellates, Unity, Diversity and Evolution 59:67–94.

Moore, R. B., M. Obornik, J. Janouskovec, T. Chrudimsky, M. Vancova, D. H. Green, S. W. Wright, N. W. Davies, C. J. Bolch, K. Heimann, J. Slapeta, O. Hoegh-Guldberg, J. M. Logsdon, and D. A. Carter, 2008. A photosynthetic alveolate closely related to apicomplexan parasites. Nature 451:959–963. URL http://www.ncbi.nlm.nih.gov/pubmed/18288187.

Morii, T., 1992. A review of *Leucocytozoon caulleryi* infection in chickens. The Journal of Protozoology Research 2:128–133.

Morrison, D. A., 2009. Evolution of the Apicomplexa: where are we now? Trends in Parasitology 25:375–382.

Morrissette, N. S. and L. D. Sibley, 2002. Cytoskeleton of apicomplexan parasites. Microbiology and Molecular Biology Reviews 66:21–38.

Münster-Swendsen, M., 1991. The effect of sublethal neogregarine infections in the spruce needleminer, *Epinotia tedella* (Lepidoptera: Tortricidae). Ecological Entomology 16:211–219. URL https://onlinelibrary.wiley.com/doi/abs/10.1111/j.1365-2311.1991.tb00211.x.

Nakamura, K., Y. Mitarai, N. Tanimura, H. Hara, A. Ikeda, J. Shimada, and T. Isobe, 1997. Pathogenesis of reduced egg production and soft-shelled eggs in laying hens associated with *Leucocytozoon caulleryi* infection. The Journal of Parasitology 83:325–327. URL http://www.jstor.org/stable/3284467.

Norén, F., Ø. Moestrup, and A.-S. Rehnstam-Holm, 1999. *Parvilucifera infectans* Norén et Moestrup gen. et sp. nov. (Perkinsozoa phylum nov.): a parasitic flagellate capable of killing toxic microalgae. European Journal of Protistology 35:233–254.

O'Donoghue, P. J., 1995. *Cryptosporidium* and cryptosporidiosis in man and animals. International Journal for Parasitology 25:139–195. URL http://www.sciencedirect.com/science/article/pii/0020751994E0059V.

Okamoto, N. and P. J. Keeling, 2014. The 3D structure of the apical complex and association with the flagellar apparatus revealed by serial TEM tomography in *Psammosa pacifica*, a distant relative of the apicomplexa. PLoS ONE 9:e84653.

Ormières, R., 1965. Recherches sur les sporozoaires parasites des tuniciers. Vie Milieu 15:823–946.

Page, M., M. Kelly, and B. Herr, 2019. Awesome ascidians, a guide to the sea squirts of New Zealand. Version 3. NIWA. URL https://niwa.co.nz/coasts-and-oceans/marine-identification-guides-and-fact-sheets/seasquirt-id-guide.

Palmer, J. D., 2003. The symbiotic birth and spread of plastids: How many times and whodunit? Journal of Phycology 39:4–12.

Panciera, R. J., S. A. Ewing, J. S. Mathew, C. A. Cummings, A. A. Kocan, M. A. Breshears, and J. C. Fox, 1998. Observations on tissue stages of *Hepatozoon americanum* in 19 naturally infected dogs. Veterinary Parasitology 78:265–276.

Pereira, S., N. Ramirez, L. Xiao, and L. Ward, 2002. Pathogenesis of human and bovine *Cryptosporidium parvum* in gnotobiotic pigs. The Journal of Infectious Diseases 186:715–718.

Perkins, F. O., J. R. Barta, R. E. Clopton, M. A. Pierce, and S. J. Upton, 2002. Phylum Apicomplexa. Allen Press Inc., Lawrence, KS.

Petersen, E. and J. P. Dubey, 2001. Biology of toxoplasmosis. Toxoplasmosis: A comprehensive clinical guide Pp. 1–42.

Plattner, H. and N. Klauke, 2001. Calcium in ciliated protozoa: sources, regulation, and calcium-regulated cell functions. International Review of Cytology 201:115–208.

Portman, N., C. Foster, G. Walker, and J. Šlapetaa, 2014. Evidence of intraflagellar transport and apical complex formation in a free-living relative of the apicomplexa. Eukaryotic Cell 13:10–20.

Potter, T. M. and D. K. Macintire, 2010. *Hepatozoon americanum*: An emerging disease in the south-central/southeastern United States. Journal of Veterinary Emergency and Critical Care 20:70–76.

Ralph, S. A., G. G. van Dooren, R. F. Waller, M. J. Crawford, M. J. Fraunholz, B. J. Foth, C. J. Tonkin, D. S. Roos, and G. I. McFadden, 2004. Metabolic maps and functions of the *Plasmodium falciparum* apicoplast. Nature Reviews Microbiology 2:203–216.

Ramirez, N. E., L. A. Ward, and S. Sreevatsan, 2004. A review of the biology and epidemiology of cryptosporidiosis in humans and animals. Microbes and Infection 6:773–785.

Ray, H. N., 1930. Studies on some sporozoa in polychaete worms. I. Gregarines of the genus *Selenidium*. Parasitology 22:370–398.

Robert-Gangneux, F. and M. L. Dardé, 2012. Epidemiology of and diagnostic strategies for toxoplasmosis. Clinical Microbiology Reviews 25:264–296.

Ronquist, F., M. Teslenko, P. Van Der Mark, D. L. Ayres, A. Darling, S. Höhna, B. Larget, L. Liu, M. A. Suchard, and J. P. Huelsenbeck, 2012. Mrbayes 3.2: Efficient Bayesian phylogenetic inference and model choice across a large model space. Systematic Biology 61:539–542.

Rueckert, S., C. Chantangsi, and B. S. Leander, 2010. Molecular systematics of marine gregarines (Apicomplexa) from North-eastern Pacific polychaetes and nemerteans,

with descriptions of three novel species: *Lecudina phyllochaetopteri* sp. nov., *Difficilina tubulani* sp. nov. and *Difficilina paranemertis* sp. nov. International Journal of Systematic and Evolutionary Microbiology 60:2681–2690.

Rueckert, S. and B. S. Leander, 2008. Morphology and phylogenetic position of two novel marine gregarines (Apicomplexa, Eugregarinorida) from the intestines of North-eastern Pacific ascidians. Zoologica Scripta 37:637–645.

———, 2009. Molecular phylogeny and surface morphology of marine archigregarines (Apicomplexa), *Selenidium* spp., *Filipodium phascolosomae* n. sp., and *Platyproteum* n. g. and comb. from North-Eastern Pacific peanut worms (Sipuncula). The Journal of eukaryotic microbiology 56:428–39. URL `http://www.ncbi.nlm.nih.gov/pubmed/19737195`.

Rueckert, S., T. G. Simdyanov, V. V. Aleoshin, and B. S. Leander, 2011a. Identification of a divergent environmental DNA sequence clade using the phylogeny of gregarine parasites (Apicomplexa) from crustacean hosts. PLoS ONE 6:e18163. URL `http://dx.plos.org/10.1371/journal.pone.0018163`.

Rueckert, S., P. M. Villette, and B. S. Leander, 2011b. Species boundaries in gregarine apicomplexan parasites: A case study-comparison of morphometric and molecular variability in *Lecudina* cf. *tuzetae* (eugregarinorida, lecudinidae). Journal of Eukaryotic Microbiology 58:275–283.

Rueckert, S., K. C. Wakeman, H. Jenke-Kodama, and B. S. Leander, 2015. Molecular systematics of marine gregarine apicomplexans from Pacific tunicates, with descriptions of five novel species of *Lankesteria*. International Journal of Systematic and Evolutionary Microbiology 65:2598–2614.

Rueckert, S., K. C. Wakeman, and B. S. Leander, 2013. Discovery of a diverse clade of gregarine apicomplexans (apicomplexa: Eugregarinorida) from pacific eunicid and

onuphid polychaetes, including descriptions of *Paralecudina* n. gen., *Trichotokara japonica* n. sp., and *T. eunicae* n. sp. Journal of Eukaryotic Microbiology 60:121–136.

Ryan, U., A. Paparini, P. Monis, and N. Hijjawi, 2016. It's official – *Cryptosporidium* is a gregarine: what are the implications for the water industry? Water Research 105:305–313. URL http://dx.doi.org/10.1016/j.watres.2016.09.013.

Sato, S., 2011. The apicomplexan plastid and its evolution. Cellular and Molecular Life Sciences 68:1285–1296.

Schilder, R. J. and J. H. Marden, 2006. Metabolic syndrome and obesity in an insect. Proceedings of the National Academy of Sciences of the United States of America 103:18805–18809.

Schlüter, D., W. Däubener, G. Schares, U. Groß, U. Pleyer, and C. Lüder, 2014. Animals are key to human toxoplasmosis. International Journal of Medical Microbiology 304:917–929. URL http://dx.doi.org/10.1016/j.ijmm.2014.09.002.

Schnepf, E. and G. Deichgräber, 1984. "Myzocytosis", a kind of endocytosis with implications to compartmentation in endosymbiosis - Observations in *Paulsenella* (Dinophyta). Naturwissenschaften 71:218–219.

Schnittger, L., A. E. Rodriguez, M. Florin-Christensen, and D. A. Morrison, 2012. *Babesia*: a world emerging. Infection, Genetics and Evolution 12:1788–1809. URL http://dx.doi.org/10.1016/j.meegid.2012.07.004.

Schrével, J., 1971. Observations biologiques et ultrastructurales sur les Selenidiidae et leurs consequences sur la systematique des grkgarinomorphes. The Journal of Protozoology 18:448–470.

Schrével, J., A. Valigurová, G. Prensier, A. Chambouvet, I. Florent, and L. Guillou, 2016. Ultrastructure of *Selenidium pendula*, the type species of archigregarines, and phylogenetic relations to other marine Apicomplexa. Protist 167:339–368. URL http://dx.doi.org/10.1016/j.protis.2016.06.001.

Siddall, M. E., 1995. Phylogeny of adeleid blood parasites with a partial systematic revision of the Haemogregarine complex. Journal of Eukaryotic Microbiology 42:116–125. URL https://onlinelibrary.wiley.com/doi/abs/10.1111/j.1550-7408.1995.tb01551.x.

Simdyanov, T. G., 1996. The morphology and ultrastructure of the gregarine *Loxomorpha harmothoe* from the White Sea. Parazitologiya 30:174–180.

Simdyanov, T. G., A. Y. Diakin, and V. V. Aleoshin, 2015. Ultrastructure and 28S rDNA phylogeny of two gregarines: *Cephaloidophora* cf. *communis* and *Heliospora* cf. *longissima* with remarks on gregarine morphology and phylogenetic analysis. Acta Protozoologica 54:241–263.

Simdyanov, T. G., L. Guillou, A. Y. Diakin, K. V. Mikhailov, J. Schr?vel, and V. V. Aleoshin, 2017. A new view on the morphology and phylogeny of eugregarines suggested by the evidence from the gregarine *Ancora sagittata* (Leuckart, 1860) Labbé, 1899 (Apicomplexa: Eugregarinida). PeerJ 5:1–46. URL https://peerj.com/articles/3354.

Simpson, A. G. and D. J. Patterson, 1996. Ultrastructure and identification of the predatory flagellate *Colpodella pugnax* Cienkowski (Apicomplexa) with a description of *Colpodella turpis* n. sp. and a review of the genus. Systematic Parasitology 33:187–198.

Sitnikova, T. Y. and A. Shirokaya, 2013. New data in deep-water Baikal limpets found in hydrothermal vents and oil-seeps. Archiv für Molluskenkunde 142:257–278.

Smith, H. V., R. A. Nichols, and A. M. Grimason, 2005. *Cryptosporidium* excystation and invasion: getting to the guts of the matter. Trends in Parasitology 21:133–142. URL http://www.sciencedirect.com/science/article/pii/S1471492205000243.

Smith, T. and F. L. Kilborne, 1893. Investigations into the nature, causation, and prevention of Texas or southern cattle fever. 1. US Department of Agriculture, Bureau of Animal Industry.

Smith, T. G., B. Kim, H. Hong, and S. S. Desser, 2000. Intraerythrocytic development of species of *Hepatozoon* infecting ranid frogs: evidence for convergence of life cycle characteristics among apicomplexans. The Journal of Parasitology 86:451–458. URL `https://doi.org/10.2307/3284856`.

Stach, T. and J. M. Turbeville, 2002. Phylogeny of Tunicata inferred from molecular and morphological characters. Molecular Phylogenetics and Evolution 25:408–428.

Stamatakis, A., 2014. RAxML version 8: A tool for phylogenetic analysis and post-analysis of large phylogenies. Bioinformatics 30:1312–1313.

Starcovici, C., 1893. Bemerkungen über den durch Babes entdeckten Blutparasiten und die durch denselben hervorgebrachten Krankheiten, die seuchenhafte Hämoglobinurie des Rindes (Babes), das Texasfieber (Th. Smith) und der Carceag der Schafe (Babes). Zentralblatt fur Bakteriologie, Parasitenkunde, Infektionskrankheiten und Hygiene. Erste Abteilung: Originale 14:1–8.

Sunnotel, O., C. J. Lowery, J. E. Moore, J. S. Dooley, L. Xiao, B. C. Millar, P. J. Rooney, and W. J. Snelling, 2006. *Cryptosporidium*. Letters in Applied Microbiology 43:7–16.

Swedlow, J. R., K. Hu, P. D. Andrews, D. S. Roos, and J. M. Murray, 2002. Measuring tubulin content in *Toxoplasma gondii*: a comparison of laser-scanning confocal and wide-field fluorescence microscopy. Proceedings of the National Academy of Sciences of the United States of America 99:2014–2019.

Tengs, T., O. J. Dahlberg, K. Shalchian-Tabrizi, D. Klaveness, K. Rudi, C. F. Delwiche, and K. S. Jakobsen, 2000. Phylogenetic analyses indicate flint the 19'hexanoyloxyfucoxanthin containing dinoflagellates have tertiary plastids of haptophyte origin. Molecular Biology and Evolution 17:718–729.

Théodoridès, J., 1967. Sur la position systématique du genre *Lankesteria* Mingazzini, 1891 (Eugregarina). Comptes rendus hebdomadaires des séances de l'Académie des Sciences 265:1995–1996.

Tomley, F. M. and D. S. Soldati, 2001. Mix and match modules: structure and function of microneme proteins in apicomplexan parasites. Trends in Parasitology 17:81–88.

Trampuz, A., M. Jereb, I. Muzlovic, and R. M. Prabhu, 2003. Clinical review: severe malaria. Critical Care 7:315–323.

Turon, X. and S. López-Legentil, 2004. Ascidian molecular phylogeny inferred from mtDNA data with emphasis on the Aplousobranchiata. Molecular Phylogenetics and Evolution 33:309–320.

Tyzzer, E., 1907. A sporozoan found in the peptic glands of the common mouse. Proceedings of The Society for Experimental Biology and Medicine 5:12–13.

Uilenberg, G., 2006. *Babesia* - a historical overview. Veterinary Parasitology 138:3–10.

Valkiunas, G., 2005. Avian malaria parasites and other haemosporidia. CRC Press, Inc., Boca Raton, Florida.

Vivier, E. and J. Schrével, 1964. Etude au microscope électronique d'une Grégarine du genre Selenidium parasite de *Sabellaria* alveolata. Journal de Microscopie (Paris) 3:651–670.

———, 1966. Les ultrastructures cytoplasmiques de *Selenidium hollandei*, n. sp., Grégarine parasite de *Sabellaria alveolata*. Journal de Microscopie 5:213–228.

Wakeman, K. C., M. B. Heintzelman, and B. S. Leander, 2014a. Comparative ultrastructure and molecular phylogeny of *Selenidium melongena* n. sp. and *S. terebellae* Ray 1930 demonstrate niche partitioning in marine gregarine parasites (Apicomplexa). Protist 165:493–511. URL `http://www.ncbi.nlm.nih.gov/pubmed/24998785`.

Wakeman, K. C. and B. S. Leander, 2012. Molecular phylogeny of pacific archigregarines (Apicomplexa), including descriptions of *Veloxidium leptosynaptae* n. gen., n. sp., from the sea cucumber *Leptosynapta clarki* (Echinodermata), and two new species of *Selenidium*. Journal of Eukaryotic Microbiology 59:232–245.

———, 2013a. Identity of environmental DNA sequences using descriptions of four novel marine gregarine parasites, *Polyplicarium* n. gen. (Apicomplexa), from capitellid polychaetes. Marine Biodiversity 43:133–147. URL http://link.springer.com/10.1007/s12526-012-0140-5.

———, 2013b. Molecular phylogeny of marine gregarine parasites (Apicomplexa) from tube-forming polychaetes (Sabellariidae, Cirratulidae, and Serpulidae), including descriptions of two new species of *Selenidium*. Journal of Eukaryotic Microbiology 60:514–525. URL http://doi.wiley.com/10.1111/jeu.12059.

Wakeman, K. C., J. D. Reimer, H. Jenke-Kodama, and B. S. Leander, 2014b. Molecular phylogeny and ultrastructure of *Caliculium glossobalani* n. gen. et sp. (Apicomplexa) from a pacific *Glossobalanus minutus* (Hemichordata) confounds the relationships between marine and terrestrial gregarines. Journal of Eukaryotic Microbiology 61:343–353.

Wakeman, K. C., A. Yabuki, K. Fujikura, K. Tomikawa, and T. Horiguchi, 2017. Molecular Phylogeny and Surface Morphology of *Thiriotia hyperdolphinae* n. sp. and *Cephaloidophora oradareae* n. sp. (Gregarinasina, Apicomplexa) Isolated from a Deep Sea *Oradarea* sp. (Amphipoda) in the West Pacific. Journal of Eukaryotic Microbiology Pp. 1–10. URL http://doi.wiley.com/10.1111/jeu.12480.

Wang, Z. D., H. H. Liu, Z. X. Ma, H. Y. Ma, Z. Y. Li, Z. B. Yang, X. Q. Zhu, B. Xu, F. Wei, and Q. Liu, 2017. *Toxoplasma gondii* infection in immunocompromised patients: a systematic review and meta-analysis. Frontiers in Microbiology 8:1–12.

Watts, J. G., M. C. Playford, and K. L. Hickey, 2016. *Theileria orientalis*: a review. New Zealand Veterinary Journal 64:3–9.

White, N. J. and G. C. Cook, 1996. Manson's tropical diseases. Pp. 1124–1130, *in* Malaria. Saunders Philadelphia.

WHO, 2019. World malaria report 2018. World Health Organization P. xii.

Wilson, I. R., P. W. Denny, P. R. Preiser, K. Rangachari, K. Roberts, A. Roy, A. Whyte, M. Strath, D. J. Moore, P. W. Moore, and D. H. Williamson, 1996. Complete gene map of the plastid-like DNA of the malaria parasite *Plasmodium falciparum*. Journal of Molecular Biology 261.

Yamaguchi, A. and T. Horiguchi, 2005. Molecular phylogenetic study of the heterotrophic dinoflagellate genus *Protoperidinium* (Dinophyceae) inferred from small subunit rRNA gene sequences. Phycological Research 53:30–42.

Yoshimura, A., M. Koketsu, H. Bando, E. Saiki, M. Suzuki, Y. Watanabe, H. Kanuka, and S. Fukumoto, 2014. Phylogenetic comparison of avian Haemosporidian parasites from resident and migratory birds in Northern Japan. Journal of Wildlife Diseases 50:235–242.

Yubuki, N. and B. S. Leander, 2013. Evolution of microtubule organizing centers across the tree of eukaryotes. Plant Journal 75:230–244.

Zhan, A., E. Briski, D. G. Bock, S. Ghabooli, and H. J. MacIsaac, 2015. Ascidians as models for studying invasion success. Marine Biology 162:2449–2470.

Zhu, G., M. J. Marchewka, and J. S. Keithly, 2000. *Cryptosporidium parvum* appears to lack a plastid genome. Microbiology 146:315–321.

Zuk, M., 1987a. Seasonal and individual variation in gregarine parasite levels in the field crickets *Gryllus veletis* and *G . pennsylvanicus*. Ecological Entomology 12:341–348.

———, 1987b. The effects of gregarine parasites on longevity, weight loss, fecundity and developmental time in the field crickets *Gryllus veletis* and *G.pennsylvanicus*. Ecological Entomology 12:349–354. URL http://doi.wiley.com/10.1111/j.1365-2311.1987.tb01014.x.